CHAPTER 1

INTRODUCTION

1.1 Importance of Nanoscience and Nanotechnology

In a lecture by Nobel laureate Richard Feymannn in late 1959 entitled "There is Plenty of Room at the Bottom", he mentioned about a fascination world of nanosized materials and atoms, which is so much different from the one that we knew then and envisioned their importance. His talk took place before the word "nanotechnology" existed and he was seen by many as the person who spurred researchers to venture into the field of nanotechnology.

The prefix "nano" refers to a billionth ($1x10^{-9}$) of a unit, hence a nanometer is $1x10^{-9}$ m. Nanoscience is the study of phenomena on the scale of ~ 1-100 nm while nanotechnology is the ability to create and control novel materials or devices within this size that have specific properties and functions. There are two approaches to nanotechnology:

a) top-down; where miniaturized devices or nanostructured materials are obtained from a standard material

b) bottom up; where atoms or molecules are arranged in a desired manner to meet specific requirements

The emergence of nanoscience and nanotechnology helped to shape the world we know today. The advancement of nanotechnology helps in the miniaturization of devices especially in the field of electronics and semiconductors and also improvisation in the properties and functions of existing materials or technology. Amongst the contributions of nanotechnology include vast development in the field of nanobiotechnology, nanoelectronics and nanodevices and nanomaterials.

The conventional medical solution for curing diseases/sickness involving internal organs is through medication or surgery. Consumption of drugs often causes side-effects in other organs and damaging them in the process while wound from the surgery often takes a long time to heal and is vulnerable to infections. Advancements in the field of nanobiotechnology would allow drugs to be delivered directly to the intended organs or localized area by nanobots instead of traveling through blood stream to the entire body. Surgical robots of nanosize that can be imparted to our body through a very small hole are seen as replacements for the existing ones and avoid the post-operation complications.

Nanoelectronics and nanodevices are essential in today's world. Miniaturization leads to the reduction in the size of the electronic components. In turn, more components could be packed into the same amount of space and thus improving the performance and efficiency of the equipment and with less energy consumption. Another advantage is on overcoming the technology barrier faced in many of today's applications. One of them is the integrated circuit (IC). For decades, silicon has been used in the semiconductor devices and according to Moore's Law, the number of transistors in an IC doubles every two years. Eventually, there will be a limit on the number of transistors that can fit into an IC. The ever increasing number of transistors also means the amount of heat generated is greater and could cause overheating of the device. Scientists have shown that it is possible to replace silicon with quantum dot. This allows a faster rate of data transfer but with less heat generation.

Development of nanosized and nanostructured materials such as fullerenes, carbon nanotubes (CNTs), etc. is achieved via novel processing methods or breaking down the particles of traditional materials normally using mechanical means. The improvement of chemical, mechanical and electrical properties of nanomaterials is mainly attributed to the increased surface area and the quantum effect that they demonstrate due to their nanosize [1]. For instance, traditional ZnO and TiO_2 containing sunscreens reflect harmful rays but leave a white smear. Substituting with nanoparticles of ZnO and TiO_2 will make it transparent yet equally protective, thus is more suitable for commercial application.

1.2 Research Background

Nanotechnology paves way to work at the molecular level, atom by atom, to create structures with novel molecular organization. This lead to the definition of nanotechnology as materials, devices and systems where structures and components exhibit novel and significantly improved physical, chemical and biological properties because of their nanoscale size.

An announcement was made by the US government that a tire pressure monitoring (TPM) system is mandatory for vehicles sold in North America beginning 2004 and by September 2007, all new vehicles should be installed with this capability as per the requirement of the National Highway Traffic Safety Administration (NHTSA) [2]. This comes into ruling after a series of accidents due to tire failures involving highly underflated vehicles. On top of that, vehicles running on properly pumped-up tire will consumed less fuel by as much as 1% or amounting 1.2 billion gallons of petrol in US alone [3]. With the increase in fuel pricing like the one experienced in year 2008 and potentially in the near future, the importance of running on well-inflated tires with the assistance of a TPMS cannot be undermined. Although overseas car makers are not required to comply, they are expected to follow this ruling for safety and fuel efficiency reasons.

Tire pressure monitoring system is not new to the automotive industry since it has been implemented as factory-installed feature for quite a number of years albeit for the high-end vehicles only. However, with the new ruling, which also involves those in the middle range, would require the system to be more cost effective. In this measuring system, each tire has its own monitoring sensor and the information will be transferred and evaluated by a central control unit.

Under normal circumstances, the pressure inside the tire will vary slightly due to air diffusion and the change in the temperature of the pressurized air. With proper calibration, variation due to temperature change can be rectified using an embedded temperature sensor. The driver will not be alarmed about this until it has exceeded the threshold. Motorist will be warned about the condition of their tires by the signal displayed on the dashboard (Figure 1.1).

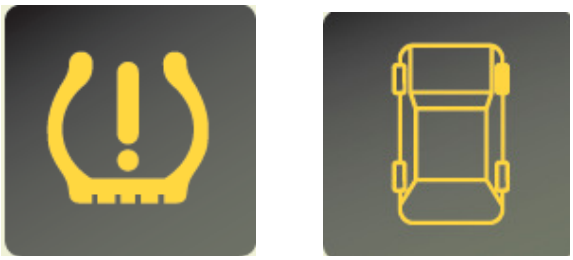

Figure 1.1 Warnings lights indicating one or more tires significantly under-inflated (left) and position of the affected tire (right) [4]

Current TPM sensors mostly use MEMS technology, doped silicon operating on the piezoresistive nature of silicon. Silicon is preferred because their electrical properties are well-known, it is of single crystal structure and has higher piezoresistive effect compared to metals.

Piezoresistive effect describes the changing electrical resistance of a material due to applied mechanical stress. The degree of the material's sensitivity towards the applied stress is known as gauge factor, K, and is defined as:

$$K = (\Delta R/R)/\varepsilon_L \tag{1.1}$$

where R is the resistance and ε_L the strain. The gauge factor depends on the impurity level in the sensing material, temperature and crystal orientation. Materials having high K values are more sensitive to strain.

Advantage of using piezoresistive sensors are their small size, rugged construction, high speed of response and self-generated signal. However, the limitations include limited to dynamic measurements, sensitive to temperature variations and required special cabling and output signal amplification [5].

1.3 Silicon as Sensor Material

Current pressure sensors that use MEMS technology, employ single-crystal Si as the sensing material since Si can be found in abundance in the environment where they exist naturally in the form of silica (SiO_2) and can be processed into single crystal

relatively easily. Being single crystal, their electrical and mechanical properties are superior and can be manipulated by means of doping.

To make a pressure sensor, a piece of Si, usually (1 0 0) orientation, is etched from the backside, to create a diaphragm, like in Figure 1.2, and should be as thin as possible for better sensitivity. For example, a 20-micron diaphragm has approximately 4 times the sensitivity of a 40-micron diaphragm [6]. Four doped polycrystalline silicon which display piezoresistive characteristic, or piezoresistors, are then diffused onto the selected spots on the surface of the diaphragm so that when it bends (elastically) as a result of pressure, there will be changes in the electrical resistance at these areas. The design of the pressure sensor normally uses four piezoresistors, usually in a "Wheatstone bridge" configuration in Figure 1.3 with three resistors having fixed resistance. Compared to a single resistor, the output voltage is less susceptible to external influence, i.e. temperature, as all four resistors would experience equal changes thus minimizing the temperature effects. Any differences in the resulting voltage can then be related to the change in resistance of the sensor.

One major setback for silicon-based sensors is that their electrical resistance is sensitive towards the effect of temperature, especially for TPM due to the harsh operating environment. This is primarily due to the current-leakage across a back-biased P-N junction and it doubles every 8^{o}C of temperature. At elevated temperature, the error is large and consequently limiting the maximum operating temperature of silicon sensors (usually at 120^{o}C). A simple comparison of the phenomena is tabulated in Table 1.1 [6]. In order to increase the operating temperature, the silicon is normally doped, however this will incur additional cost.

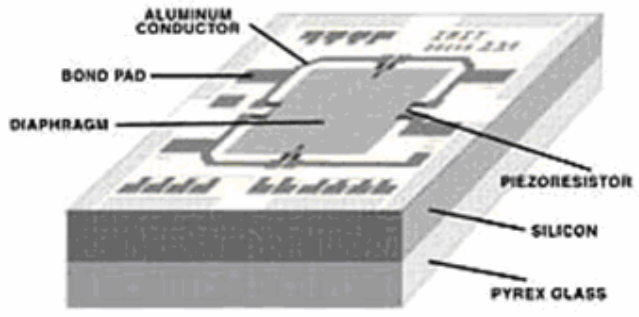

Figure 1.2 Example of a silicon pressure sensor [7]

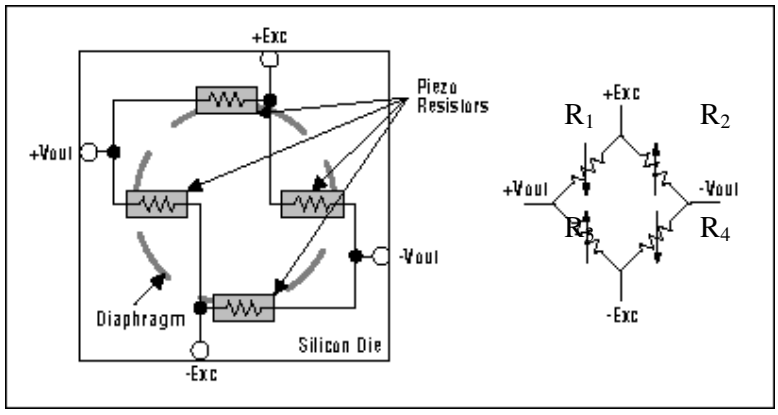

Figure 1.3 Typical pressure sensors with equivalent circuit [6]

Table 1.1 Current leakage across back-biased P-N junction in Si at different temperature [6]

Operation temperature (^{o}C)	Current leakage (μA)
25	5×10^{-3}
120	20
170	1.3×10^{3}

Another limitation is the diaphragm thickness over diameter ratio. In most devices, they are diced into the same size (diameter). Thus, the range of pressure measurement is tailored by varying the thickness of the diaphragm. While it was mentioned earlier that a thinner diaphragm would be more sensitive towards pressure, there is however, a lower limit to it. As it becomes thinner, the diaphragm will undergo larger bending or distortion at a given pressure until it reached a threshold limit. Further thinning will result in a situation whereby the deformation no longer corresponds linearly to the applied stress (non-linearity). As technology continues to strive for miniaturization, this can only be overcome by sourcing for alternative materials.

1.4 Carbon Nanotubes as Alternative Sensing Elements

At the moment, researchers worldwide see carbon nanotubes (CNTs) as potential materials for a vast number of applications, including as an active element in pressure

sensing. This is because of the superior properties that CNTs have over most conventional materials due to their unique structure.

Fullerenes and carbon nanotubes (CNTs) are new allotropes of the carbon family (apart from diamond and graphite) that were only discovered recently. A fullerene consists of C atoms bonded to 3 other carbon atoms in a hybridized sp2 bonding and could be found as C_{60} (Figure 1.4 (a)), C_{70}, C_{76}, C_{78} and C_{84} [8]. Due to its dome shape, which resembles a ball, thus fullerene or Buckminsterfullerene are also known as "buckyball". The discovery of fullerenes is seen as significant due to the characteristics and properties that it possesses, as a result of the unique carbon atoms arrangement, and the vast potentials that scientists and engineers can tap into.

This eventually led to Harold W. Kroto, Robert F. Curl Richard E. Smalley, who discovered fullerenes in 1985, of being awarded the Nobel Prize in Chemistry in 1996. CNTs (Figure 1.4 (b)) are similar to fullerenes as they have end-caps that resemble fullerene hemispheres and are found to be of better importance compared to fullerenes. CNTs have captured the attention of the researchers around the globe since their discovery in 1991 because of their endless possibilities for various applications.

CNTs are one of the nanostructured materials that received a lot of attentions from researchers across the globe. This is mainly due to their remarkable mechanical properties, unique electrical properties as well as high thermal and chemical stability. Mechanically, they are light but very strong. Young's modulus of CNTs is almost 10 times higher than steel and yet they are not brittle. Instead, they would undergo an elastic bending upon deformation (Figure 1.5) [9]. Electrical properties of CNTs are a strong function of their atomic structure and mechanical deformation. This is useful especially when developing tiny sensors that are sensitive to chemical, mechanical or physical environment.

Researches so far have found that CNTs can be used for chemical and physical sensors. Kong [10] has shown that the electrical resistance of CNTs changes when the nanotubes are exposed to a small amount of nitrogen dioxide and ammonia at room temperature while most sensors demonstrate high sensitivity only at temperature above 600^{o}C. This occurs as the gas molecules react with the C-C bonds, leading to electron withdrawal or donation in a process called electrochemistry.

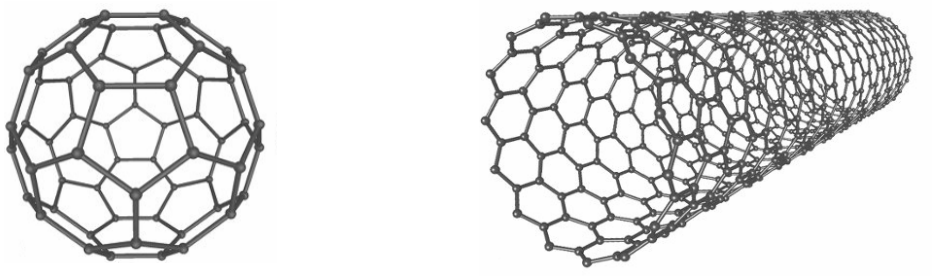

(a) (b)

Figure 1.4 Structure of a (a) C_{60} buckminsterfullerene and (b) carbon nanotube [8]

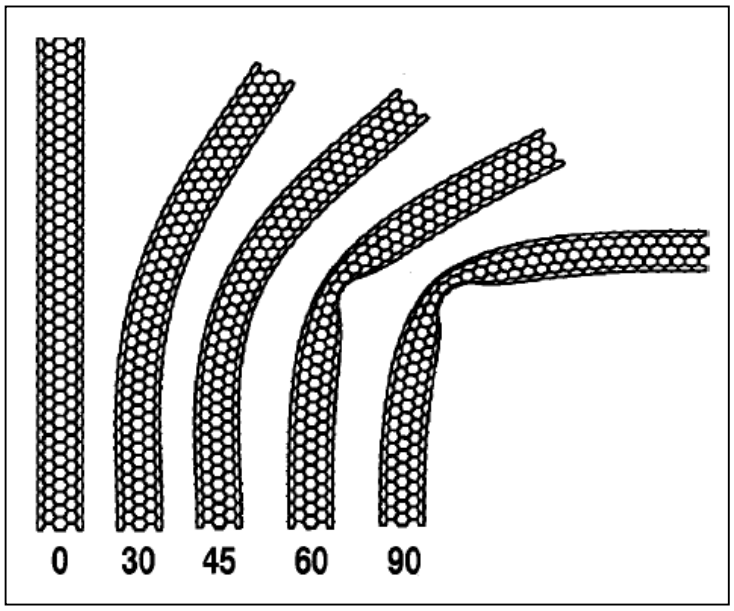

Figure 1.5 Schematic diagram of a carbon nanotube at various bending angle [9]

Beside chemical reaction, CNTs also exhibit piezoresistvity characteristics, like Si. Mechanical distortion like bending and twisting of the nanotubes will also affect their electron transport properties, which is useful for detecting mechanical stress [9]. Some advantages of CNTs over silicon as pressure sensor include having larger K values [11], indicating they are more sensitive towards changes in the strain and a lower temperature coefficient of resistivity (~5 times) [12]. On top of that, CNTs have higher Young's modulus compared to Si, meaning CNTs are able to withstand higher

pressure level before experiencing non-linearity. CNTs also offer a possibility for gearing towards the next technological frontier, replacing MEMS (Micro ElectroMechanical Systems) with NEMS (Nano ElectroMechanical Systems). Further details regarding the properties of CNTs will be discussed in Chapter 2.

1.5 Critical Issues of Si-based Pressure Sensor

As described in Section 1.3, the electrical changes of Si-based sensors is highly sensitive to temperature causing it to be useless beyond the operating temperature of 120^{o}C. The thickness of the sensing element is another issue that will not be resolved with the current trend of miniaturization of components in the devices.

1.6 Objective and Scope of Work

Driven by the need to address the challenges encountered by the Si-based pressure sensor, an alternative material is being sought after. It is believed that CNTs would be a good candidate as the pressure sensing element as it can provide the thermal stability and nanoscale required. The objective is to develop the nanostructure material namely CNTs as the active element for pressure sensing applications. To achieve this, the following research elements need to be carried out:

1) Produce good quality aligned carbon nanotubes with desired characteristics. This would involve synthesis of vertically aligned carbon nanotubes via thermal chemical vapor deposition method through optimization of the growth parameters. The scope of work consists of:

    a) Study on the synthesis of CNT growth involves investigating various growth parameters and its effect towards the CNTs film. This includes the effect of buffer layer preparation, growth configuration (sandwich and conventional stacking) and catalyst precursor selection (pellet and powder).

    b) Characterization of the synthesized CNTs film requires selecting appropriate characterization tools suitable for nanosize materials like

Raman spectroscopy, field emission scanning electron microscopy (FESEM) and transmission electron microscopy (TEM) to study their properties. The physical properties of CNTs that can be characterized using these analytical tools are diameter distribution, wall thickness, cyrstallinity, purity, density, length or thickness of the film, etc.

2) Characterization of the electrical response of carbon nanotubes as sensing element in a test unit and evaluating the performance of the sensing element when subjected to pressure and temperature. The activities to be carried out encompass the following:

    a) Integration of the CNTs film into a test unit that involves the designing the experimental setup in which the electrical measurement can be carried out not only effectively and efficiently, without damaging the CNTs film, but also one that is repeatable.

    b) Evaluation of the CNTs film performance that involves collection and interpretation of the data obtained (resistance change of the film with time, temperature and pressure) to validate the feasibility of using CNTs film for pressure sensing application.

1.7 Originality of Work

The originality of this PhD work includes the use of metal catalyst in powder form when most work uses pellets (electron beam or ion beam evaporation) or disc (sputtering), growth of aligned carbon nanotubes (CNTs) film in the sandwich configuration using two substrates of equal size and successfully performed electromechanical measurements on as-grown CNTs film assisted by conductive buffer layer. The use of metal catalyst offers another option for CNTs as it is readily available unlike pellets and discs. Formation of conductive buffer layer means electrical measurement can be made on the as-grown or pristine aligned CNTs film without having to resort to transferring it to a conductive substrate using a conductive paste.

1.8 Thesis Online

This thesis is separated into five chapters. This outline is to provide information on the discussions in each chapter.

Chapter One provides an introduction about nanotechnology and its importance, the background issue of this research and reasons for the use of carbon nanotubes as the topic of research.

Chapter Two gives an overview about the general information on the structure, important growth parameters, electrical and mechanical properties and past research on carbon nanotubes that are relevant to the scope of study.

Chapter Three charts the flow of the project and the methods used to synthesize and characterize the carbon nanotubes required and equipments employed to analyze the carbon nanotubes obtained.

Chapter Four discusses the observations and results from the synthesis and characterization of the carbon nanotubes and the importance of these findings, for the application of carbon nanotubes as an active element in pressure sensing application.

Chapter Five concludes the findings in Chapter Four and their importance. Some recommended works to be undertaken are also listed here.

CHAPTER 2

CARBON NANOTUBES – STRUCTURE, PROPERTIES AND APPLICATIONS

2.0 Overview

Carbon nanotube is one of the most important nanostructured materials as it revolutionizes the way we produce devices or systems. As CNTs is the material chosen to be developed as the pressure sensing element, an extensive background study starting with its structure to applications need to be presented here. This would give a better understanding in order to establish the structure-property behavior.

2.1 Background

Carbon nanotubes (CNTs), together with fullerenes, are considered as the third allotropes of the carbon family. Existence of carbon filaments with diameter smaller than 10 nm have been known for quite some time since 1970's as they have been found to present albeit randomly during the synthesis of carbon fibers [13, 14]. However, not much attention was to given them until Iijima discovered multi-walled carbon nanotubes (MWCNTs) in 1991 [15] while running high resolution TEM (HR-TEM) on the filament which he used for the synthesis of fullerenes. The main reasons were lack of proper instrumentations to study them scientifically due to their nanosize and failure to synthesize them in a consistent manner. Single-walled carbon nanotubes (SWCNTs) were discovered two years after the discovery of MWCNTs, independently and at the same time, by two different groups; Iijima at NEC Laboratory and Bethune from IBM Laboratory [16, 17].

The discovery of SWCNTs is significant as it allows researchers, for the first time, to study the behavior and characteristics of a one-dimensional material that exhibits quantum effect due to its geometry. The smallest tube diameter reported is 0.4 nm [18] while their length can reach up to a few millimeters [19-21] meaning that their length-to-diameter ratio can reach a remarkable value of 10^6 or more.

The exceptional properties and characteristics exhibited by CNTs as compared to diamonds and graphite are largely attributed to the C-C bonding in their structure. Regardless of their allotrope, a carbon atom has four valence electrons occupying the $2s^2$ and $2p^2$ orbits to form either the sp, sp^2 or sp^3 hybrid orbital (Figure 2.1).

In diamond [21], the carbon atoms are bonded together by four equivalent σ covalent bonds, forming sp^3 bond. This 3-D structure makes diamond the hardest known material and also electrically insulating since there's no delocalized π bonds. For graphite [23], each carbon atoms along the same planar is held together by three in-plane σ bonds to give sp^2 bonds with an out-of-plane π orbital. The σ and π orbitals cannot mix as they are at right angle of each other. For that, graphite is stronger in-plane than diamond and also more electrically and thermally conductive as a result of the π orbital. The weak van der Waals bond that exists between adjacent graphite sheets explains the soft nature of graphite and allows the use of graphite as lubricants as the sheets can easily glide on top of each other.

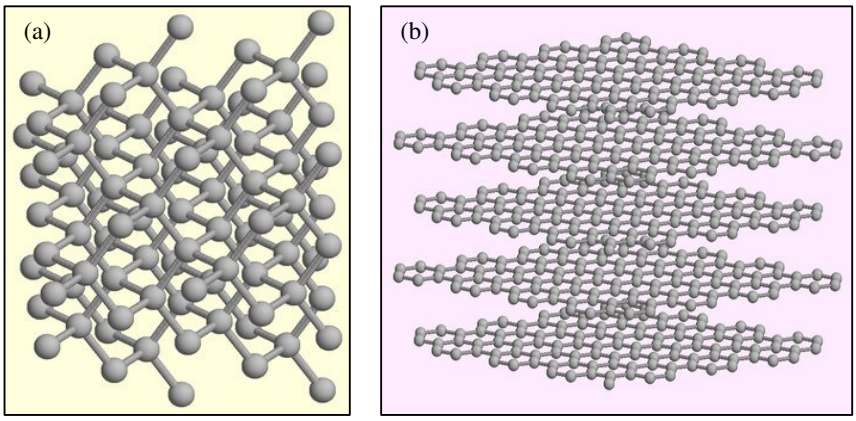

Figure 2.1 Structure of (a) sp^3 hybrid in diamond (b) sp^2 hybrid in graphite [24]

For a CNT, since it is a rolled-up graphene sheet, the C-C bonding is basically sp^2, similar to that of graphite. However, the curvature effect or rolling of the graphene sheet leads to the deformation of the three σ bonds, with further delocalization of the π orbital and this enables the π and σ states to mix and form hybrids that are partly sp^2 and sp^3. This effect is known as σ-π rehybridization and contributed to the CNTs having better mechanical strength, higher electrical and thermal conductance and chemically more reactive than graphite [25].

2.2 Classifications of Carbon Nanotubes

In general, CNTs can be categorized into two groups; single-wall and multi-walled, depending on the number of walls (Figure 2.2). A single-wall CNTs (SWCNT) is a hollow cylinder of a graphene sheet while a multi-walled CNT (MWCNT) is the plural form of coaxial SWCNTs. Each "layers" or walls in the MWCNTs is separated by an interlube spacing of 0.34 nm [26].

2.2.1 Single-walled Carbon Nanotubes

SWCNTs are the basic structure of all CNTs with average diameters of about 1.4 nm. They are an important variety of CNTs since most SWCNTs are perfectly formed and offers as potential materials for various applications as mechanical reinforcement, catalyst, electronic devices, etc. The hollow structure within the SWCNTs has the potential to be utilized for hydrogen storage since the walls of the CNTs are chemically very stable. Depending on the chirality and diameter of the nanotubes, SWCNTs can be found to behave either as metallic, semi-metallic or semiconducting [26].

2.2.2 Multi-walled Carbon Nanotubes

MWCNTs refer to all CNTs that have more than one wall in their structure. However, in recent times, specific names have been given to MWCNTs of simpler forms having

double wall and triple wall, known as double-walled and triple-walled CNTs, respectively [27-30]. Although much of the focus is on SWCNTs due to their superior properties, nevertheless the study on MWCNTs is still relevant as they possess several advantages namely can be grown without the use of catalytic particles, enables study of quantum interference phenomena using magnetic fields accessible at laboratory level and better mechanical stability and rigidity for scanning probe tip applications.

2.3 Structure of Carbon Nanotubes

Since the structure of a CNT has very close resemblance to a graphene, the structure is normally explained using the graphene lattice vectors, $\boldsymbol{C_h}$ and $\boldsymbol{T}$ (Figure 2.3). A single-wall carbon nanotube can be seen as a capsule consisting of a graphene sheet being rolled together to form a seamless cylinder about the axis $\boldsymbol{T}$, which is at the right angle to graphene sheet, and capped with a hemisphere of fullerene at both ends.

The circumference of a SWCNT is influenced by the circumferential vector (also known as chiral vector) since the diameter of the tube, $d_t = \boldsymbol{C_h}/\boldsymbol{\pi}$ with $\boldsymbol{C_h} = n\mathbf{a_1} + m\mathbf{a_2}$, where $\mathbf{a_1}$ and $\mathbf{a_2}$ represent the unit vectors of the honeycomb structure with n and m as integers. The characteristics of the nanotubes are determined by chirality, the manner in which the CNTs are rolled with respect to the direction of the $\boldsymbol{T}$ vector. Chirality is specified by the two integers (n, m) as summarized in Figure 2.4, and has huge significance on the properties of the resulting nanotubes.

The three main structures of CNTs are zigzag, armchair and chiral (Figure 2.5). The direction of the chiral vector is measured by the chiral angle, θ. When $\theta = 0^o$, the vector is (n, *0*) and the structure is known as "zigzag" because they exhibit a zigzag pattern along the circumference. At chiral angle $\theta = 30^o$, the structure is "armchair", a (n, n) nanotube. All other vectors (n, m) correspond to chiral nanotubes [34].

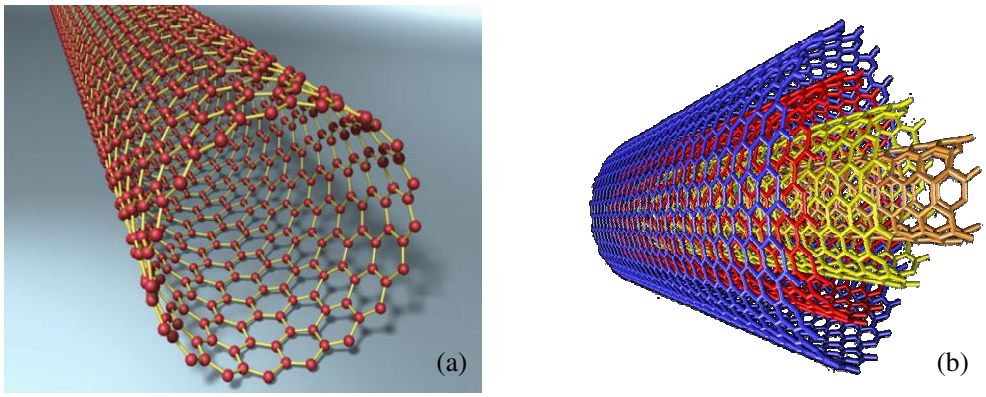

Figure 2.2 Schematic image of (a) single-walled [31] and (b) multi-walled carbon nanotubes [32]

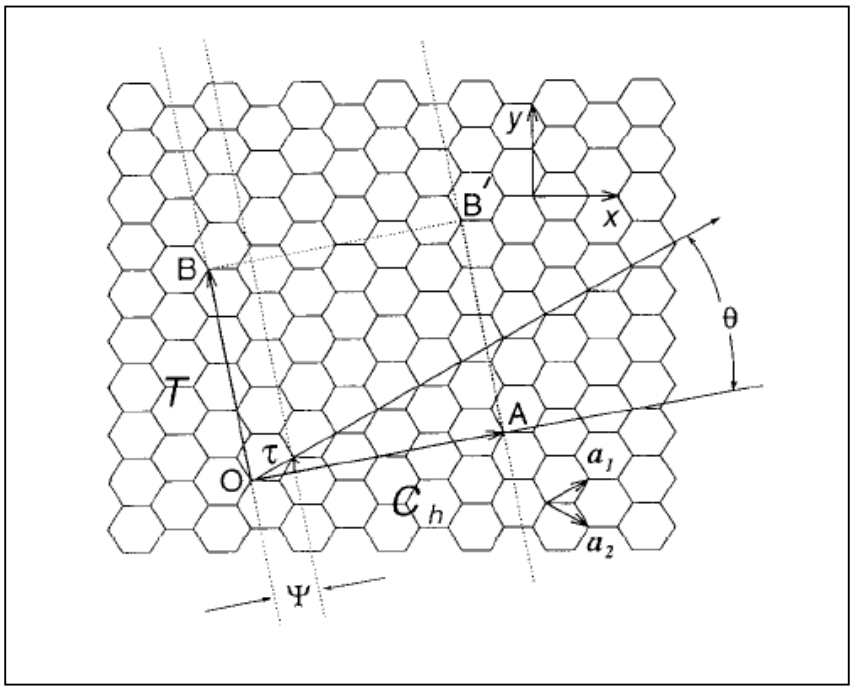

Figure 2.3 Structure of a graphene sheet showing the unit vectors $\mathbf{a_1}$ and $\mathbf{a_2}$ as well as the definition for $\mathbf{C_h}$ and **T** [31]

The abovementioned nanotubes are based on the model of a perfect structure. However, in reality, it is impossible to have defect-free structures of CNTs. Capped, bent, branched (L, Y, T), helical and toroidal are amongst the defective types of CNTs that have been found [35-40]. These topological deformities occur when pentagons

and heptagons structures are incorporated into the hexagonal network instead. But generally speaking, most SWCNTs are defect-free compared to MWCNTs where structural defects like discontinuous or cone-shaped walls or bamboo structures may also occur on top of the topological defects listed above. This can be analytical proven using Raman spectroscopy, whereby the defective band (D-band) of MWCNTs is always higher than that of SWCNTs.

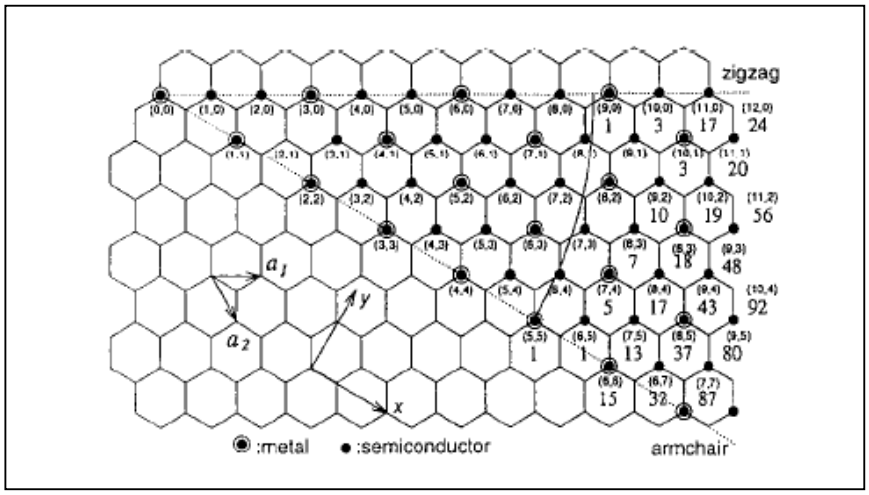

Figure 2.4 Possible vectors specified by the integers (n, m) including zigzag, armchair and chiral nanotubes [26]

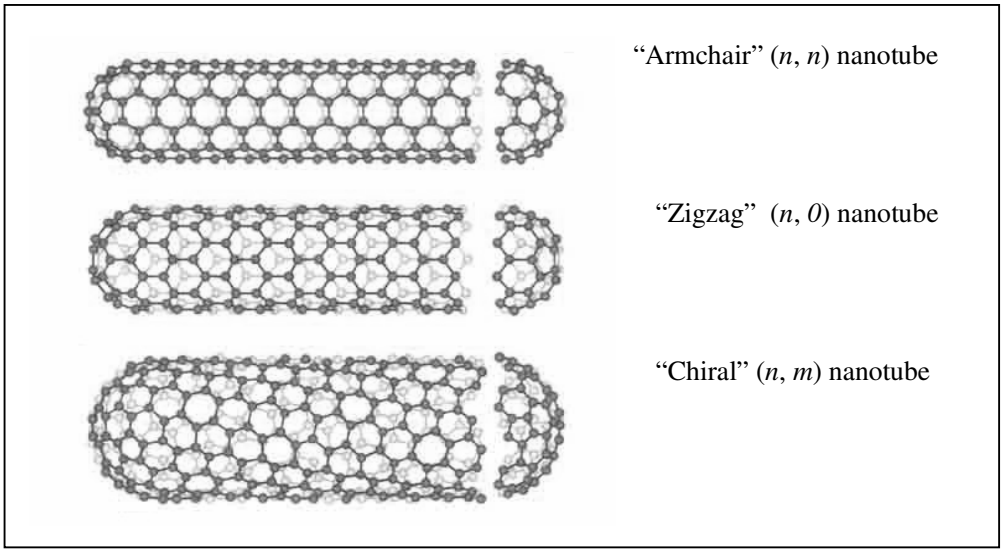

Figure 2.5 Schematic models for single-wall carbon nanotubes of different chirality [31]

2.4 Methods for growing Carbon Nanotubes

Like all other materials, the study of CNTs intensified once they can be produced or synthesized with great consistency. There are three common methods of synthesizing CNTs namely are arc discharge, laser ablation and chemical vapor deposition (CVD).

2.4.1 Arc discharge

The earliest method used for the production of MWCNTs is arc-discharge (Figure 2.6), first discovered by Iijima [14] but further improvised by Ebbesen and Ajayan [41]. Opposing graphite electrodes are used as anode and cathode with a gap of 1 to 4 mm between them in an inert atmosphere. The orientation, whether vertically or horizontally, is insignificant as they have been found to have non-noticeable affect on the quality and quantity of resulting nanotubes. In order to have a better yield, a helium gas atmosphere is preferred compared to argon.

An arc, with temperature approaching 3700^{o}C [42], is created between these two electrodes when high currents passed through these electrodes, resulting in the carbon atoms getting evaporated due to the high temperature. This is possible as the temperature produced is approximately the melting point of graphite. To regulate the temperature of the chamber, water is used as cooling substance. As a result, the anode is consumed while cylindrically shaped deposit is grown on the negative electrode.

As for the production of SWCNTs, a composite anode made of graphite embedded with metal catalyst (cobalt) is required [16]. Further improvements have been achieved using Ni/Y and Co/Ni [43-45].

The advantage of using this method is the ability to produce CNTs of high crystalinity in large quantities but the setback of using this method is the high temperature required making it not plausible for large scale production. It also requires careful control of the process conditions i.e constant current flow to achieve a stable arc, constant inert gas pressure inside the chamber, proper spacing between the electrodes, etc [46].

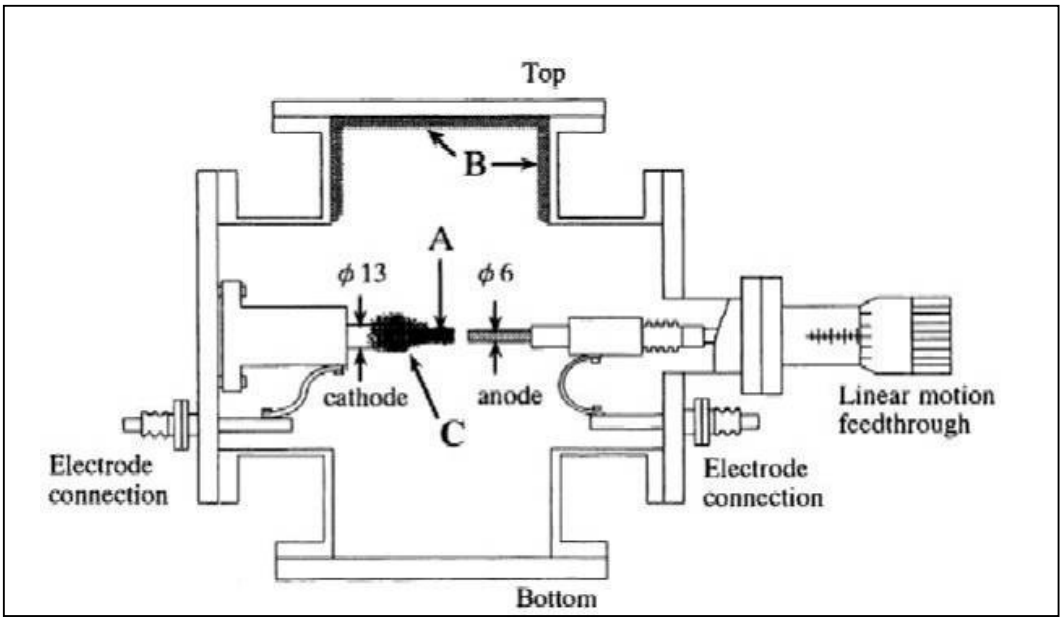

Figure 2.6 Schematic diagram of an arc discharge method [42]

2.4.2 Laser Ablation

This method of synthesizing CNTs was first performed by Smalley's group [47, 48] in 1995. The furnace was heated up to 1200^{o}C and pumped with Ar gas (carrier gas) at a pressure of 500 Torr. Pulse (Nd:YAG) or continuous laser is focused onto the block of graphite containing a small amount of metal catalyst (target) to ablate the graphite block. Upon impingement by the laser, the carbon and metal atoms vaporized and form a mixture of vapor plume. This plume later condensed and collected at the Cu collector due to the action of the Ar gas flow. In this experimental setup (Figure 2.7), CNTs were collected but in the absence of the metal catalyst, fullerene was observed instead.

It is speculated that in the presence of metal catalyst, the atoms of the catalyst somehow got attached to a half-formed fullerene or graphite sheet. This prevented the hemisphere of a fullerene to close. Instead, carbon atoms continue to build onto it to form tubules. Additional attachment of carbon atoms lead to the lengthening of these tubes. This growing process of the nanotubes continued until termination where it

was poisoned as the catalyst gets over-coated with carbon [49]. All these occurred over a short period of time.

It was also observed by Guo *et al* [47] that the quality of the MWCNTs deteriorated with decreasing growth temperature from 1200^{o}C, where the nanotubes are almost defect-free until 200^{o}C, where no CNTs were observed. It was also reported in another paper by Guo that, bi-metallic catalyst system was found to give better yield of SWCNTs compared to mono-metallic [48].

2.4.3 Chemical Vapor Deposition (CVD)

CVD method, by far, has been the more successful and preferred method of producing CNTs. This method allows the aligned growth of CNTs on a substrate, where all the CNTs are growing in the same direction and subsequently formed a dense film, something not achievable with the other two methods. It is also scalable up to industrial level [28, 50]. Typically, CVD refers to a process where a substrate is exposed to volatile precursors to form deposits on the surface of the substrate. The types of CVD are classified according to the method use to apply the energy necessary to activate the CVD reaction i.e. temperature, photon or plasma. In fact, most of the recent advancements in the synthesis of CNTs are achieved via CVD methods.

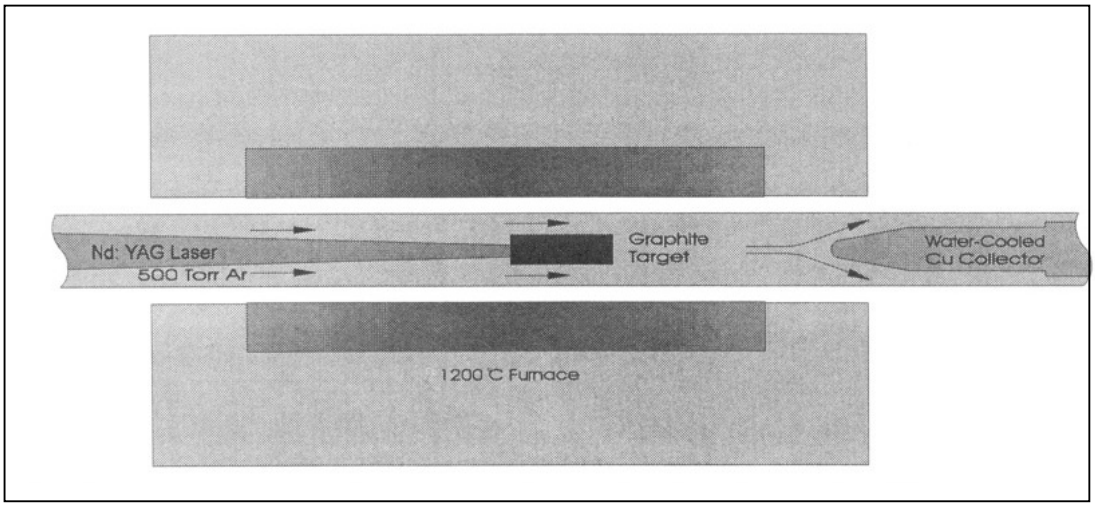

Figure 2.7 Schematic of laser-ablation apparatus [47]

For CNTs growth using CVD, a substrate is required for the formation of CNTs over a specific area. The selection of substrates has been studied [50-55] and they can be of silicon wafer, quartz, glass, silica, alumina, zeolite etc. According to Ward *et al* [54], the surface morphology, rather than the type of substrate, is found to have a profound significance on the CNTs obtained. There are two types of CVD method, thermal CVD and plasma enhanced CVD (PECVD).

In thermal CVD (Figure 2.8), the reactor is filled with inert gas like Ar while the temperature inside is being raised. Once it reached the reaction temperature, the metered flow of feedstock gas, normally CO [56], alcohols (methanol and ethanol) [57] or hydrocarbon gas like methane [58], ethylene [59], acetylene [60], etc is purged into the reaction chamber over a stipulated period for the CNTs growth to take place on the substrate. After that, the chamber is filled with inert gas again and is allowed to cool to room temperature before the CNTs are collected.

In the case whereby the substrate cannot tolerate the high temperature associated to a thermal CVD, an alternative method would be using PECVD [61]. In this method, the dissociation of precursor is by high energy electrons in cold plasma while the substrate is kept at a relatively low temperature. CNTs are formed when the exposed substrate is impinged with ions from the plasma generated using DC, hot-filament, microwave and radio frequency (r. f.), etc. Whereas thermal CVD normally produced aligned CNTs as a result of crowding effect (nanotubes supporting each other by van der Waals interaction), individual, free-standing and vertically oriented structures are possible with PECVD [24]. However, the CNTs formed using PECVD has a high content of amorphous carbon as the decomposition of pure hydrocarbon feedstock by plasma leads to formation of reactive radicals. Thus, usually inert gases are used to dilute the pure hydrocarbon.

2.5 Selection of catalyst

Growth of CNTs generally involves the use of hydrocarbon feedstock gas (discussed in Section 2.4) and catalyst at the suitable growth environment.

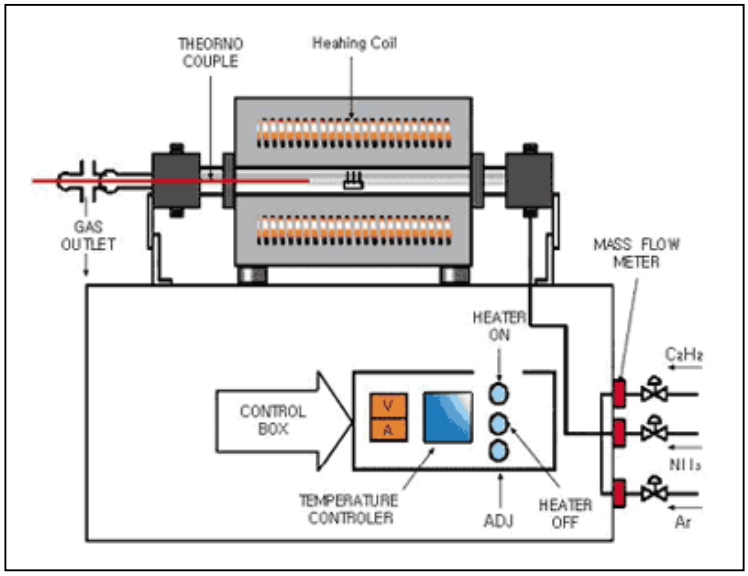

Figure 2.8 Schematic of thermal chemical vapor deposition [62]

Catalyst is a vital ingredient in the growth of CNTs as they act as nucleation sites. The type of catalyst used for the synthesis of CNTs are normally single element of transitions metals like Fe, Ni, Co, Mo, oxides of these elements (CoO, NiO, Fe_2O_3) or binary alloys like Fe/Ni, Fe/Co, Fe/Mo, Co/Ni and NiO/CoO [52,60,62-68].

Although CNTs were only discovered in 1991, studies have been performed on the growth of filamentous carbon since 1970's. Thus, the use of catalyst is not an entirely new subject. Catalyst selection is a vital step in growing CNTs. The type of catalyst used has adverse effect on the crystallinity and growth rate. Lee *et. al.* [67] reported that Ni gives the best growth rate of MWCNTs compared to Co and Fe, but the CNTs obtained using Fe have higher cyrstallinity.

Kong *et. al.* [58] have studied using oxides of Fe, Ni and Co as catalysts for SWCNTs growth. In their report, SWCNTs were only obtained under certain situation, either on alumina or silica, when using CoO or NiO/CoO. In contrast, Fe_2O_3 was found to be producing abundant amount of CNTs under both conditions studied while no SWCNTs were formed when using NiO as catalyst. On top of that, Baker *et. al.* [69] had earlier shown that the catalytic action for the growth of filamentous carbon differs with various oxides of iron as precursor. The order of activity is: $FeO > Fe \sim Fe_2O_3$.

Ivanov *et. al.* [60] and Ng *et. al.* [68] both reported that combination of two elements/binary alloys produce better outcome compare to single elements. These findings agree with earlier reports [44, 45, 48]. All these could be due the synergistic effect when combining two or more elements.

All these and many other reports are proofs that the selection of the types of catalyst is crucial towards the synthesis of CNTs. Based on the reports that Fe_2O_3 can produce abundant CNTs of highest crystallinity in alumina and silica substrates in addition to being the best catalyst for thermal CVD [70], Fe is selected as the catalyst for the purpose of this study.

2.6 Preparation of catalyst

There are two types of catalyst deposition for CNTs growth. One method is the fixed catalyst, whereby the catalyst is deposited on top of the substrate as thin film, either using solution or by physical techniques while the second method is using floating catalyst i.e. in gaseous form.

2.6.1 Solution-based Catalyst

Numerous researches have been performed on the use of solution-based catalyst. Amongst the methods used to deposit solution-based catalyst are spin coating, dip coating and contact printing. The desired catalyst mostly is in the form of chemical salt and a support, dissolved in alcohol solution. The purpose of adding a support is to disperse the particles of the dissolved catalyst as agglomeration is common in small-sized particles. This way, lesser starting material is required and the amount of catalyst used can be optimized. In theory, the particle size of the catalyst obtained through chemical reaction that takes place is favorably smaller but that may not necessary be true as these particles tend to aggregate due to van der Waals force. In addition, the preparation work involved is cumbersome such as dissolution and mixing of chemical salts, separation of unwanted by-product from the precursor and calcinations/annealing of the gel or precipitate (before or upon deposition on the

substrate). All these are time consuming, not to mention the difficulties to confine the catalyst solution over a selected growth area [24]. Deposition methods of solution are also not favorable when a large area is involved due to concern of uniformity.

2.6.2 Physical Techniques of Catalyst Deposition

This technique involves deposition of a thin film of catalyst onto the substrate. Amongst the methods are electron beam evaporation, thermal evaporation, ion beam sputtering, magnetron sputtering, etc. Their names are reference to the method in which the evaporative materials, mostly in solid forms like pellets or disc, are vaporized to form a thin film on the substrate/target. Typical catalyst thickness deposited is less than 20 nm as it has been shown that there's a correlation between film thickness and diameter of the resulted CNTs [71-73].

Nanoislands of the catalyst are observed upon annealing as a result of surface tension and also due to mismatch in the coefficient of thermal expansion between Si and the catalyst [74, 75]. Formation of such small islands is said to be critical as they act as nucleation sites for CNTs growth. An increase in the catalyst thickness will lead to an increased in the average size of these islands as well [71, 74] and subsequently have a significant impact on the resulting CNTs structure. Increasing the thickness of Ni from 2 nm to 10 nm [71] will decrease the average density of CNTs by a factor of 3, reduce the average length of CNTs by 4 times while the tube diameter will be twice as large. Similar results were also reported by Ren *et. al.* [52]. Chhowalla *et. al.* [71] reported that when the thickness of the Co layer is 20 nm, no island formation is observed. The catalyst layer, however, can be fragmented upon etching with NH_3 plasma akin to other reports. In those reports, the etchant used are diluted HF [52] and NH_3 gas [75].

Thus, it is important to have a thin layer of catalyst. At the same time, there is a threshold on the lower limit of the thickness. When the thickness is decreased, the number of these nanoislands also decreased and causes discontinuity in the catalytic layer [71]. This reduces the number of nucleation site and catalytic reactivity for the formation of CNTs. As the growth of aligned CNTs is due to the crowding effect of

nanotubes, when the growth becomes sparse, the alignment of CNTs may be compromised [76]. However, there is no study on this threshold value although most of these reports used catalyst thickness no less than 1 nm.

2.6.3 Floating Catalyst

As opposed to the methods described earlier, where the catalyst and feedstock gas are introduced in two steps, floating catalyst is an in-situ process of introducing them (Figure 2.9). This method usually involves a two-stage furnace. The first furnace is used for decomposition of the catalyst source where the catalyst will be collected on the substrate and transfer to a second furnace whereby the carbon-containing feedstock is introduced.

This method was first reported by Sen *et. al.* [77] via pyrolysis of metallocene like ferrocene, nickolecene and cobaltocene since they contained both the transitional metals and hydrocarbon fragments required for CNTs formation. That paper also explored the difference of using benzene with or without an addition of metallocene on the CNTs obtained. Later, studies conducted by others use other hydrocarbon gaseous like acetylene [36] and CO [56] with ferrocene. Studies on substituting ferrocene with iron pentacarbonyl $Fe(CO)_5$ and use together with other hydrocarbon gases have also been conducted [56, 78].

2.7 Growth Mechanisms of Carbon Nanotubes by CVD method

Although there are reports about success in growing CNTs even in the absence of catalyst [79, 80], most researchers still uses catalytic method for growing CNTs. The focus of discussion is on the growth mechanism of CNTs in a thermal CVD using fixed catalyst deposited via e-beam deposition. The reason for selecting transitional elements is that carbon has finite solubility in these elements at elevated temperature. Although the exact growth mechanism of CNTs has not been identified, researchers adopt a model similar to that of the carbon filament formation from catalytic pyrolysis. This can be described as dissociation of hydrocarbon into carbon atoms followed by

dissolution and diffusion of carbon atoms onto catalytic particles. The result is the supersaturation of carbon precipitation into tubular forms before finally terminating the growth and capping the tubes.

Inside a CVD system, the hydrocarbon feedstock gas decomposed at high temperature. The carbon atoms will then dissolve and diffuse on the surface of these catalytic particles. As the solubility of carbon in the metal catalyst is finite, upon reaching a saturation limit, these carbon atoms will precipitate and form tubules as they are energetically favored. Carbon atoms continue to add onto the sidewall, contributing to the increase in the length.

At this stage, there could be two possible mode of growth (Figure 2.10). If the bonding between the particles and substrate is strong, base growth will occur whereby the catalytic particle remains at the bottom while the tube lengthens. If the bonding is loose, tip growth will happen where the catalytic particle is lifted as the tube grows. The metal-support interactions are highly dependent on the type of support materials and the metal precursor for the catalyst used [65]. Annealing can also be performed to enhance the bonding and to avoid from being over-sintered at elevated temperature [59].

During the growth of nanotubes, the open ended theory suggests that the C_2 dimers continuously add to the dangling bonds at the open ends on the sidewall, forming hexagons [35,81]. Sometimes C_3 dimers are required for continual additions of the hexagons. Otherwise, pentagons will formed and this will lead to capping and termination of the growth. But researchers are still uncertain what kept the tubes from closing at this stage. On the other hand, formation of heptagons will cause changes in the orientation of the growth. Another theory, closed ended theory [82, 83], proposed that the CNTs are always capped and that the C_2 dimers absorbed through the pentagonal defects at the tube end. While the two theories on the growth are still debatable as there is no concrete evidence to support, the open-ended theory seems to be more plausible.

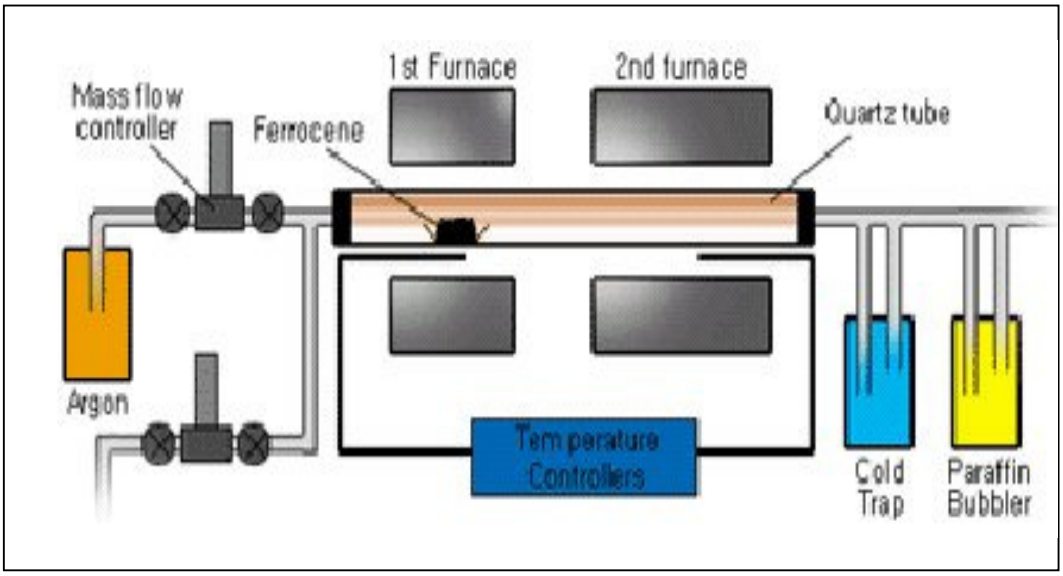

Figure 2.9 Schematic diagram of a two-stage furnace [62]

On the termination of CNTs growth, most agree that at certain point, the growth stops when the catalytic particles get poisoned by the impurities or due to formation of carbide. This hinders further addition of dimers. In view of this, Hata *et. al.* introduced a method to include a "small and controlled amount of water vapor" during the synthesis of CNTs [20] to obtain a 'supergrowth' of SWCNTs forest that can reach 1 mm in height in 10 minutes with carbon purity above 99.98% and SWCNT-to-catalyst mass ratio of 590. The introduction of water vapor in a balanced ratio to ethylene claimed to help to ensure the surface of the catalytic particles remain clean and this prolong their reactivity up to 30 minutes compared to 1 minute using conventional method. This was followed up with a paper that deals with the kinetics behind [84]. Even though the task to create CNTs consisting of a single chirality and tubes of similar diameter is still almost impossible, efforts have been made to separate metallic SWCNTs from semiconducting [85], to obtain SWCNTs of selected chirality [86] and nanotubes with a narrower range of diameters [87, 88].

2.8 Inclusion of buffer layer

There are instances where an additional layer called buffer layer, is deposited between the Si substrate and the metal catalyst. This is normally performed in the absence of a thick layer of SiO_2. The concern with the catalyst layer is that, it may form metal silicides with the silicon wafer at high temperature that could hinder the growth of CNT. It has been proven that the native oxide of SiO_2 layer with only a few nanometers thick, is too thin to act as a barrier and to provide support for CNTs growth [59]. To overcome this, a buffer layer between the wafer and metal catalyst, like Si_3N_4, TiN and Al_2O_3 is introduced [89], which can act as a barrier layer between the metal and wafer. Depending on the type of materials used, the presence of a buffer layer may also enhance the growth of the CNTs [68].

2.9 Orientation of CNTs growth

In general there are two orientations of CNTs grown, namely bulk and array,. While researchers may not have fully understood the growth mechanisms of CNTs, current understanding of this subject does enable us to grow the required orientation of CNTs.

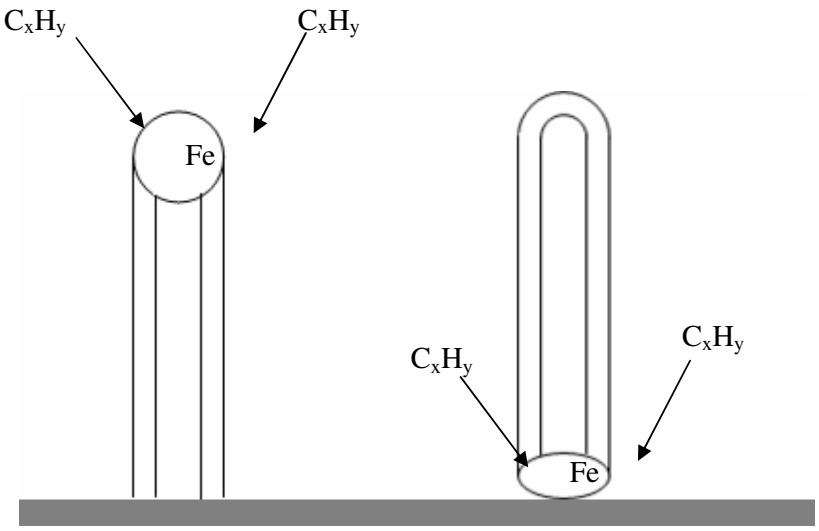

Figure 2.10 Tip growth (left) and base growth (right) mode of carbon nanotubes

Bulk CNTs are actually clusters of CNTs that grow in multiple directions, often overlapping each other, thus the spaghetti-like appearance under SEM at high magnification (Figure 2.11) [96]. This growth orientation is mainly used for mechanical reinforcement. The type of catalyst used is solution based. The diameter of the nanotubes depends on the size of the catalytic particles while its length is determined by the growth period (exposure time of catalyst to feedstock gas).

In array CNTs, all the nanotubes grow in a single direction (Figure 2.12). The preparation process is more tedious as a lot of parameters are involved namely distribution of catalyst, substrate and catalyst interaction, growth duration, growth temperature, etc. Catalyst layer is usually prepared using physical vapor deposition. The aligned CNTs are formed as a result of crowding effect with adjacent nanotubes due to van der Waals forces along the wall of the nanotubes. Theoretically, there is no limit to length that the CNTs can grow as ultra long CNTs film of 2.5 mm has been reported [20**Error! Reference source not found.**, as long as the catalyst particles remain active. There is no actual application for aligned CNTs at the moment, but they have been earmarked for application like sensors, field emission (FE) and field effect transistors (FET), etc in the future [24]. Their high aspect ratio (length to diameter ratio) makes them a highly suitable material for this application.

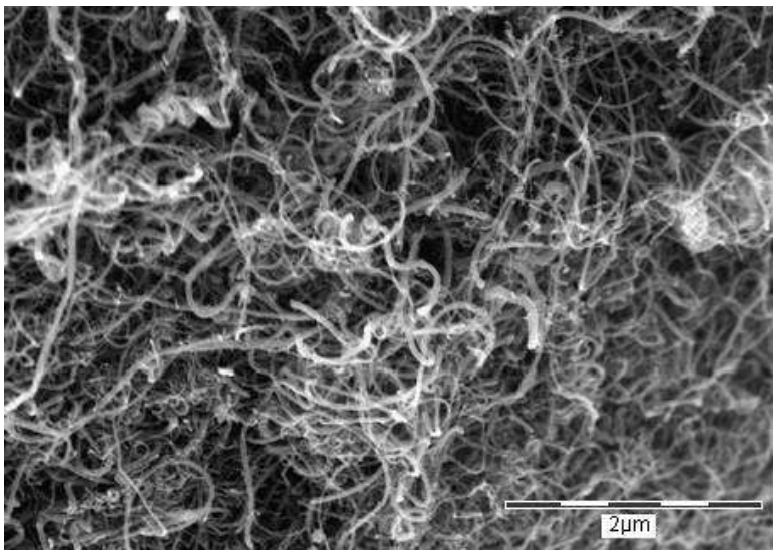

Figure 2.11 SEM image of bundled CNTs

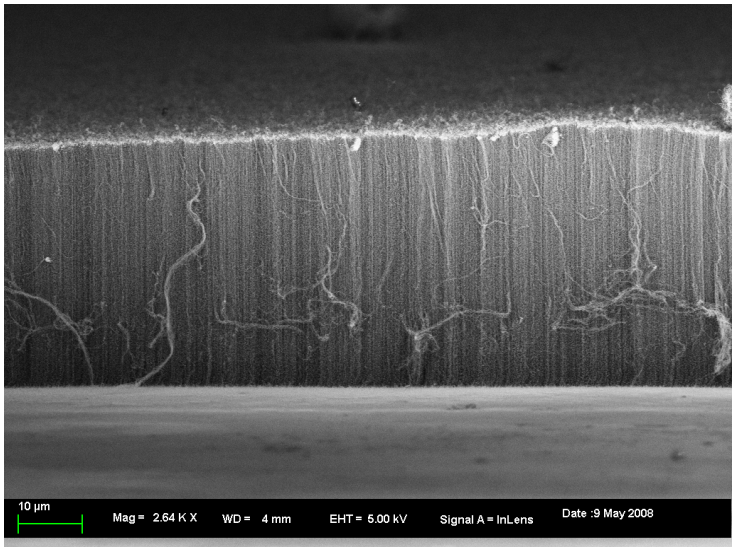

Figure 2.12 SEM image of aligned CNTs film

2.10 Characterization Techniques for Carbon Nanotubes Study

Upon obtaining the CNTs, it is important to have suitable analytical tools to characterize them as they appear like black substance. Amongst the commonly used characterization techniques are Raman spectroscopy, scanning electron microscopy (SEM), transmission electron microscopy (TEM), etc. Only these electron microscopy techniques can reveal the intrinsic properties of CNTs

2.10.1 Raman Spectroscopy

The use of Raman spectroscopy, Figure 2.13 [90] for studying CNTs is mainly to validate the existence of CNTs and to provide physical properties such as crystallinity, types of CNTs (SWCNTs, MWCNTs), tube diameter, chirality and etc. This technique, of analyzing, was initially used on carbon-based materials like graphite and fullerene and was later extended to CNTs study, pioneered by Dresselhaus [25, 91].

Generally, there are three major peaks in a Raman spectrum of CNTs. The first peak is the radial breathing mode or RBM, which exists between 100 and 400 cm^{-1} [92] as a result of vibration in carbon atoms along the radial direction (Figure 2.14).

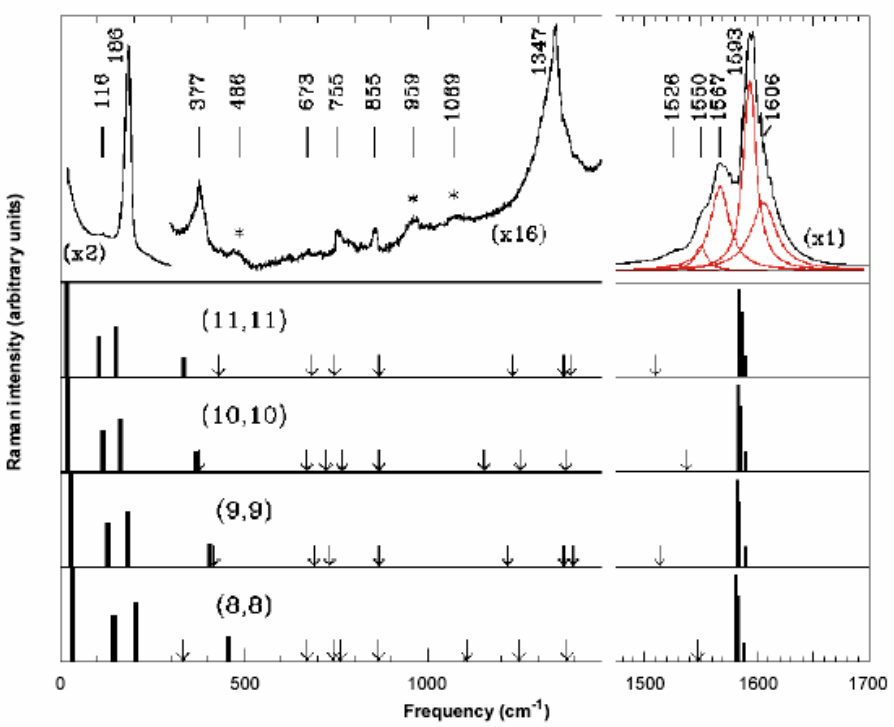

Figure 2.13 Example of Raman spectrum for armchair (*n, n*) nanotubes, *n*=8 to 11 [90]

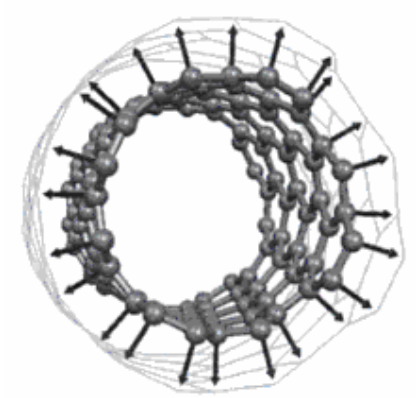

Figure 2.14 Radial breathing mode of a nanotube. The arrows indicate the motion of the carbon atoms during vibration while the lines indicate the changes in the diameter as it vibrates [92]

The existence of RBM usually indicates the presence of SWCNTs (Figure 2.15) [93] while no one has observed the presence of RBM in MWCNTs [94]. Theoretically, RBM can be observed in MWCNTs, which indicates the nanotubes having co-axial

structures. But since the wall of a MWCNT is composed of multiple layers of carbon, the nanotubes are deemed rigid to vibrate in the radial axis thus explaining the absence of RBM in MWCNTs (Figure 2.16). One of the significance of RBM is that it can be used to calculate the theoretical value of the diameter of SWCNTs. For isolated carbon nanotubes [95], the value is governed by $\omega_{RBM} = 248/d_t$, where ω_{RBM} is the Raman shift (cm^{-1}) and d_t refers to the diameter of the nanotubes.

The other two major peaks are known as disordered band (D-band) and graphitic band (G-band). D-band in carbon nanotubes is related to the structural defects presence in the nanotubes and normally occurs at ~1350 cm^{-1}. Another important feature in a Raman spectrum is the G-band (~1590 cm^{-1}). This peak represents the vibration of carbon atoms along the tangential direction of the nanotubes. To quantitatively represent the crystallinity of the nanotubes, the intensity of the D-band (I_D) is normalized against that of the G-band (I_G). Thus, the preferred ratio of I_D/I_G would be as low as possible as it would indicate a low concentration of defects. In general, this value is greater in MWCNTs compared to SWCNTs as SWCNTs are mostly made up of structurally perfect nanotubes.

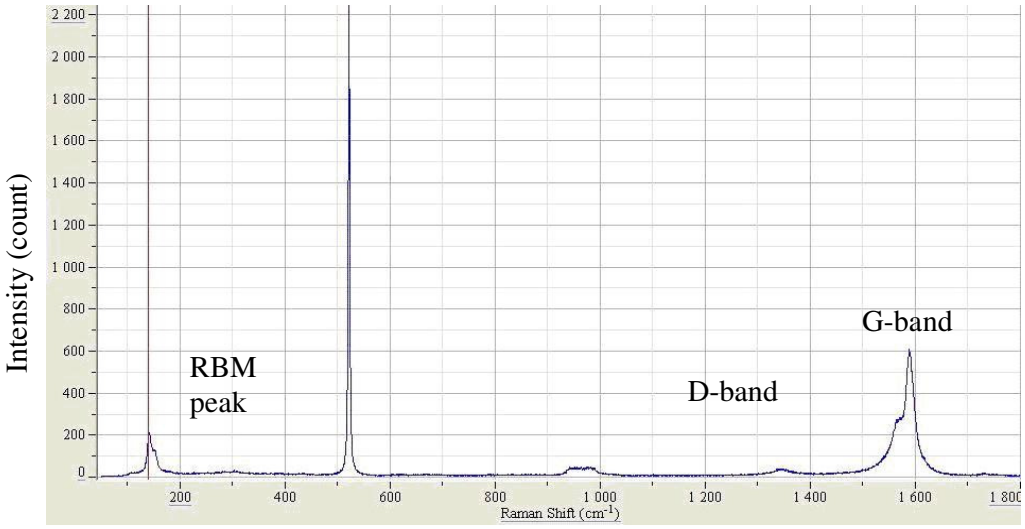

Figure 2.15 RBM peaks occur at 170 cm^{-1} and 185 cm^{-1} resulting in diameter of 1.46 nm and 1.34 nm, respectively.

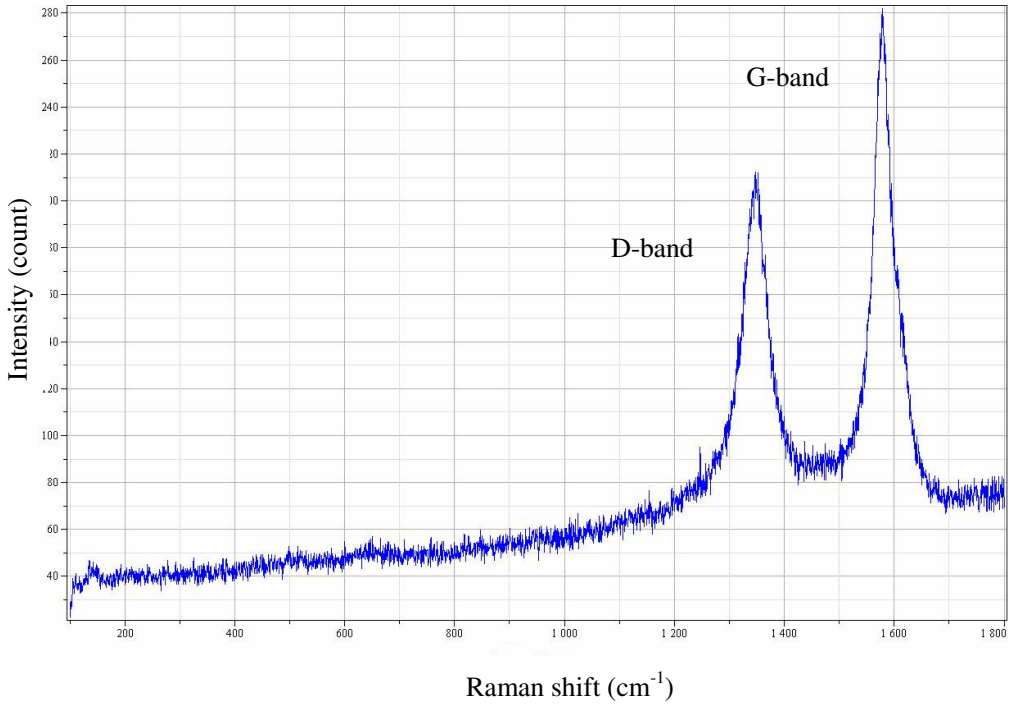

Figure 2.16 Example of Raman spectra for MWCNT. RBM is absent while intensity of D-band is prominent

2.10.2 Scanning Electron Microscopy (SEM)

In most experimental research, "seeing is believing". While Raman spectra provides qualitative analysis, the use of SEM or field emission SEM (FESEM), which provides a higher resolution, gives researchers visual image or morphology of the nanotubes (Figure 2.17). This is useful especially when looking for any anomalies within the sample like presence of impurities i.e. amorphous carbon, catalytic particles that could provide supporting proof to explain the Raman results. Beside the morphology study, energy dispersion X-ray (EDX) spectroscopy that comes with the SEM enables the element study of the samples i.e. chemical composition and distribution.

2.10.3 Transmission Electron Microscopy (TEM)

TEM differs from SEM as TEM offers image on the internal structure of CNTs while SEM only scanned the external structure (Figure 2.18). This tool can be used to

measure the internal and external diameter of selected nanotubes, the number of walls it consists as well as the defects on the walls. It can also be used to determine the type of growth, whether tip or base by looking at the location of the catalytic particles embedded.

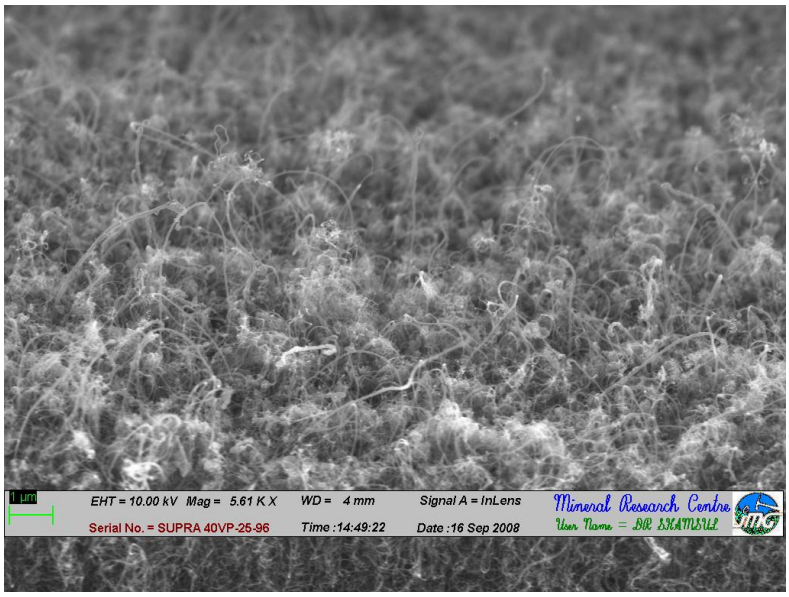

Figure 2.17 Example of SEM image on the surface of aligned CNTs

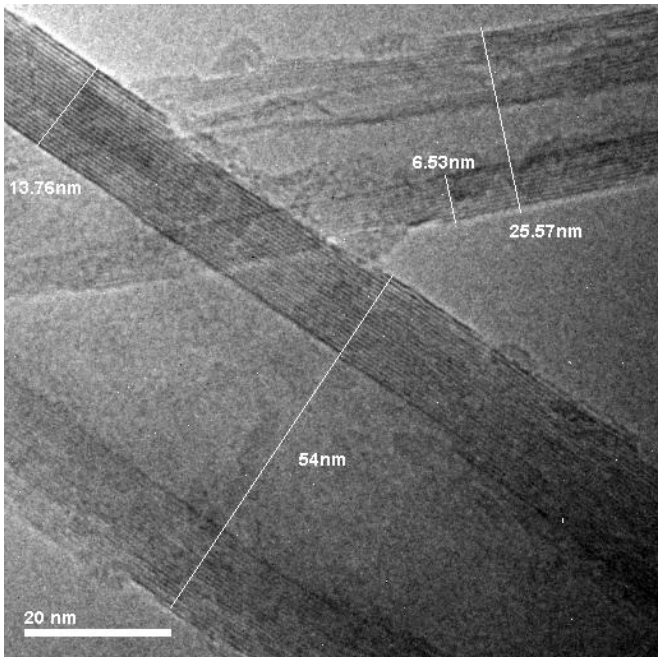

Figure 2.18 Example of TEM image of a CNT illustrating the outer diameter of a CNT and thickness of its wall. Also seen is the number of walls within a nanotube

2.10.4 Atomic Force Microscopy (AFM)

AFM is a scanning probe to study the topography of the sample, in the scale of nanometers. As the tip at the end of the cantilever in AFM scans the area of sample, interaction between the tip and the surface causes the tip to deflect. In the process, it provides information of the roughness of the area being studied.

2.11 Properties of Carbon Nanotubes

Carbon nanotubes possess an enormous potential for future applications (electronic, mechanical, chemical and biological) because of the unique properties and characteristics that they display, partly attributed to the quantum effect displayed due to their nanosize. Although it is still too early to incorporate CNTs into applications, studies have shown that CNTs could be the paradigm shift in materials technology since the materials currently used are being pushed to their limit.

2.11.1 Electronic Properties

Although researchers have long came up with the prediction on the theoretical values of SWCNTs based on the C_{60} model [96-99], their experimental values often turn out to be otherwise. Theoretically, since SWCNTs have structures similar to that of graphite, they are conductors. However, results from experimental works have shown that the electronic properties of the CNTs depend highly on their geometry structure i.e. diameter and chirality of the tubes [34, 96 , 100, 101]. Armchairs are metallic while chiral and zig-zag are semiconducting. This is made complicated by the fact that the synthesized CNTs usually consist of a mixed of semiconducting and metallic CNTs and with a wide range of tube diameters. Often, the CNTs are found in a bundle instead of individual tubes and this also alters their properties as a result of the tube-tube interaction, desribed graphically in Figure 2.19.

Electronic properties in both perfect SWCNTs and MWCNTs are similar. As CNTs have nearly one-dimensional electronic structure, the electronic transport

occurs ballistically (without scattering) over long lengths. This enables CNTs to carry high currents with negligible heat dissipation [102, 103] as there will be essentially zero intrinsic resistance. The current densities of CNTs can reach up to 10^9 A/cm^2 over extended periods of time at temperature up to 250^{o}C as compared to a maximum of ~10^5 A/cm^2 in metals [103-105], making them potential materials as interconnects for nanoelectronics devices.

2.11.2 Mechanical Properties

CNTs are the strongest known materials to date, as a result of the σ bonding between C atoms in the graphite structure. Treacy et. al. [106] was the first to study the strength of CNTs and estimated the average Young's modulus of MWCNTs to be 1800 GPa. However, there were flaws in the methodology used. Wong et. al. [107] later introduced atomic force microscopy (AFM) as a method to determine the mechanical properties of MWCNTs and found the average to be 1280 GPa while Yu et. al. [108, 109] reported the Young's modulus of SWCNTs between 320-1470 GPa and that of MWCNTs between 270-950 GPa. These values are confusing as they appear to be inconclusive about the Young's modulus of CNTs. There seem, however, a correlation between the strength and chirality of the nanotubes [110, 111]. But all these reports have the same conclusion; that CNTs are many times stronger than steel with an even greater strength-to-weight ratio, making them an ideal alternative for light weight structural applications.

On top of that, CNTs also undergo significant elastic deformation before failing. Most hard materials have a strain of 1% or less, but CNTs can sustain up to 15% of elastic strain before fracture, as tabulated in Table 2.1. This is another remarkable characteristic of CNTs as a result of the deformation modes originated from σ-π rehybridization, through which the high strain gets released.

Table 2.1 Mechanical Properties of Nanotubes [112]

	Young's modulus (GPa)	Tensile strength (GPa)	Density (g/cm^3)
MWCNT	1200	~150	2.6
SWCNT	1054	75	1.3
SWCNT bundle	563	~150	1.3
Graphite (in-plane)	350	2.5	2.6
Steel	208	0.4	7.8

2.11.3 Piezoresistive Properties

Early works, both experimental and theoretical [9, 112, 113], have demonstrated that inducing structural deformation of the nanotubes will lead to changes in the electrical conductance of CNTs. Tombler used an AFM tip [113] to bend a strand of SWCNT that was affixed to a metal electrode on both ends and suspended over a fabricated trench about 600 nm wide as illustrated in Figure 2.20.

When the tip is pushed down, it forced the nanotubes to deflect downward and resulted in a reduction in the conductance. The magnitude of reduction increased when it experienced a greater deflection (larger bending angle). When the tip is retracted, the nanotubes return to its initial state and a recovery in the electrical conductance is observed as well, indicating a reversible process. Liu [114] later related the change in the conductance to be due to transition change in the carbon bonding configuration, from sp2 to sp3. Table 2.2 shows the comparison of gauge factors amongst metal and semiconductors, including CNTs. Gauge factor (GF), K is attributed by geometrical change ($1 + 2\nu$) and/or electrical resistivity change of the material ($d\rho/\rho_0 d\varepsilon$) as derived from the equation [116]:

$$K = 1 + 2\nu + \frac{d\rho}{\rho_0 d\varepsilon} \tag{2.1}$$

where ν is Poisson's ratio of the films, ρ and ρ_0 are resistivities for strain ε and at original, respectively. In most materials, the geometrical change is relatively small (Table 2.2). This explains the low GF values in metals whereas the large gauge factor in semiconductor materials is governed by the changes in resistivity of the material.

Table 2.2 Gauge factors for typical materials [115]

Materials	Gauge Factors (GF)
Platinum	4.0
Aluminum	2.5
Copper	2.2
Gold	2.1
Small gap semiconducting CNT	600-1000
CNT (Semiconducting)	150
Silicon (p-doped)	126
CNT (metallic)	40-60

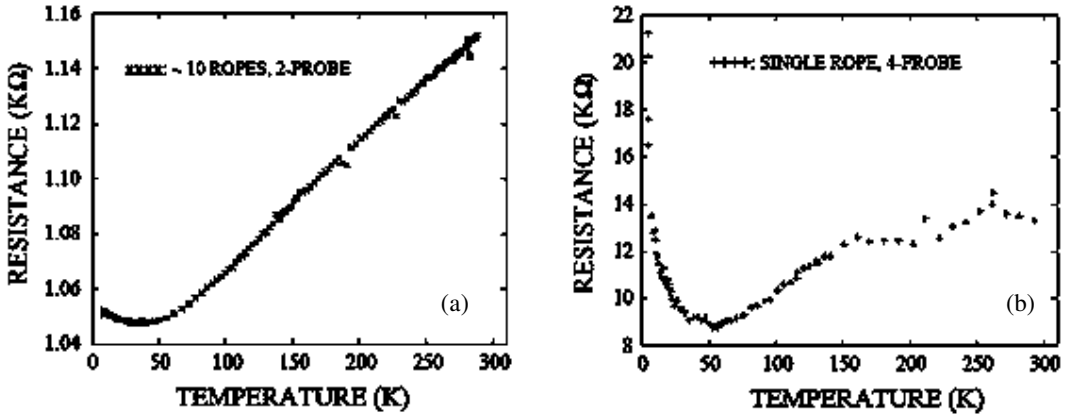

Figure 2.19 Measured resistivities of samples of carbon nanotubes. (a) 2-probe measurement on several ropes in parallel. (b) 4-terminal measurement of a single rope [12]

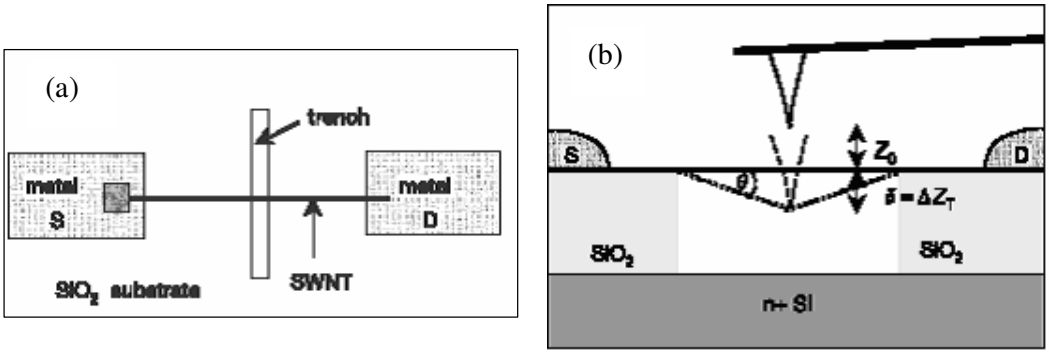

Figure 2.20 Schematic diagram showing (a) top view of the experimental setup and (b) side view on the movement (pushing and retracting) of the AFM tip [113]

2.12 Potential applications of Carbon Nanotubes

2.12.1 Nanoelectronics

In the effort of miniaturization of electronic components, the traditional materials currently used in the electronics industry are consistently being pushed to their limit. As a result of the scaling down of their sizes, the resistance of interconnects (mostly using Au or Cu) for example, becomes higher as a result of decreased in cross-sectional area as well as the need to carry a higher current density. This in turn requires better heat dissipation capability. In comparison, CNTs have higher current carrying capacity, better thermal conductivity and length independent resistance. Kreupl et. al. made a paper on the possibility of implementing CNTs to replace gold as interconnect applications [117].

One of the most common method of electron extraction, known as thermionic emission refers to the mechanism in which the solid is heated at high temperature to provide sufficient energy to the free electrons to free themselves from the surface potential barrier. This effect can be found in applications like CRT display, vacuum electronics, x-ray generation, etc. Although this is a simple method, it is not power efficient due to the high temperature required. Among the alternative means of electron generation is through field emission. Field emission involves extraction of electrons from a conducting solid by an extremely high electric field (several kV/μm), usually under ambient condition and can provide very high current densities (up to 10^7 A/cm^2 at the emitting site). A sharp tip however can significantly reduced the electric field required as a result of geometrical enhancement, with the electric field line concentrating around the tip area. Given the nature of the CNTs, the small diameter of its tips can achieve a high concentration of localized electric field. For example, Saito and Uemura [118] performed studies on the use of CNTs as field emitters for cathode-ray tube (CRT) type lighting-elements and vacuum-fluorescence display (VFD) panels. In both cases, the CNTs are found to have many advantages, amongst them are stable emission of electrons, provide adequate luminance and a long life.

2.12.2 Sensors

CNTs have huge potentials as sensors for a variety of applications such as electronics, mechanical, chemical and biological and mechanical probes due to their excellent properties. Their nanosize means CNTs have a very large surface-to-volume ratio, which translate into larger amount of detectors over a specific area thus increasing the sensitivity of the sensor towards the changes in the environment. These changes will cause a difference, usually, in the conductivity of the CNTs and becomes the fundamental in the application of CNTs as sensors. Their high tensile strength and chemical inertness suggest that CNTs can endure a harsh environment. And because they are carbon, they are environmentally friendly too. Amongst the problems faced in application of scanning probes are constant replacement of the probe tip as a result of fracture and the limitation in the probing capability. Instead of breaking, the CNT probe will only bend upon hitting a hard surface. Like a drinking straw, simply retracting the probe and projecting it out again to return to its original position can reverse this type of elastic deformation.

Conventional probes are mostly made of pyramidal-shaped Si at the end of the cantilever, with tip apex of curvature of about 10 nm. Due to its angled shape and low aspect ratio, such probes have problems detecting objects smaller than its tip diameter and shapes with deep and narrow features. These raise a major concern when facing with the ever decreasing in size of the electronic components and the complexity in the features. Replacing such tips with CNTs can help to overcome much of these problems.

2.12.3 Composites

CNTs are found to be very suitable for reinforcement applications. Additional of CNTs as fillers have been known to have improve the mechanical strength as well as electrical and thermal conductivity of composites materials. This offers a new dimension towards the development of new conducting polymers, structural polymer composites, conducting metal matrix composites and ceramics composites with superior strength. On top of that, the low density of CNTs means their weight,

especially polymer composites, will not be compromised while achieving a tremendous improvement in the conductivity and/or structural strength. In ascending order of conductivity level, these polymers can be made into electrostatic dissipative (ESD) materials (10^{12}-10^{5} Ω/square), electromagnetic interference (EMI) materials (10^{5}-10^{2} Ω/square) and highly conducting materials (less than 10^{2} Ω/square) [24]. High-conducting materials can also be used as multifunctional composites (mechanical/electrical) as replacements for metallic materials.

Earlier, carbon nanotubes functions as fillers within the composites. Now, they can be made into long, continuous fibers using the "direct spinning" method [119], which is more effective as reinforcement compared to the short ones. On top of that, functionalization of CNTs, refers to the additional of functional groups onto the CNTs structure, enable the nanotubes to react with other functional groups from chemical reagents to form strong matrix-fillers bonds.

2.12.4 Hydrogen Storage

The hollow core of the CNTs can be utilized for hydrogen storage through capillary effect. In spite of the safety concerns (mainly due to the lack of understanding on the storage mechanisms involved), extraordinarily high and reversible hydrogen adsorption in SWCNTs [120-123], lightweight properties and chemically inert CNTs are and no oxidation until almost 600^{o}C could be the reasons why they continue to attract vast interest for this application. Beside hydrogen, CNTs has been shown to be able to store liquid and gas in their core as well [124].

2.13 Carbon Nanotubes As Pressure Sensor

The sections reviews for a good sensor are high sensitivity, fast response time, low cost and high volume production. Being nanosize (20-50 nm in diameter and its nanometers length), CNT should be able to meet the first two requirements. These are achieved through the variation in the electrical resistance of CNT when pressure is applied.

Liu and Dai [125] demonstrated that CNT can be made into piezoresistive pressure sensor. When a uniform pressure is applied, it resulted in a change in the resistance of the CNT. Upon removal, it is restored to its original state thus demonstrating that the change is reversible. Bozhko *et al* [126] has investigated and found that the resistance change of bulk nanotubes decreases with the increase in pressure (up to 20 GPa), as depicted in Figure 2.21. This finding is interesting but not surprising considering the fact that CNT is known to have very high Young's modulus (even higher than steel). The same phenomenon was also observed when Tang *et al* [127] performed similar investigation using aligned multi-walled CNTs, Figure 2.22.

Dharap *et al* [128] showed that CNT has advantages over conventional sensors as they are discrete points, fixed directional and are not embedded at the material level. Randomly oriented CNT is isotropic in nature and this enables the measurement of strains on various locations at multiple directions. Also, miniaturized sensors can lead to reduced weight, lower power consumption and at a low cost.

Piezoresistive characterization of the CNTs can either be performed on a single strand of nanotube [112, 115, 129, 130], bundled nanotubes [126-128], on the CNTs film [131, 132] or CNTs reinforced composites [133-134]. It has been shown that the change in electrical resistance of nanotubes depends on the type of CNTs (metallic or semiconducting) [112].

While it is relatively easy to carry out electrical measurement on a single strand or bundle, the task for studying the piezoresistive characteristics of the aligned CNTs film includes configuring the film such that it is feasible for the electrical measurement to be carried out. Previous reports involve performing on the CNTs film/block that was removed from the Si wafer and coat with conductive thin film on both ends [135] or transferring the film onto a conductive substrate by using a conductive adhesive paste [136, 137]. The purpose is to allow electrical measurement to be carried out accurately since most of the substrates used for CNTs growth are dielectric. So far a number of models have been reported on carrying out the piezoresistive measurements of the CNTs.

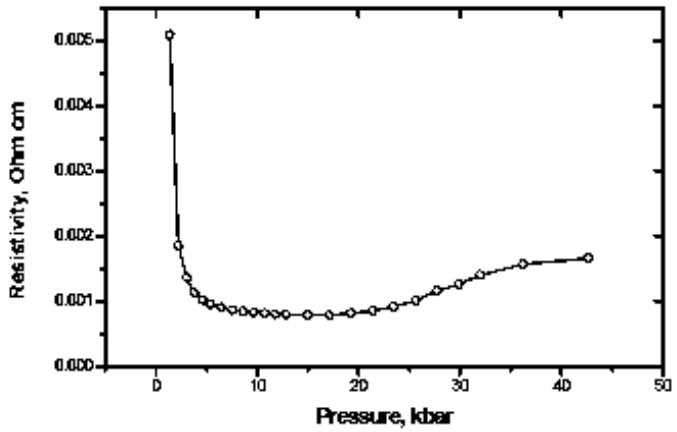

Figure 2.21 Directionally averaged 2-probe resistivity measured in the lenticular cell at 300 K [126]

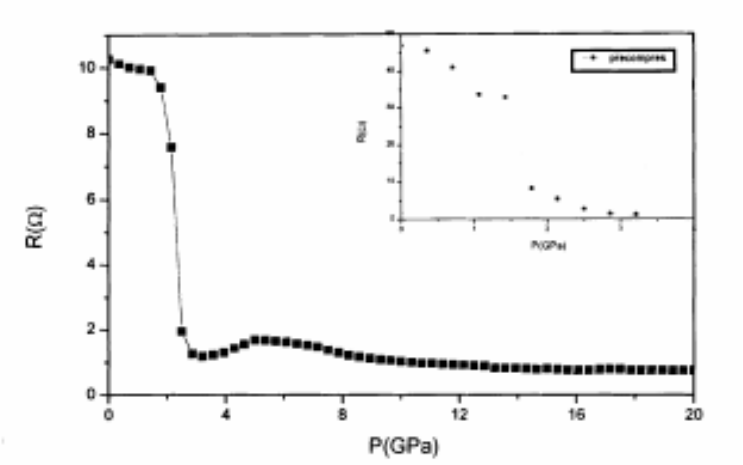

Figure 2.22 The dependence of resistance on pressure for multiwalled carbon nanotubes from the first compression and the inset from the precompression [127]

At room temperature, Pushparaj [135] induced stress on a block of CNTs at the parallel and perpendicular directions, relative to the tubes axis (Figure 2.23). In both cases, compression of the block also leads to increase in conductivity of the CNTs. At the parallel direction, it was found that the compressive stress caused the nanotubes to buckle, starting from the bottom end of the block (Figure 2.24). As the compressive stress increases, the block becomes denser as the number of buckles increases, until there is little room left for the nanotubes to buckle further thus leading to sudden increase in the compressive stress versus compressive curve. When the stress is

imposed perpendicular to the axis, increment in the compressive strain is gradual even at high compressive stress level. At this mode of compression, the gap between the nanotubes started to reduce resulting in a more compact block. However, in both modes, the process is reversible, mechanically and electrically.

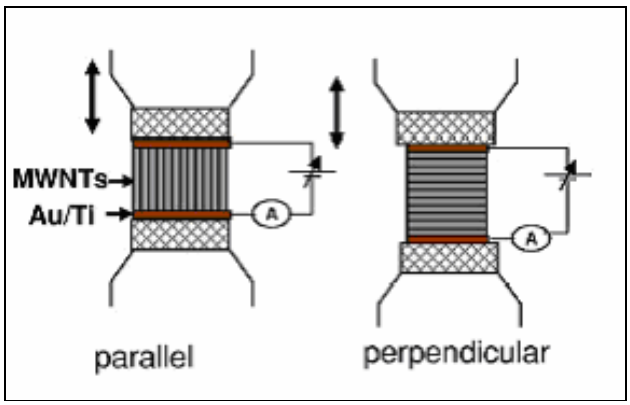

Figure 2.23 Schematic diagram of the electrical conductivities and compressive strain response measurements carried out on CNTs block either perpendicular or parallel to the CNTs tube axis [135]

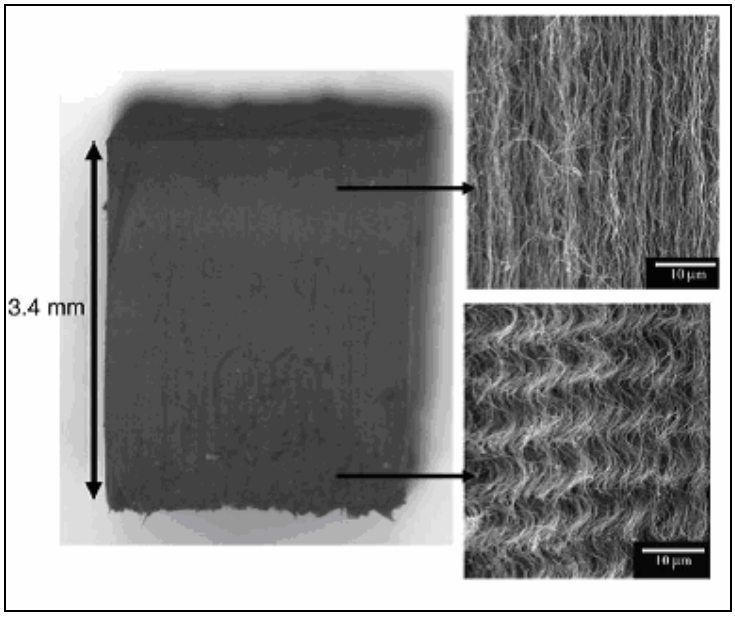

Figure 2.24 Optical image of CNT block. The CNT block is subjected to mechanical compressive strain (25%), which results in the buckling (SEM image, bottom) at the lower portion while the remaining portion of the CNT is straight (SEM image, top) [135]

In another work, Cao et al [138] studied the piezoresistive properties of strained bulk CNTs using a three-point bend test (Figure 2.25). However, the result may differ from compressing aligned CNTs since bulk CNTs does not have a common growth direction. In aligned CNTs, each of the nanotubes connects one end of the terminal to the other, thus electrical conduction occurs as a result of electrons traveling along the walls of the nanotubes. For bulk CNTs, the structure consists of individual strands of CNTs that are compressed to form a conductive thin film. Although electrical conduction still occurs from one end to another, but microscopically, the electrons are traveling along and/or transverse to the walls of the CNTs. As pointed out by Cao, electrical conductivity transverse the walls is lower compared to along the wall and may have compromise in the sensitivity of the sensor. Also, the temperature studied (up to 50^{o}C) is too low for most real life application. CNTs are also known to exhibit variation in electrical resistance at high temperature. The resistance of SWCNTs increases with temperature [12] while in MWCNTs, the resistance decreases with temperature [139, 140].

Based on the above review, it is felt that the work done so far is not suffice to reflect the whole picture about the suitability of CNTs for pressure sensing. Pusharaj et al studied the pristine CNTs block but only at room temperature while Cao used bulk CNTs to measure their piezoresistivity properties. Thus, this work is designed to study CNTs in their pristine structure and measure their respond towards applied pressure at elevated temperature beyond 120^{o}C (the threshold for most Si-based pressure sensors) in order to test their thermal stability.

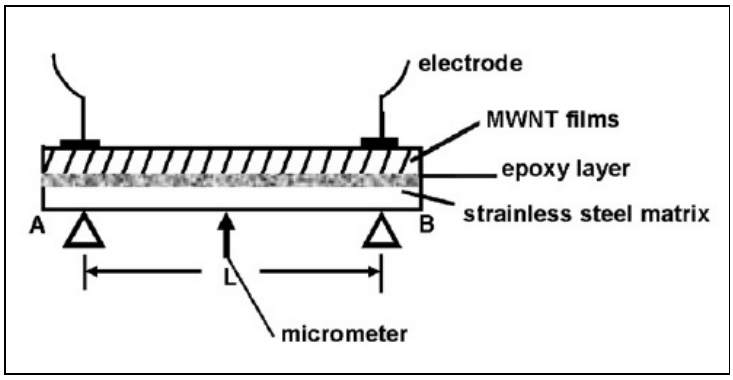

Figure 2.25 Schematic diagram of experiment setup for piezoresistance measurement [138]

CHAPTER 3

EXPERIMENTAL PROCEDURE

3.1 Introduction

Synthesis of CNTs is the biggest challenge of producing nanostructured materials. This is due to the fact that the characteristics such as type and chirality of CNTs largely depend on the growth parameters, which in turn will determine their electrical and mechanical properties. Since the early 1990s until now, this aspect or research work has contributed to a significant volume of published papers in the subject of CNTs, making it a research is on its own. To produce CNTs will require careful and systematic approach of experimental work which is laid out in this chapter.

3.2 Methodology for Growing Aligned Carbon Nanotubes (CNTs)

The growth of carbon nanotubes depends critically on the preparation of the substrate hence a great amount of work was focused on it. Figure 3.1 illustrates the process flow chart, starting from the as-received wafer to the growing of CNTs, as well as the substrate configuration at the end of each stage. Also listed are some of the equipments used to carry out the respective process. The methodology employed for the synthesis of carbon nanotubes (CNTs) growth in this study involves the following:

1. Cleaning of silicon wafer
2. Formation of silicon oxide
3. Preparation of buffer layer
4. Preparation of catalyst layer
5. Growth of carbon nanotubes

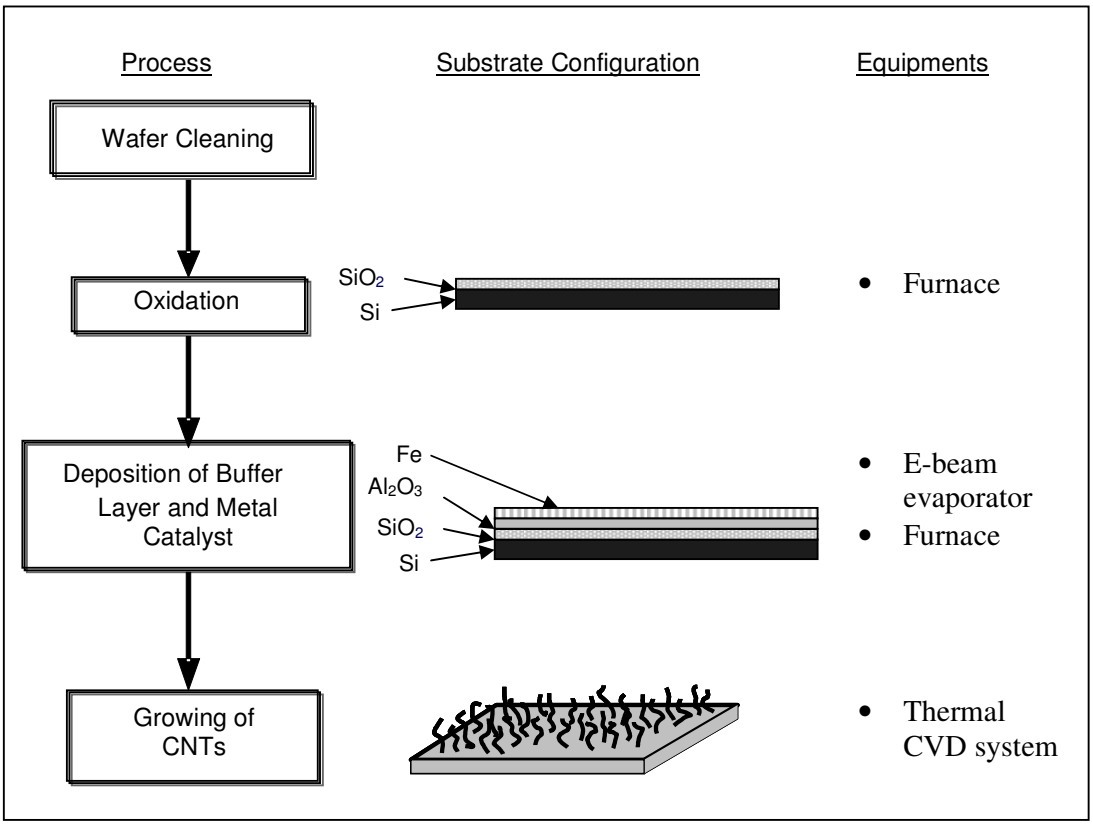

Figure 3.1 Methodology of producing CNTs film

1. Cleaning of silicon wafer

As-received wafer contains a thin layer of silicon oxide known as native oxide. This thin layer of oxide is formed as Si reacts readily with oxygen in air and is not favorable for CNTs growth [141] since it is not capable of providing sufficient support for CNTs growth and worse still, can form metal silicides with any metallic element deposited on top. The wafers are cleaned using the RCA method. RCA, named after the company where the method was developed, is commonly used for wafer cleaning. It is a two-step procedure with an additional etching process using HF as etchant.

First step involves the use of SC1 solution which consists of distilled $H_2O/NH_4OH/H_2O_2$ at a ratio of 5:1:1 and is used for removal of organic contaminants. The temperature of the solution should be maintained around 70^{o}C. In order to

achieve that, deionized water is heated up to about 90°C before NH_4OH and H_2O_2 (both at room temperature) are added into it. Wafers, cut into squares of 2 cm are soaked in the solution for 10-15 minutes and are rinsed thoroughly.

In the additional process, HF is used for removal of the native oxide layer. The concentration of HF used is 4%. Wafers are soaked in the diluted HF solution for 2 minutes and then rinsed thoroughly before the final cleaning procedure.

In the final step, the wafers are cleaned with SC2 solution, made of distilled $H_2O/HCl/H_2O_2$ at a ratio of 6:1:1. SC2 solution helps to remove metallic contaminants. They are rinsed several times with water and finally dried.

2. Formation of silicon oxide

A fresh layer of SiO_2 is grown from the cleaned wafer using the Deal-Grove model [142], shown in Figure 3.2. A sufficiently thick layer of SiO_2 (300-500 nm) can provide necessary support for the growth of aligned carbon nanotubes. It also acts as a barrier against the formation of silicides with the catalyst used for CNTs growth. Formation of SiO_2 can be done using either dry oxidation or wet oxidation method using the furnace.

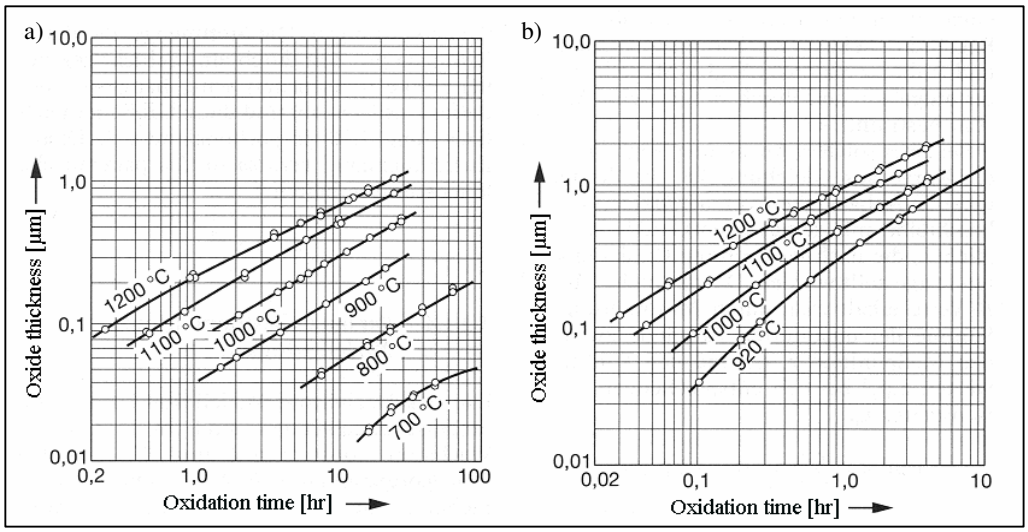

Figure 3.2 Deal-Grove model for determination of silicon oxide thickness using a) dry oxidation and b) wet oxidation [142]

Dry oxidation refers to where oxygen (as oxidant) is supplied during the oxidation process. For wet oxidation, the oxidant is steam. In both cases, oxidation occurs at the Si-SiO_2 interface and Si is consumed in the process. As a result, newly formed SiO_2 will always be on top of the Si layer, beneath the existing SiO_2. This explains the importance of having a clean, contamination-free top surface of the wafer.

For the purpose of this study, the thickness of the SiO_2 layer is around 300 nm and the method employed is dry oxidation. The temperature used is 1100^{o}C and the duration is 4 hours. The thickness of the SiO_2 layer obtained is then cross-examined with a color chart that can be used to estimate the thickness (Appendix A) [143]. The reason being, the color of the SiO_2 layer varies with thickness. Based on the color chart, the thickness of the SiO_2 obtained is found to be consistent with the Deal-Grove model. Although color chart comparisons are subjective and are therefore not the most accurate method for determining the oxide thickness, but it is the simplest way for rough estimation.

3. Preparation of buffer layer

A buffer layer beneath the catalyst is sometimes deposited mainly to act as a barrier between the silicon substrate to avoid the formation of FeSi which is unfavorable for the growth of CNTs [72]. The formation of silicides was found to cause a decrease in the catalytic efficiency as there will be less active Fe particles left. Al_2O_3 buffer layer is chosen as it also helps to enhance the growth of the CNTs [144]. This is achieved by oxidation of the Al thin film (deposited using electron beam evaporator) on the wafer at 600^{o}C for 2 hours. The source of Al used is Al pellet (99.99%).

4. Preparation of catalyst layer

The catalyst used in this study is Fe. Justification on the selection of Fe as catalyst has been discussed in Chapter 2. The source is Fe pellet (99.95%) while deposition is via electron beam deposition. As-deposited Fe is then annealed in air at 400^{o}C for 2 hours. Annealing process is important as it allows a strong bonding between the catalyst and substrate and avoids sintering of catalyst at elevated temperature during the CNTs growth [141] that can lead to the increase in particle size.

This is followed by dry etching using NH_3 as the etching agent [144]. Etching is considered to be essential since small-sized catalytic particles are preferred as it provides a more favorable condition for the growth of carbon nanotubes i.e. CNTs having smaller diameters [145] and is performed at 850^{o}C for 10 minutes at a flow rate of 10 sccm (standard cubic centimeter).

5. Growth of carbon nanotubes

The growth conditions also have a big influence over the carbon nanotubes obtained. Flow rate, types of carrier gases, growth duration, etc can largely affect the outcome of the carbon nanotubes in terms of length, tube diameters, overall structures and the likes. The growth of CNTs, schematically presented in Figure 3.3, is performed using thermal chemical vapor deposition (CVD) with ethylene as the feedstock gas. The settings for the growth of CNTs shown in Table 3.1 are in accordance to the standard recipe developed for EasyTube^{TM} 2000 CVD system.

Table 3.1 Sequence in thermal chemical vapor deposition (CVD) for CNTs growth

Sequence	Process
1	Purge Ar (1000 sccm) and heat to 700°C
2	Purge H_2 (500 sccm) at 700°C and heat for 4 min
3	MWNT growth – 10 min ethylene (700 scm) and H_2 (700 sccm)
4	Purge H_2 (500 sccm), cool to 300°C
5	Purge Ar (1000 sccm), cool to room temperature

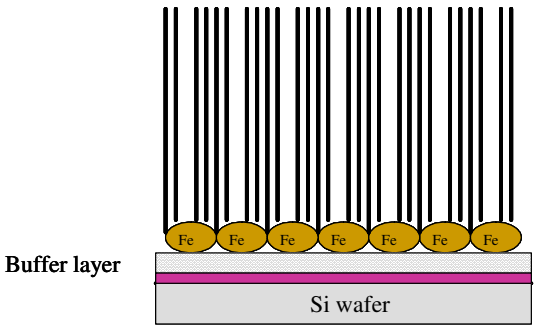

Figure 3.3 Schematic diagram on the growth of carbon nanotubes on substrate

Sequence 1 and 2 are to condition the environment inside the furnace. Sequence 1 is to create an inert environment by flushing out the oxygen while Sequence 2 is to anneal the substrate for better CNT growth. The growth of the CNTs takes place in Sequence 3. Feedstock gas is ethylene while H_2 is required to remove amorphous carbon from CNTs. Sequence 4 and 5 are for cooling down the furnace in an inert environment.

3.3 Parametric Study of Carbon Nanotubes

The area of study on the growth of CNTs includes optimization of buffer layer preparation, selection of catalyst precursor and stacking orientation for sandwich growth.

3.3.1 Optimization of buffer layer preparation

Studies have shown that the addition of alumina can assist in improving the density and subsequently the alignment of the CNTs film. The manners in which the alumina layer can be incorporated include direct deposition of aluminum oxide, oxidation of as-deposited aluminum and anodized aluminum oxide (AAO). In this work, the aspect of study is on the buffer layer preparation to understand which method would provide the best outcome (Table 3.2). The source is the pellet form of aluminum (99.99% pure, Kurt J. Lesker) or aluminum oxide (99.99% pure, single crystal sapphire, Kurt J. Lesker).

3.3.2 Selection of catalyst precursor

Very few works have been reported on the effectiveness of using metal in powder form as the source of catalyst for e-beam process. Bimetallic catalyst are found to be able to produce CNTs of better quality compare to monometallic and it is easier to produce them using the powder metallurgy method. Here, the objective is to make

comparison between the CNTs film obtained using Fe pellets and Fe powder as source.

Table 3.2: Different methods for preparing Al_2O_3 buffer layer

Sample	Method of Preparation
A1	Deposition of Al_2O_3
A2	Deposition of Al, oxidized in air at 5°C/min until 600°C and soak for 2 hours
A3	Deposition of Al, pre-heat in Ar. Soak for 2 hours in oxygen environment at 600°C
A4	Deposition of Al, followed by Fe. Soak for 2 hours in oxygen environment at 600°C
A5	Deposition of Al in partial oxygen environment

3.3.3 Stacking orientation for sandwich growth

Earlier procedures discussed about the CNTs growth using the conventional method, a single substrate with SiO_2, Al_2O_3 and metal catalyst as depicted in Figure 3.3. For the pressure sensing applications, this setup is not suitable and will be explained in Section 4.5. A more appropriate approach will be using a two-terminal device that was first reported by Chen [146]

Initial substrate preparation, from the cleaning of as-received Si wafer until the creation of Al_2O_3 buffer layer are the same as the abovementioned. For the interest of this study, we used Fe pellet as our catalytic source. The detail on the selection of Fe pellets will be reported in the Chapter Four (Results and Discussions).

The two substrates are stacked such that the polished surfaces of the wafers are in contact with each other, in three different configurations described below (refer to Figure 3.4):

a) Sample S1: sandwich type with catalyst coated top substrate
b) Sample S2: sandwich type with catalyst coated bottom substrate
c) Sample S3: sandwich type with catalyst coated top and bottom substrate

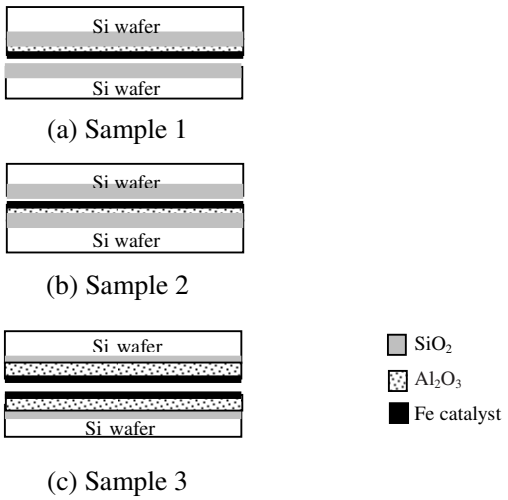

Figure 3.4 Schematic diagram shows the variation in the sandwich stacking configuration of the sandwich stacking

In order to monitor and compare the growth of CNTs against those obtained via the conventional, single substrate method tagged as "Conventional". By doing so, we can conduct a direct comparison between these two methods. Any difference between the CNTs film produced by the two methods can then be attributed to the stacking configuration.

3.4 Integration of Carbon Nanotubes

Before the CNTs film can be utilized for pressure sensing application, it is necessary to integrate them into a measurement unit so that the required investigations can be carried out to evaluate their performance. For that, a pressure chamber is constructed to measure the change in electrical resistance with respect to applied pressure (Figure 3.5). This chamber is consists of three components; top lid, bottom lid and body that is fastened together using bolts and nuts. Electrical connections are then made onto the sample to measure the response of the CNTs film towards applied pressure.

Figure 3.6 provides an overview of the setup for electromechanical analysis of the CNT film. The objective of the experimental work is to measure the changes in the electrical resistance of the CNTs as a result of variation in the pressure and

temperature. In order to determine the resistance of the film, a voltage source is used to provide constant voltage supplier while the current flowing through the CNTs film is measured.

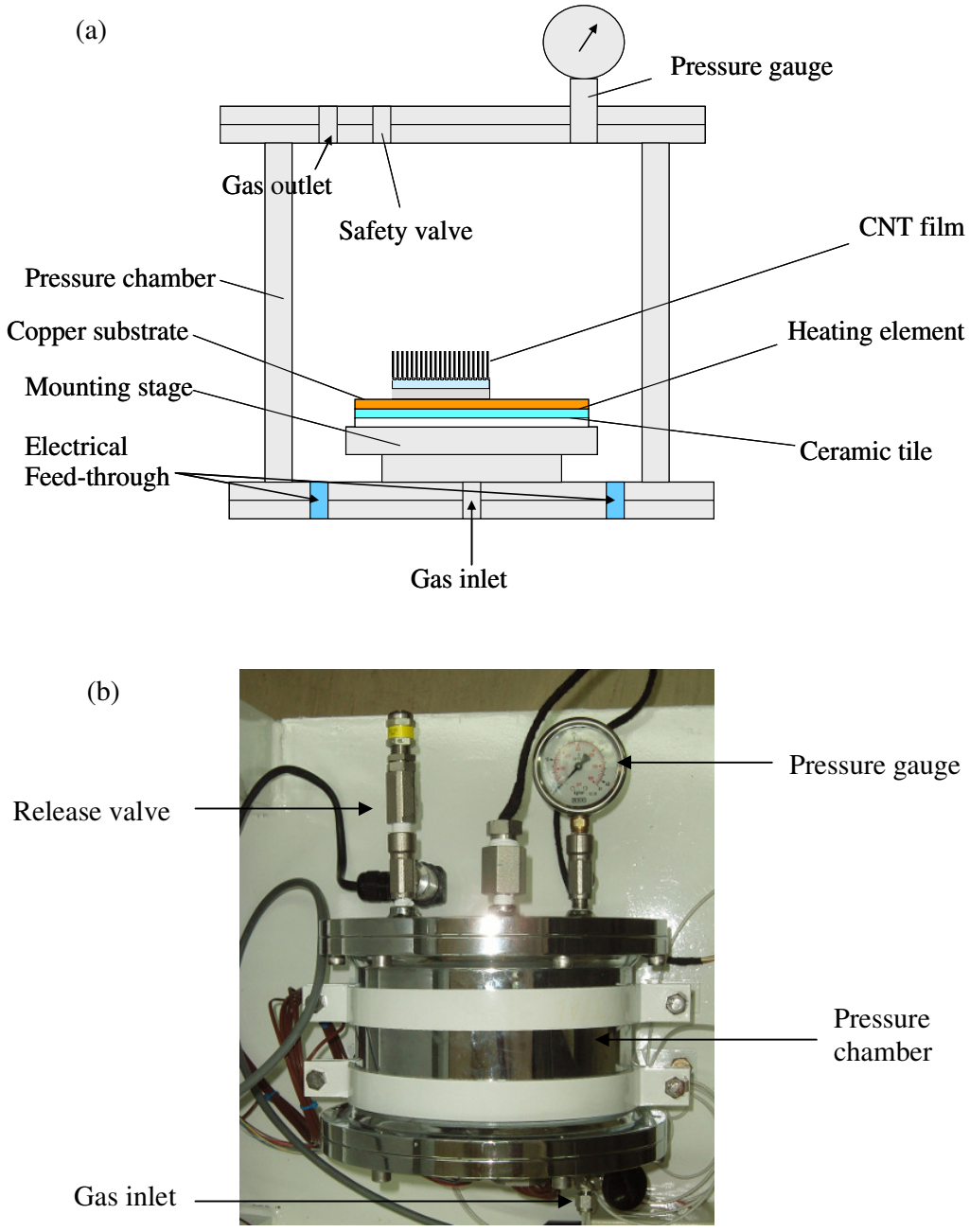

Figure 3.5 (a) Schematic diagram of pressure chamber together with fittings and (b) photograph image of the pressure chamber

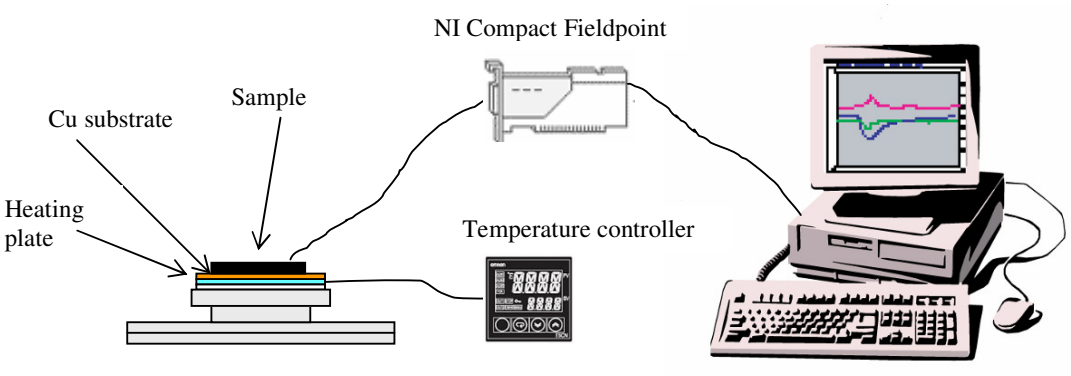

Figure 3.6 Schematic diagram on the setup for electrical measurement

Inert gas i.e. nitrogen gas will be purged into the chamber, at the designated pressure, from the nitrogen gas tank. Once the pressure inside the chamber is equivalent to the required pressure level, gas flow will stop. For better control of the pressure inside the chamber, there will be a bleed valve at the gas outlet flow. Inside the chamber, there is a stage welded to the bottom lid where the sample is mounted and secured in order to carry out the measurement.

When heating of the sample is required, the temperature controller regulates the temperature of the heating plate via a close loop PID (Proportional-Integral-Derivative) to ensure temperature of the sample is close to the setpoint temperature (Figure 3.7). This ensures temperature of the heating plate is close to the setpoint temperature and is much better compared to the on/off profile. Details on the working mechanism are available in Section 3.7.

Initial efforts are focused on measuring the change in the resistance of the grown CNTs inside a custom-made pressure chamber. As the substrate (Si wafer) is non-conductive, measurement cannot be performed across the length of the as-grown CNTs, similar to Figure 2.23. Additional steps are required to convert the films into a measurement unit either. Several methods have been identified and their feasibility tested including transferring the CNTs film onto a conductive substrate (Cu), as illustrated in Figure 3.8 and on a setup shown in Figure 3.9.

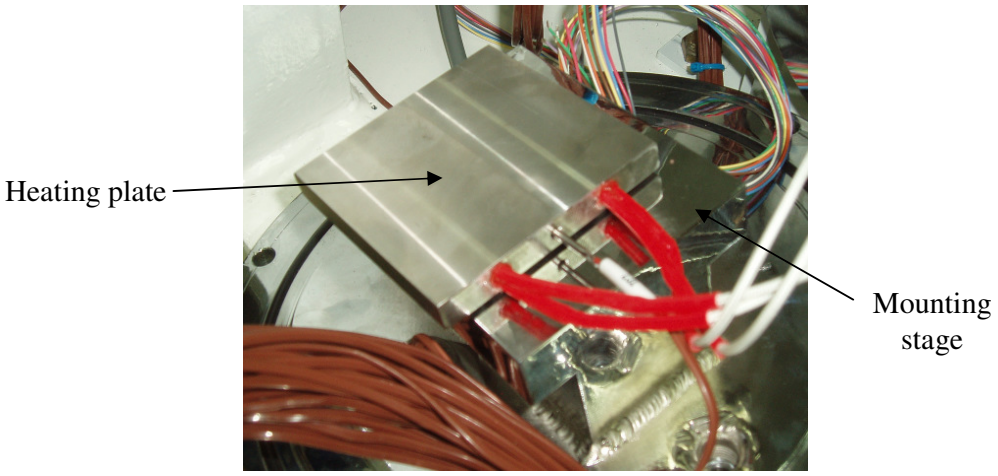

Figure 3.7 Photograph image of mounting stage with heater plate inside the chamber

As MWCNTs are synthesized at temperature around 700^{o}C, the substrate used is normally Si wafer, glass or quartz, etc which are mostly non-conductive. Recent reports suggest transferring synthesized CNTs film from these substrates to a copper substrate [132,136] for electrical resistance measurement (Figure 3.8). Top electrode is a layer of deposited Cu (using e-beam) while the metal adhesion layer used is solder paste. The main reason for their selection is due to their better electrical conductance and also ability to withstand high operating temperature. This setup is then connected to a power source and the current output is measured. For better accuracy, the voltage across the CNTs film was measured as well. However, there are some setbacks with the model. The thickness of the CNTs film in these reports is about 80 μm, probably for the ease of transfer but could be too thick for some application (i.e. interconnects) while the transfer process itself is another challenge. It has to be performed carefully to ensure all the CNTs are transferred without causing damage to the nanotubes. For this, the adhesive layer will need have a good compatibility with the substrate and the CNTs. In addition, it may also need to be able to withstand any extreme condition (e.g. elevated temperature, corrosive environment, etc) that the CNTs film is subjected to. For these reasons, another model is proposed (Figure 3.9).

A CNTs film is grown at each end of a Si wafer using the growth method that has been established as part of the objectives for this research. This is achieved by only depositing catalyst on the required area. This way the CNTs structures are not disturbed. Connection points are made on the Al plates using silver-loaded epoxy (by RS). The plates are then placed on each of the CNTs film. Current is able to flow between the two CNTs film as it is believed only the surface of the deposited Al is oxidized while the underneath layer remained as Al.

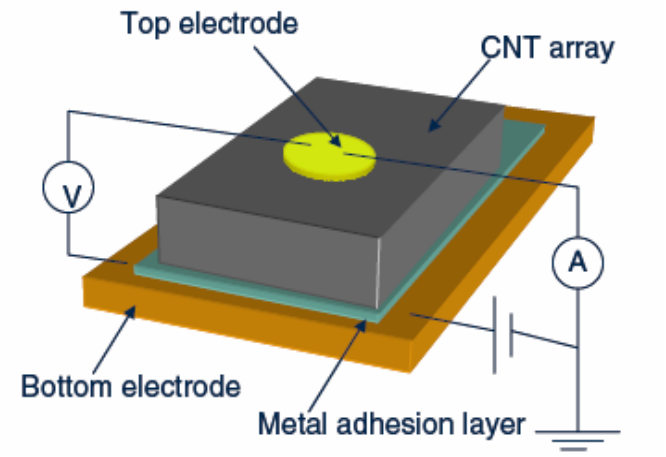

Figure 3.8 Schematic diagram of the four-point probe measurement [132]

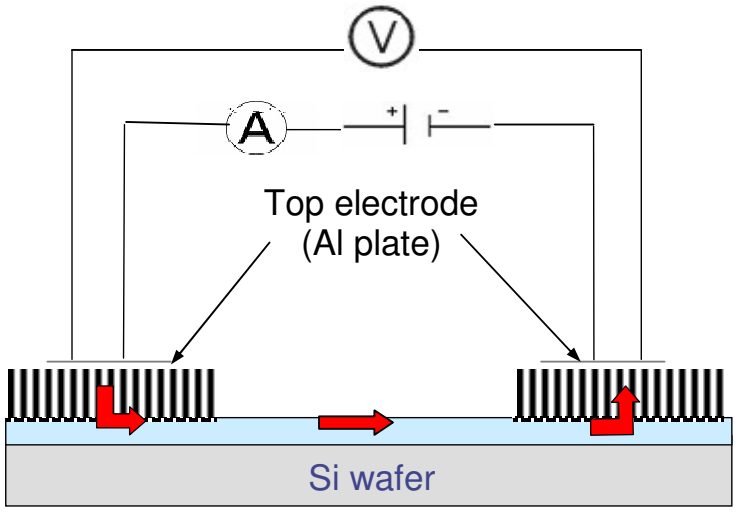

Figure 3.9 Piezoresistive measurement of CNTs film

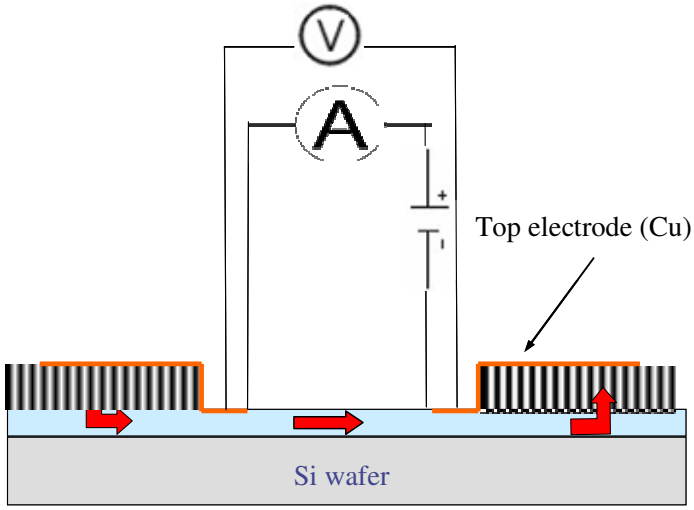

Figure 3.10 Improvised version of measurement setup

An alternative would be to replace the Al plate with a thin film of Cu (deposited using e-beam) as shown in Figure 3.10. As making direct connections onto the CNTs film will damage it due to its delicate nanostructure, connections points are made on the substrate that was coated with Cu thin film as well. Outcome for the electrical measurement for these models will be discussed in Section 4.5.

3.5 Electromechanical Measurement

After performing tests with the method proposed in Section 3.4, some shortcomings were discovered. Further modifications are required and finally come up with a measurement unit. This measurement unit (Figure 3.11) almost resembles the sandwich stacking configuration.

While the actual sandwich configuration (refer to Figure 3.4) is achieved by growing array CNTs sandwiched between two substrates, here the CNTs film were synthesized via the conventional method on two separate substrates that were later stacked together to form a double layer CNTs film. On top of that, meticulous effort was made to ensure that the oxidized Al buffer layer is electrically conductive and at the same time, promote CNTs growth. Finally, the buffer layer is partially masked before metal catalyst was deposited so that only a certain area would contain CNTs

while the remnant area is for making electrical connectivity. On top of that, two thermocouples are used to record the surface temperature of the Cu substrate to ensure that there is minimal temperature gradient across the area. Locations of these thermocouples are shown in Figure 3.12. All these information i.e. voltage, current, temperature are then recorded by the NI Compact Fieldpoint and displayed at the computer.

Weights were applied at the top of the measurement unit to generate pressure on the CNTs film and are gradually increased, from 0 to 500 g, to replicate the increase in the applied pressure. Since pressure is defined as force per unit area (where the area of the CNTs is 1 cm^2), this converts to about 0 to 50 kPa of pressure.

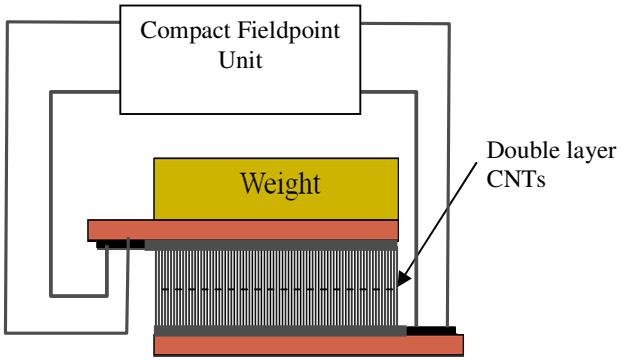

Figure 3.11 Schematic diagram of the measurement unit

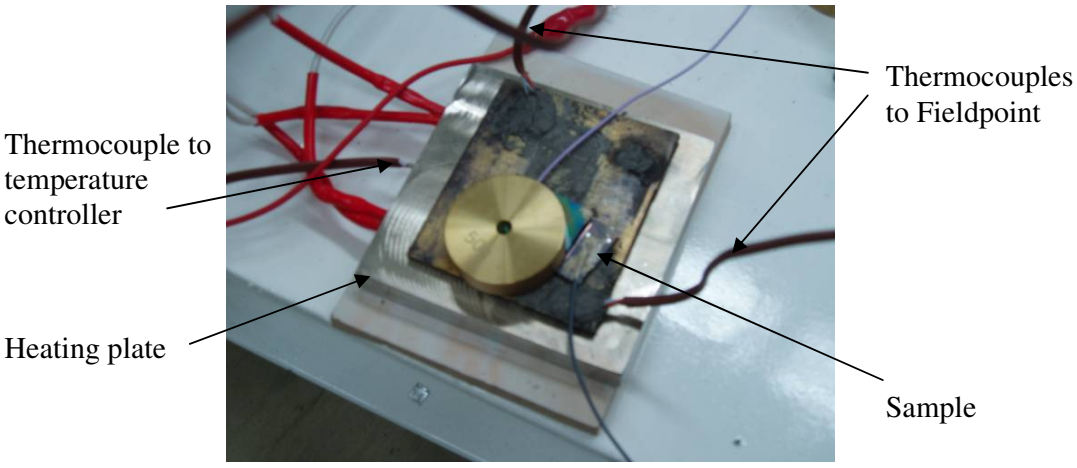

Figure 3.12 Photograph image on the location of the thermocouples

3.6 Equipments for Growth

3.6.1 Electron-beam (E-beam) evaporator

The e-beam (Figure 3.13) is used for deposition of thin film. It operates at room temperature and employs a stream of electrons to bombard the target material (material to be evaporated) at high energy, causing the target materials (held inside a graphite crucible) to melt and later vaporize and deposit onto the substrate located above. An electric or magnetic field is applied to focus and deflect the beam onto the target material. In order for the deposition to be effective, the chamber must be in vacuum environment (in the order of 10^{-6} Torr) so that the molecules can float freely and not be obstructed by the air molecules. The vacuum environment also enables the materials to evaporate at a lower temperature. Among the advantages of using e-beam are high film deposition rates, less substrate surface damage from impinging atoms as the film is being formed unlike sputtering that induces more damage because it involves high-energy particles, excellent purity of the film because of the high vacuum condition used by evaporation and less tendency for unintentional substrate heating. [147,148].

3.6.2 Thermal CVD System

The carbon nanotubes are grown using thermal chemical vapor deposition (CVD) method, procured from First Nano, see Figure 3.14. The types of CVD are classified according to the method use to apply the energy necessary to activate the CVD reaction i.e. temperature, photon or plasma [149]. Inside, it is similar to a furnace. Temperature is raised to the required level before the gases (refer to Table 3.1) are introduced for the reaction to take place. EasyTube™ 2000 is fully automated with accurate control of gases flow rate, growth temperature and faster cooling rate. It can also be programmed to clean off the carbon residue on the wall of the quartz tube.

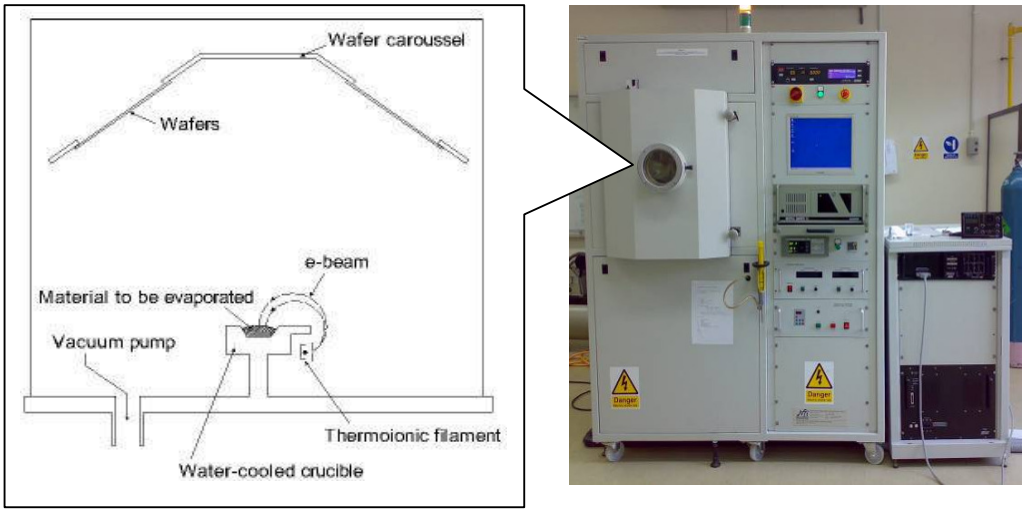

Figure 3.13 Schematic diagram [148] of the internal part of electron beam evaporator

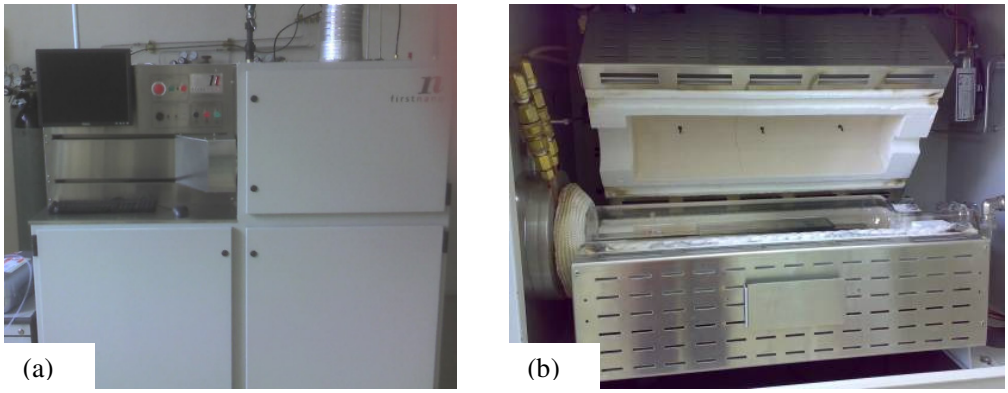

(a) (b)

Fig 3.14 Photograph image of (a) Thermal CVD EasyTube^{TM} 2000 (b) Clamshell furnace within

3.7 Equipments for Structural Characterizations

3.7.1 Raman Spectroscopy HORIBA HR800 (Jobin Yvon)

Raman spectroscopy (in Figure 3.15) is an important analysis tool for characterization of CNTs based on light scattering. Measurement is performed at ambient environment without destroying the sample and no sample preparation is required.

Figure 3.15 Photograph image of Raman Spectroscopy Horiba HR800

It operates on the principles of inelastic photon scattering (Raman effect). Inelastic scattering of photons refers to the phenomenon whereby the photons are scattered at a lower optical frequencies than the incident photons, often occurs in 10^{-14} seconds or less. The energy difference is known as Raman shift. When plot over a range of scattered light intensity, a graph known as Raman spectrum is obtained. This graph is useful and can provide information like type of CNTs, chirality, diameter of nanotubes and cyrstallinity.

3.7.2 Field Emission Scanning Electron Microscopy (FESEM)

A scanning electron microscopy (SEM) is used to observe the surface morphology of a specimen. A focused electron beam is raster over the surface of the specimen at specific rate. These electrons are then scattered depending on the collision path with the atoms. Primary electrons signals are collected by the detector to provide topographic information while the backscattered and secondary electrons are useful to provide compositional information of the specimen. A field emission scanning electron microscopy (FESEM), see Figure 3.16, is basically an improvement of SEM.

Figure 3.16 Photograph image of FESEM Supra 55VP

The inclusion of a field emission allows better resolutions at higher magnification up to order of 5-10 nm at 1 kV [150]. For carbon nanotubes, sample preparation is minimal. It is only requires a conductive carbon tape to connect CNTs to the base of the sample holder to minimize the electrons build-up that could lead to charging as the substrate (Si wafer) is dielectric.

3.7.3 High resolution Transmission Electron Microscopy (HRTEM)

For transmission electron microscopy (TEM), the specimens need to be almost transparent-like so that light could penetrate it. For this reason, sample preparations for TEM can be very tedious depending on the specimen. Before subjecting the CNTs for analysis, they need to be carefully removed from the substrate so that it will not damage their structures. Then, they are dissolved in isopropanol and are dispersed by sonicating in an ultrasonic bath for 15 minutes. 1-2 drops of the solution is placed over the copper matrix and left to dry overnight in air. This imaging technique can be

used to observe the internal structures of the CNTs like number of walls, determining external and internal diameters of individual nanotubes and type of growth based on the location of catalytic particle found, as described in Chapter 2. Compositional analysis can also be performed. An example of a TEM is shown in Figure 3.17.

3.8 Equipments for Electrical Characterization

3.8.1 National Instruments Compact Fieldpoint

The National Instruments (NI) Compact Fieldpoint (Figure 3.18) is a programmable Logic Controller (PLC) that meets industrial requirements for control and measurements applications. This instrument acquires raw information of the measurands (i.e. voltage, current, temperature, pressure), digitized and displays them in a PC (via Ethernet) using NI LabView software.

3.8.2 Heating plate with PID temperature controller

A heating plate, powered by a temperature controller with PID control, is used to heat up the sample when required. PID (Proportional-Integral-Derivative) allows a better control of the desired temperature as the combination of these three functional controls mitigates the fluctuation in the temperature. This action avoids large deviation especially at the set point temperature, which needs to be kept constant over long period of time, to reduce unwanted noise in the output data. Real-time monitoring of the temperature of the heating plate is by the thermocouple that connects the heating plate and the temperature controller. An example comparing the setpoint temperature using on/off control and PID control is shown in Figure 3.19 [152].

Figure 3.17 Photograph image of Philips Technai F20

Figure 3.18 National Instruments (NI) Compact Fieldpoint [151]

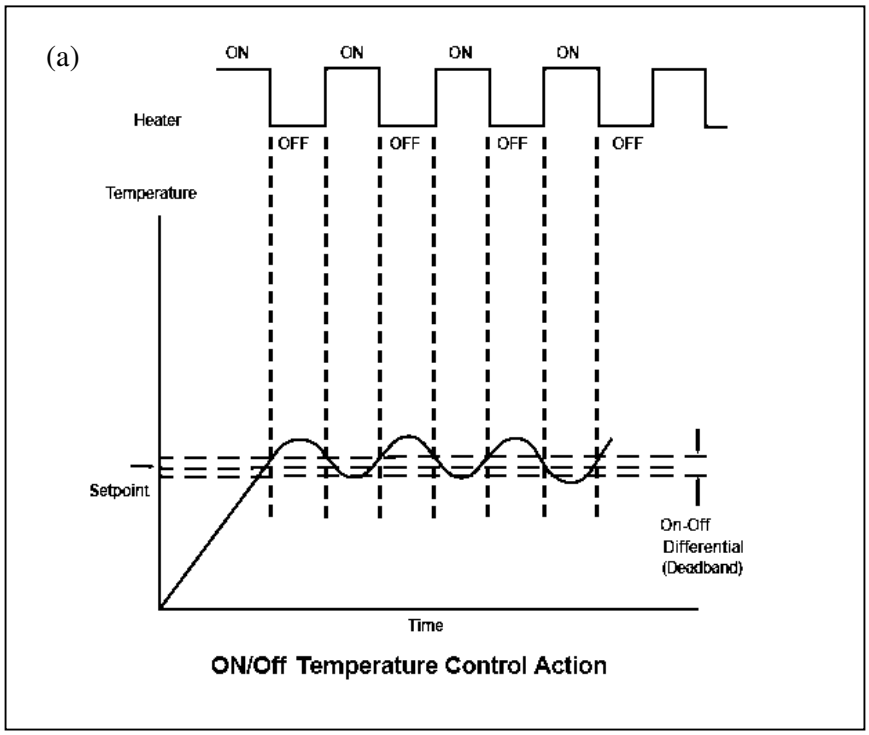

Figure 3.19 Comparison between heating profile using (a) on/off controller and (b) PID controller [152]

CHAPTER 4

RESULTS AND DISCUSSIONS

4.1 Growth of Aligned Multi-Walled Carbon Nanotubes

Despite a variety of methods reported to synthesize aligned CNTs, one still finds it important to perform a step-by-step study for a better understanding in this subject. In addition, the key parameters for growing CNTs are basically optimized according to the steps undertaken during the substrate preparation and the methods of growing CNTs and these differ from one group to another.

In this section, the focus is on determining a suitable condition for growing CNTs and to study the possibility of using Fe powder (99.5%, 10 μm particle size, Merck) as catalyst as an alternative to Fe pellet. The drive to investigate is due to the lack of work reported on the use of readily available metallic powder as catalytic source for CNTs growth. Figure 4.1 (a) shows that CNTs has been successfully synthesized using the proposed method. At the same time, the use of Al_2O_3 as buffer layer has been confirmed as an effective step towards the growth of aligned CNTs as widely reported [87]. The porous nature of Al_2O_3 allows feedstock gas to permeate into the catalyst at a higher rate, resulting in more carbon atom to dissolve into the catalyst particles, hence the growth of CNTs of higher density and yield. This has been proven based on the results shown in Figure 4.1, comparing the effect of the presence of the Al_2O_3 buffer layer.

Figure 4.1(a) shows CNTs growing from the substrate but in a random orientation while in Figure 4.1(b), the CNTs are growing almost vertically from the Si wafer and are more compact compared to Figure 4.1(a). The average length of the CNTs obtained in Figure 4.1(b) is about 10 μm, with typical diameter of 18 nm that is

comparable to those obtained using Fe pellets. SEM images of CNTs grown from buffer layer show significant improvement in the density of the CNTs as well. This is verified by Raman spectra analysis (Figure 4.2), in which the graphitic peak (G-band) intensity of sample A is much higher (176 counts) compared to from sample B (43 counts).

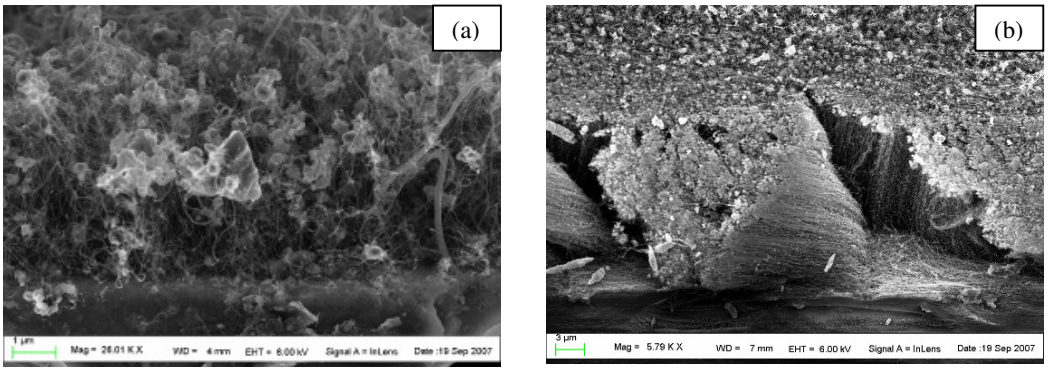

Figure 4.1 SEM images of MWNTs (a) without Al_2O_3 buffer layer and (b) with Al_2O_3 buffer layer

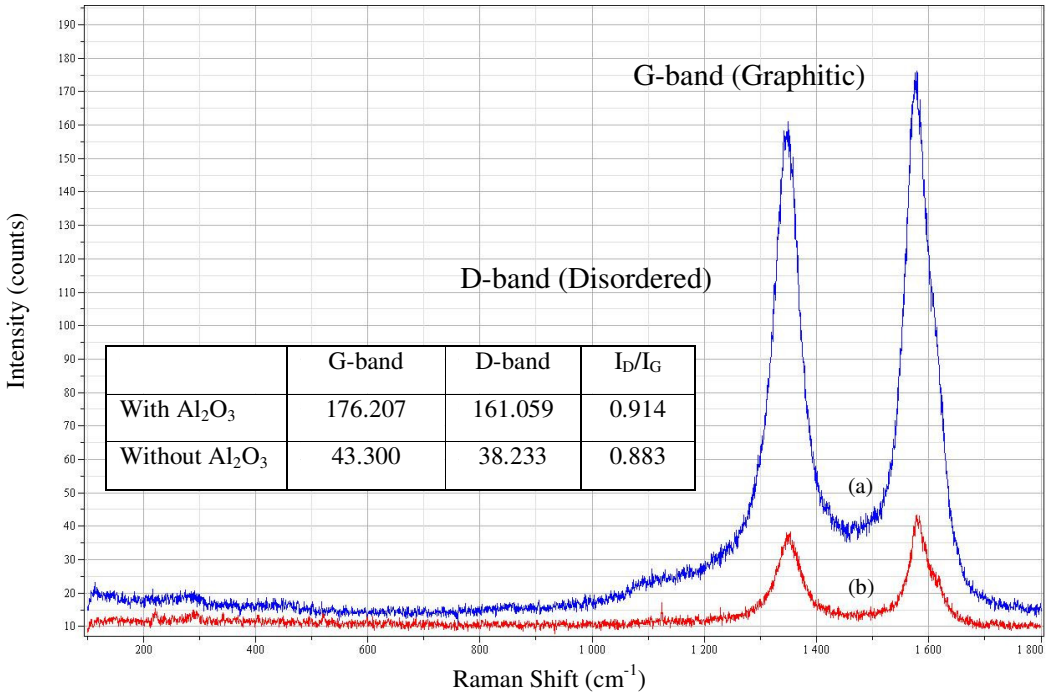

	G-band	D-band	I_D/I_G
With Al_2O_3	176.207	161.059	0.914
Without Al_2O_3	43.300	38.233	0.883

Figure 4.2 Comparison of Raman spectra between sample (a) with Al_2O_3 buffer layer and (b) without Al_2O_3 buffer layer

The driving force behind the aligned growth of the nantubes is the van der Waals interaction between adjacent nanotubes as they grow [116]. For this, in the first place, the Fe nanoparticles need to be localized, as they tend to agglomerate at elevated temperature [153]. When this happens, the resulting size of the particles will be bigger.

The size of the catalytic particles has a significant influence on the quality of the CNTs grown [154]. Particles of nanosize are necessary for the formation of small diameter CNTs. Smaller particle size also equates to having more catalytic particles per unit area. With each of these nanoparticles acting as a nucleation site for the formation of CNTs, more nanoparticles mean higher density of CNTs grown. As the CNTs lengthen, the outer wall of these nanotubes will interact with each other, thus providing the support for self-alignment to grow perpendicular to the substrate via van der Waals interaction. It is also reported that the growth rate is inversely dependent on the diameter of the catalytic particles [59,67].

Figure 4.3 summarizes the growth mechanism of the CNTs [87]. At the growth temperature, the hydrocarbon molecules from the feedstock gas will decompose on the catalytic nanoparticles and the carbon atoms will then diffuse and dissolve into catalytic particles (Step 1). Since the solubility of the carbon within these particles is finite, once it reaches a saturation limit, carbon atoms will precipitate on the surface into a crystalline tubular form (Step 2). The tubular form is favored due to its low energy. Thus, the diameter of the nanotubes is governed by the size of these nanoparticles. Further addition of carbon atoms will lead to elongation of the structures (Step 3).

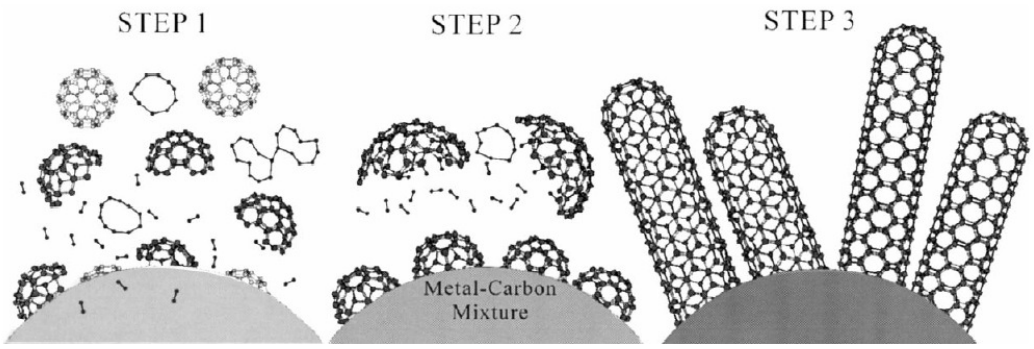

Figure 4.3 Illustration on growth of carbon nanotubes [87]

Another observation from the SEM images in Figure 4.1(a) is the presence of iron carbide. In Figure 4.1(a), it is clearly seen that there seems to be some clusters at the tip of the nanotubes whereas in Figure 4.1(b), no clusters were seen. EDX examination on one of the clusters is presented in Figure 4.4, illustrating elements of Fe and a high C content. The presence of iron carbide is consistent with that reported by Emmenegger *et al* [155]. In their paper, it is stated that carbide, resulted from the transformation of Fe_2O_3 to Fe_3C, acts as a precursor towards the CNTs growth. As for Figure 4.1(b), the presence of Al_2O_3 or Al may have hindered the formation of iron carbide. In this case all the carbon atoms will precipitate into CNTs instead of forming carbide as a by-product, thus resulting in an improved efficacy in the formation of CNTs. Replicating this by using methane as the feedstock gas at 900°C has failed to produce the clusters on the tips of the nanotubes. The absence of the cluster is evident in Figure 4.5. As the mechanism for CNT formation is almost similar, this implies that the reason is not due the selection of feedstock gases.

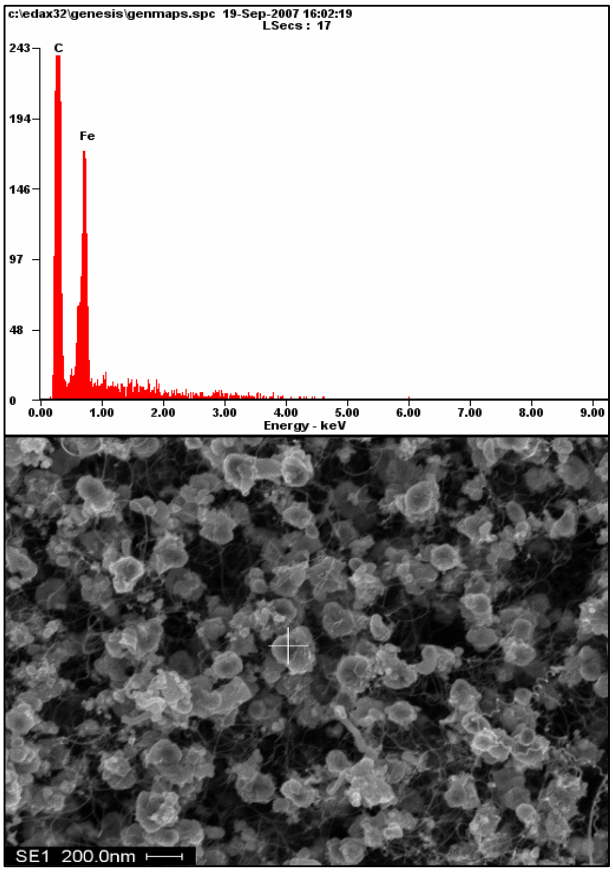

Figure 4.4 EDX results on sample without Al_2O_3 layer

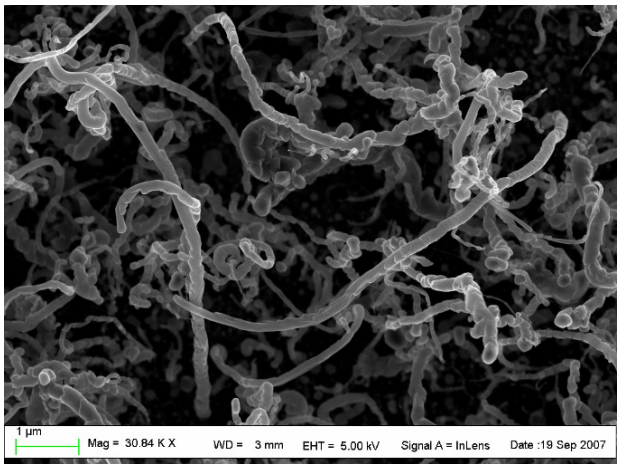

Figure 4.5 CNTs grown using methane as feedstock gas at growth temperature of 900^{o}C

The formation of carbide can be explained by examining the iron-iron carbide phase diagram (Figure 4.6). In the phase diagram, carbide formation occurs when the growth process takes place at 723^{o}C and below whilst at 900^{o}C (as in the process that uses methane), no formation of carbide is favored. Since the feedstock gas is only supplied inside the CVD chamber during the growth process and ceased before it begins to cool thus, no further reactions take place during the cooling stage. Unlike the phase transformation that occurs with the variation in temperature due to the different state of equilibrium at certain temperatures, CNTs are stable structures and once formed, will not redissolved into the Fe particles.

TEM is also performed on these samples to gather more information on the internal structures of nanotubes. From the images obtained, we noticed that for the sample having the Al_2O_3 layer, the outer diameter (OD) of the nanotubes are mostly within the range of 20-30 nm with the inner diameter (ID) between 6 and 10 nm, Figure 4.7(a). However, smaller nanotube with OD and ID of 13 and 4 nm respectively is also observed, Figure 4.7(b). In the absence of the buffer layer, the nanotubes are larger in size (Figure 4.8). OD ranges from 48-52 nm and the ID are from 13-17 nm.

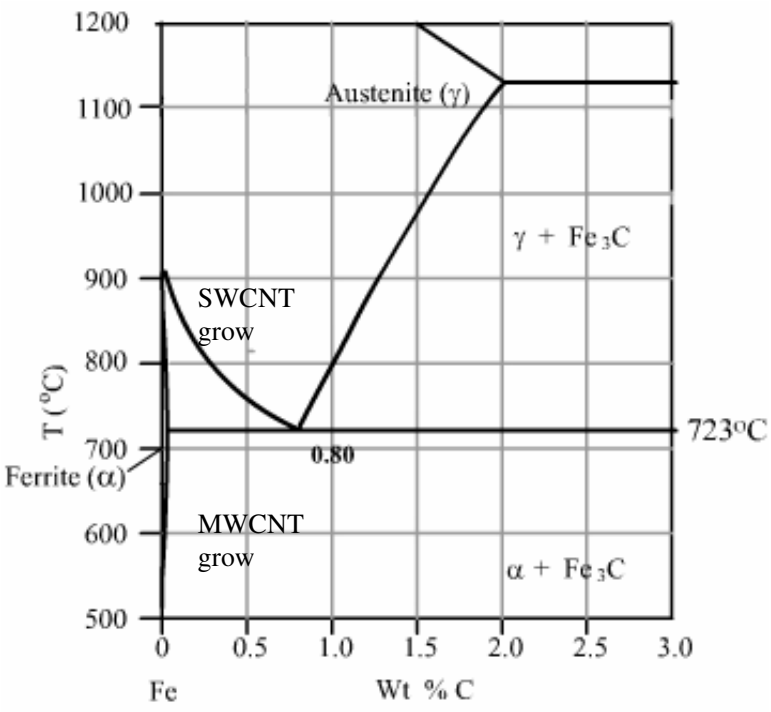

Figure 4.6 Phase diagram of Fe-FeC_3 [156]

The OD represents the size of the nanotubes whereas the ID is useful to estimate the particles size. Based on the open-end growth model proposed by Iijima [35], the first tube acts as a nucleus with the second tube grow from the side-wall of the first nanotube and the process repeats itself for the subsequent tubes. Thus, the diameter of the first nanotube or the ID of the nanotubes can be used to indicate the size of the catalyst particles. By comparing the ID for the images in Figure 4.7 and Figure 4.8, there is evidence that the Al_2O_3 buffer layer actually hinders the agglomeration of the catalyst particles at elevated temperatures i.e. growth temperature. This is consistent with the findings by others [89]. These images also provide evidence of defects in the structure of both samples and help to explain the intensity ratio I_D/I_G value obtained from the Raman spectra in Table 4.1. It is also found that performing annealing on the as-deposited Fe catalyst followed by NH_3 treatment resulted in the formation of CNTs of better quality, and was shared by Jang [154] and Moshkalyov [157]. Although different catalyst was used (Co and Ni, respectively), both came to the same conclusion, that NH_3 assisted in the formation of nanosize catalyst particles.

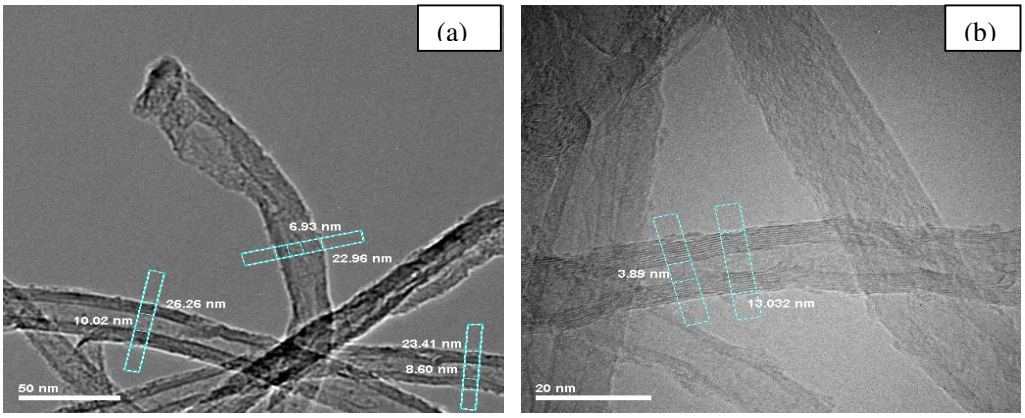

Figure 4.7 TEM images of carbon nanotubes on samples with Al_2O_3 layer

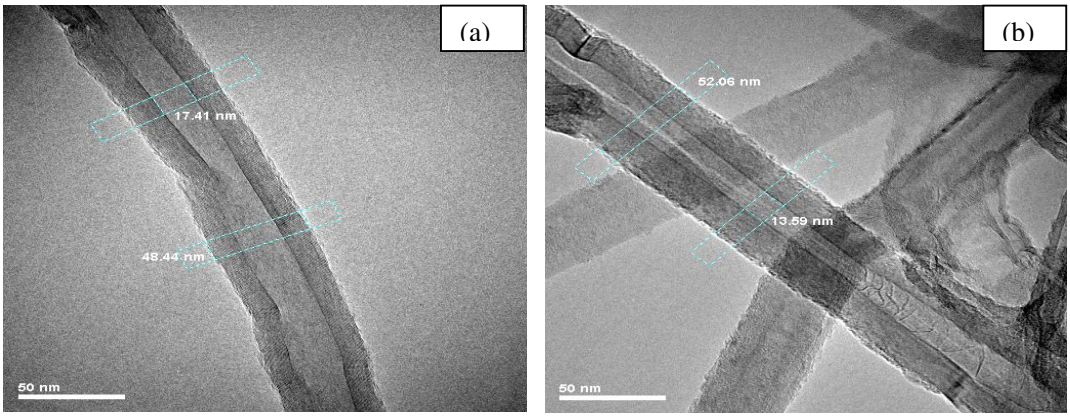

Figure 4.8 TEM images of carbon nanotubes on samples without Al_2O_3 layer

4.2 Different Methods of Preparing Aluminum Oxide Buffer Layer

Several methods of incorporating the aluminum oxide have been reported but no comparisons on these methods were made. In this section, efforts have been made to create a set of experiments on the methods that have been reported, with the addition of a couple more feasible methods. It has been shown that it is crucial to have Al_2O_3 and not pure Al as it has been shown that CNTs will not grow on pure Al [97]. This includes Sample 4 that was subjected to oxidation upon the deposition of a thin film of metal catalyst. One of the reasons, as concluded by Han *et al* [73], is that this metallic film is very thin and during annealing (performed at 400 ^{o}C), it forms nanoislands due to agglomeration of Fe particles. This causes the breaking up of this continuous film thus exposing Al layer beneath. Thus, oxidation of Al can still take

place albeit only on the exposed Al. Overall, it is critical to produce good quality buffer layer as it support the growth of good quality and highly aligned CNTs.

All the samples are analysed with Raman spectra to confirm that CNTs have been successful synthesised and to study their crystallinity. Table 4.1 records and compares of the G-band intensity and crystallinity, represented by the ratio of intensity I_D/I_G. the lower the value of I_D/I_G, the better would be the crystallinity as this means there is a higher percentage component of nanotubes with graphitic structure as compared to the defective ones. Except for sample 5, the rest of the samples have similar G-band intensity and I_D/I_G ratio.

Data from this table seems to imply that, in terms of structural crystallinity, the quality of the CNTs film obtained using an as-deposit layer of Al_2O_3 and an oxidized Al thin film is similar. It is worth mentioning that the decomposition of the hydrocarbon feedstock gas and formation of CNTs occurs in the Fe catalyst layer. The Al_2O_3 layer which lies underneath, is responsible for improving the rate at which the gas can permeate into the Fe catalyst due to its porous structure [135,158]. These seem to further strengthen the fact that the metal catalyst is the active component that is responsible for the formation of CNTs while the buffer layer only acts as the growth promoter for higher CNT yield. The surface roughness of the Al_2O_3 layer is measured using atomic force microscopy (AFM), as shown in Figure 4.9 and tabulated in Table 4.2.

Table 4.1 Results from Raman spectra analyses

Sample	G-band intensity (count)	I_D/I_G
A1	71.4	0.98
A2	66.6	1.01
A3	67.0	1.08
A4	65.0	1.03
A5	55.5	1.25

Table 4.2 Surface roughness measurement R_{ms} of Al_2O_3

Sample	R_{ms} (nm)
A1	2.638
A2	0.306
A3	2.248

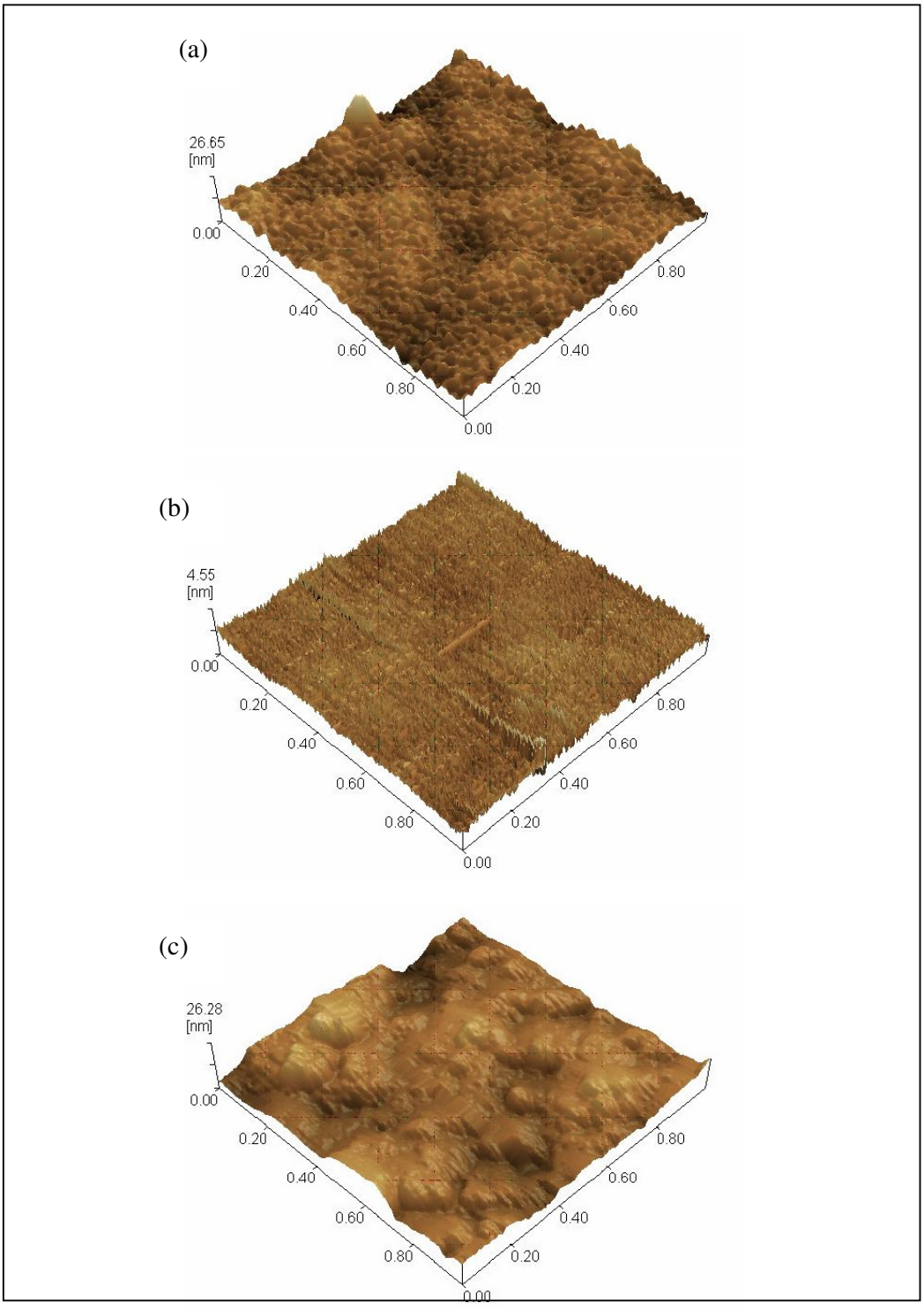

Figure 4.9 AFM measurement on (a) Sample A1, (b) Sample A2 and (c) Sample A3

As mentioned previously in Section 3.2, the buffer layer was prepared using various methods. The surface morphology of the underlying buffer layer can affect the distribution of the Fe catalyst particles and consequently the growth of the CNTs (Figure 4.10). R_{ms} means root-mean-squared of the height of the surface bump from the mean line. No measurement, however, was done on Sample A4 and A5 as the deposited Al layer was no longer at its pristine form when the measurement was taken.

These values are compared against the CNT film thickness (Table 4.3) obtained from SEM images (Figure 4.11). For sample A2 and A3, it is noticed that a lower R_{ms} in the Al_2O_3 layer will result in a thicker CNT film. This observation is shared by Han *et al* [69]. The explanation behind, could be that a lower R_{ms} reflects a smoother surface and does not encourage the agglomeration of catalytic particles. When the size of the catalytic particles is smaller, the resulting nanotubes are thinner and longer. For sample 1, since the material used is Al_2O_3 and not oxidized Al, making a direct comparison may not be appropriate. However, with the R_{ms} value close to sample A3, it still results in CNTs film thickness about the sample as sample A3. In sample A4, Al layer may have been partially oxidized and resulted in a lower thickness in the CNTs film.

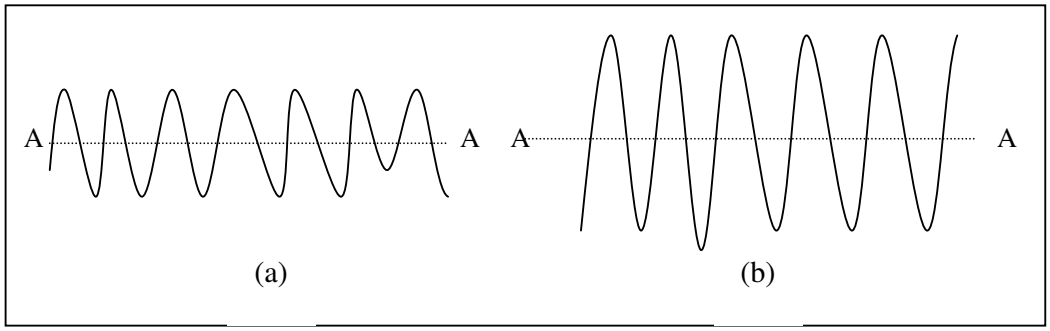

Figure 4.10 Schematic diagram showing difference between surface profile with (a) lower R_{ms} and (b) higher R_{ms}. A-A represents mean line

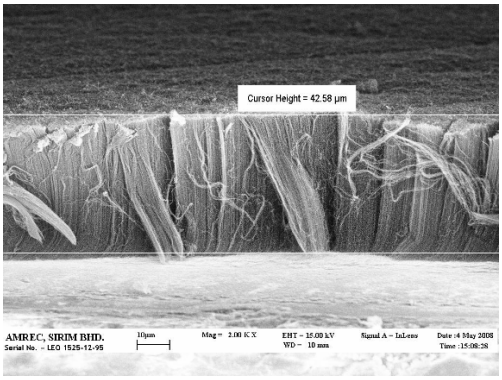

a) Sample A1

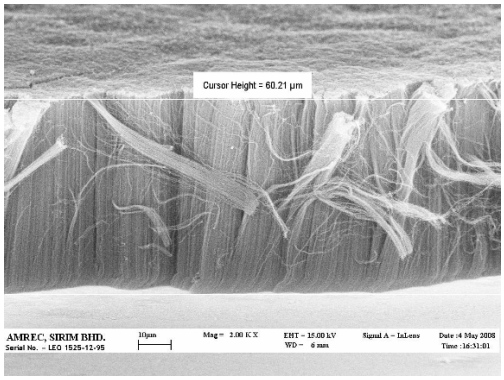

b) Sample A2

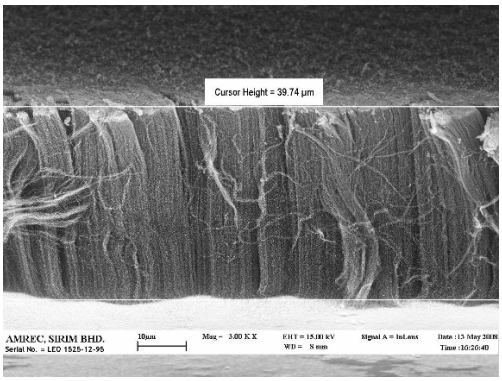

c) Sample A3

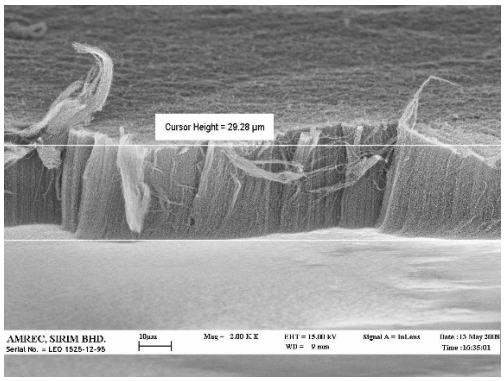

d) Sample A4

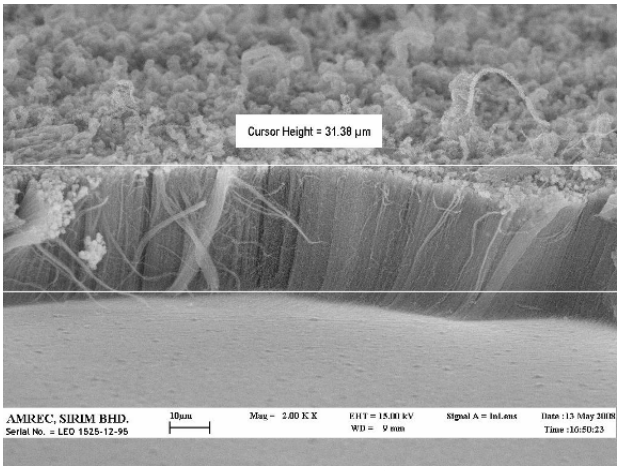

e) Sample A5

Figure 4.11 SEM images of CNTs samples grown using different method of buffer layer preparation

Table 4.3 Thickness of CNT film

Sample	Thickness (μm)
A1	42.58
A2	60.21
A3	39.74
A4	29.28
A5	31.38

For sample A5, there are a lot of clusters-like particles at the tip of the CNTs, which is likely to be amorphous carbon. This is supported by the Raman spectra, which has the highest I_D/I_G ratio indicating the presence of defective component. The result obtained here is unlike the one reported [158] where the magnetron sputtering method was used and the substrate heated to an elevated temperature. The reason could be that the e-beam deposition process does not allow purging of O_2 or any other gase as it could not maintain high vacuum environment as desired. The presence of the gases particles in the e-beam system would most likely created obstacles for the vaporized Al from reaching the substrate on top, leading to a possibly thinner Al layer. In addition, O_2 in the form of a gas may not be sufficiently reactive to oxidize the Al as the substrate is maintained at room temperature. Heating the substrate [156] and using ionized O_2 may be a better option.

4.3 Comparison between Fe powder and Fe pellet as catalyst precursor

Fig 4.12 shows the Raman spectra for both samples that used Fe powder and Fe pellet as the catalyst precursor. From the graph, it is noticed that the peak intensity of the sample using Fe pellet is higher compared to the sample using Fe powder as catalyst. However, upon calculating the I_D/I_G ratio, it is found that the values for both samples are quite similar. This could mean that the quality, in terms of crystallinity, of CNTs obtained from these methods is comparable but the density of CNTs film obtained using Fe powder is lesser.

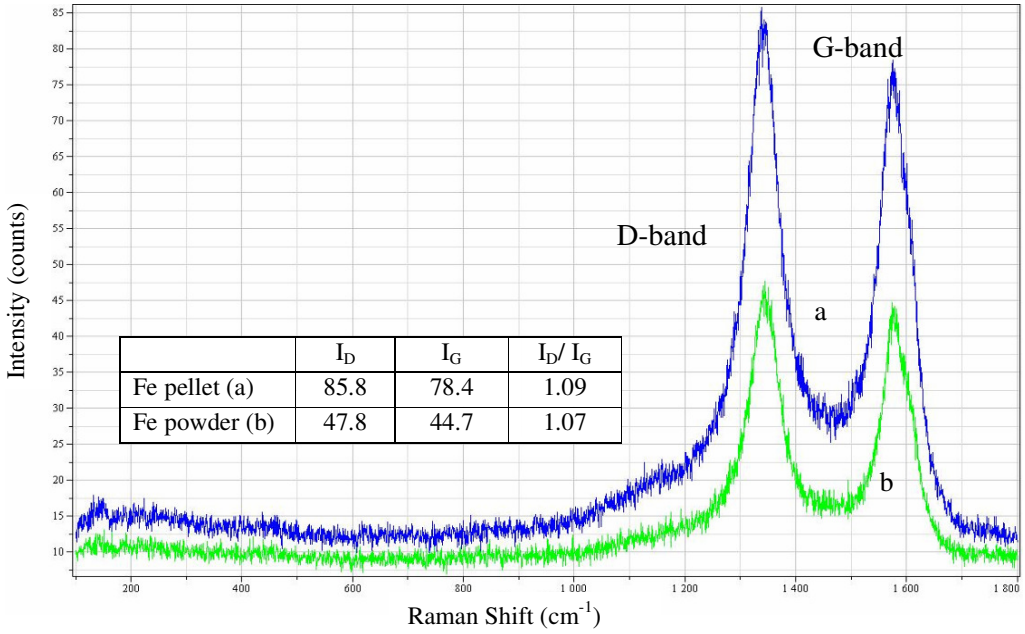

	I_D	I_G	I_D/I_G
Fe pellet (a)	85.8	78.4	1.09
Fe powder (b)	47.8	44.7	1.07

Figure 4.12 Raman spectra of sample using (a) Fe pellet and (b) Fe powder as precursors

The cross-sectional SEM images of CNTs films show that both samples using Fe pellet and powder have similar film thickness, with 49.71 μm for Fe pellet and 47.49 μm for Fe powder (Figure 4.13). From the Raman spectra and CNTs film thickness, it can be deduced that metal catalyst in their powder form is almost as effective as using metal pellets for growing CNTs.

At the surface, large particles are present in the sample using Fe powder whereas none were seen on the sample using Fe pellet as catalytic source (Figure 4.14). EDX analysis, as shown in Figure 4.15, confirmed these particles to be Fe.

A backscattered electron image (Figure 4.16) was examined to provide further information on these particles. A backscattered imaging is useful for differentiating materials since the number of backscattered electrons received by the detector increases with the atomic weight of the materials. Thus, heavier elements will appear to be brighter in the image. In Figure 4.16 (b), it shows that the core of the particles is made of heavier elements while the outer shell is made of carbon as the brightness of

the outer shell and the surrounding nanotubes is identical. Since EDX only able to detect Fe and C in the particle, thus it appears that Fe particles may have been enclosed within carbon particulates, possibly in the form of Fe carbide.

Based on the analyses performed, it is certain that metallic catalyst in the form of powder can be used as metal source. As catalyst of bi-metallic or binary alloy system is reported to be better [65,155], the composition of desired catalyst can be adjusted easily using the powder metallurgy method, which can be done inside the laboratory instead of having to cast into a solid metal like pellets. As for the presence of carbon coated Fe particles, it is believed that they could be removed using the existing purification methods available namely acid treatment for removal of catalytic particles and oxidation to burn-off amorphous carbon.

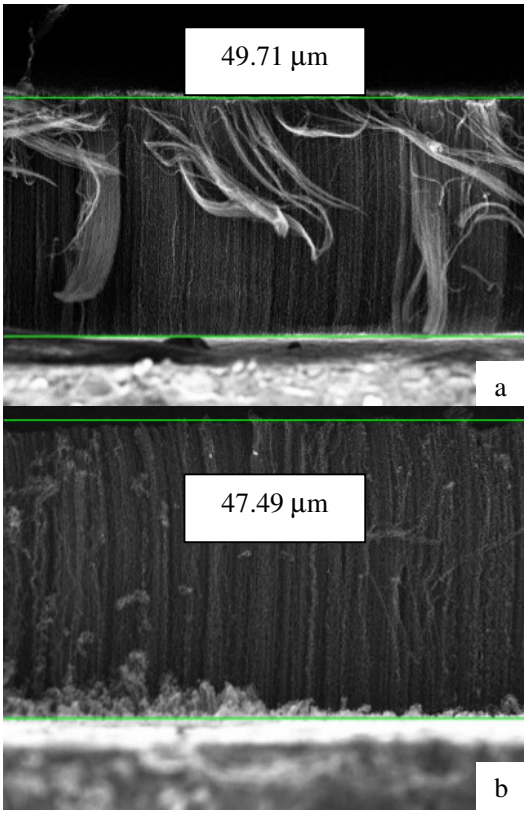

Figure 4.13 Cross-sectional view of the CNTs film for sample using a) using Fe pellet (630x magnification) and b) using Fe powder (800x magnification)

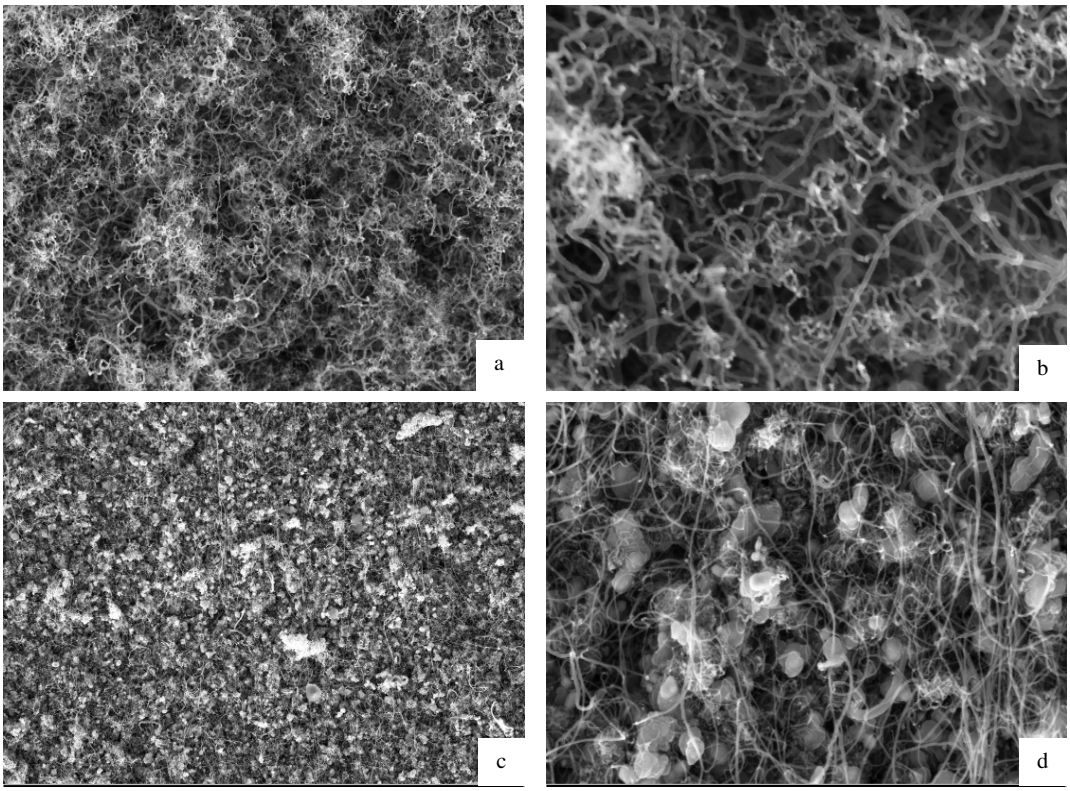

Fig 4.14 Surface morphology of CNT film of samples using Fe pellet at a) 14kx magnification b) 60kx magnification and using Fe powder at c) 7kx magnification d) 40kx magnification

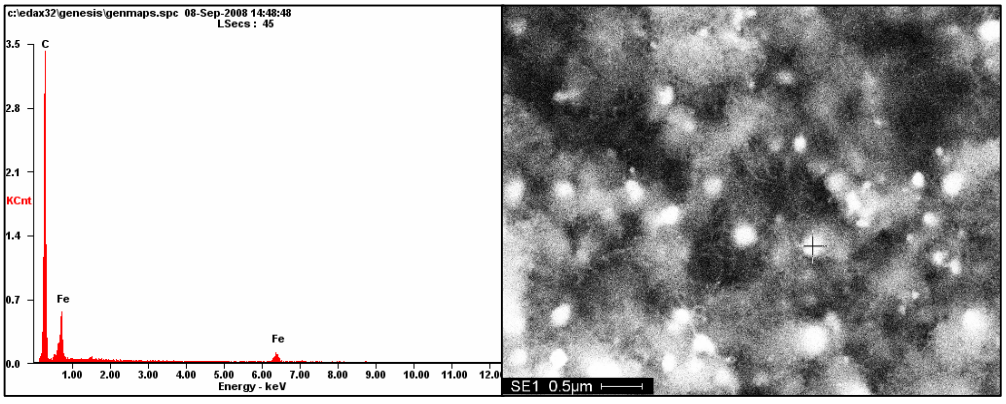

Figure 4.15 EDX analysis on the large particles found in samples using Fe powder as precursor

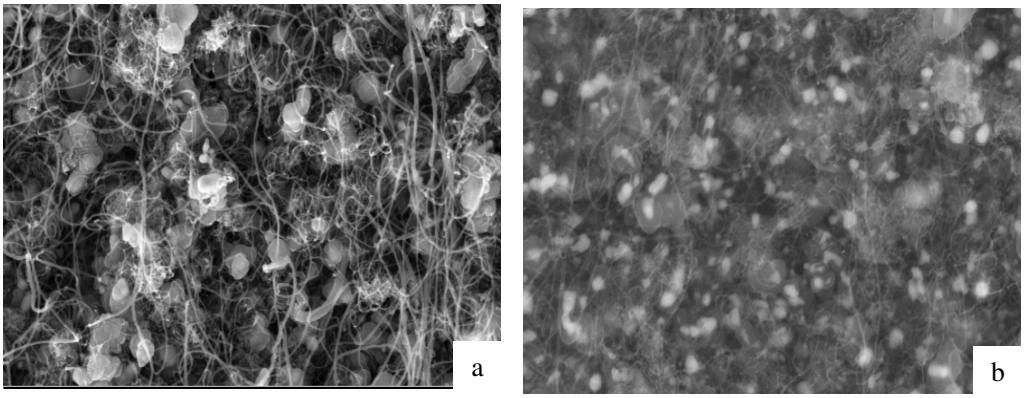

Fig 4.16 (a) In lens image and (b) Backscattered electron image of samples using Fe pellet as precursor (40kx magnification)

4.4 Sandwich Stacking Orientation and Its Effect on the CNTs Growth

So far, the effort on growing aligned CNTs is based on the conventional method that was explained extensively in Chapter 3 while the mechanism behind the growth has been discussed in great length in Chapter 2. This part of the work, however, uses a different approach which is called sandwich growth, introduced by Chen *et. al.* [146144]. Among the highlights of their findings are two CNTs grown within a catalyst particle and that the growth rate of the CNTs underneath a sandwich cover is many times higher. The CNTs were also found to have good adhesion with the sandwich cover and this may lead to the feasibility of having an in-situ growth of a two-terminal electronic device.

Chen *et al* [146] had incorporated an additional small cover substrate (Figure 4.17) to the conventional configuration with the purpose of providing "shielding effect" for the CNTs from direct ion bombardment in the microwave plasma CVD. In his report, the area with a cover lid was reportedly contains longer CNTs due to an exceptionally higher growth rate and strong adhesion between CNTs and the top cover. The catalyst particles were found to have CNTs growing from both ends instead of the usual one. However, the reasons for these phenomena were not fully understood.

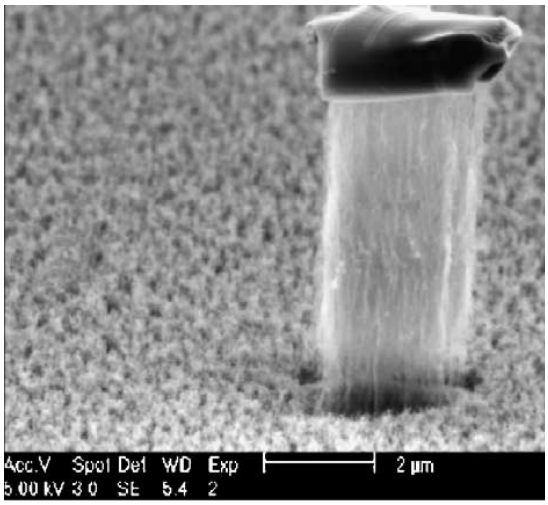

Figure 4.17 SEM image showing sandwich cover lifted by growing CNTs [146]

Figurative description of the sandwich stacking is demonstrated in Figure 4.18. The designation of the samples and details on the procedure for sandwich growth CNTs is according to that described in Section 3.2:

a) Conventional sample (without top substrate)
b) Sample S1: sandwich type with catalyst coated top substrate
c) Sample S2: sandwich type with catalyst coated bottom substrate
d) Sample S3: sandwich type with catalyst coated top and bottom substrate

SEM images in Figure 4.19 show that CNTs have been successfully produced via the sandwich method using the methods described in Section 3.2. This is significant, considering that CNTs can grow on catalyst in concealed area in between two substrates when the only access is only through the sides. In order for the analysis to be done, the top substrate is carefully removed as illustrated in Figure 4.19. Upon removing the top substrate, it can be seen that the CNT film remained intact, and no noticeable amount of CNTs which will appear as black spots is seen sticking onto the other substrate. Thickness of each film is tabulated in Table 4.4.

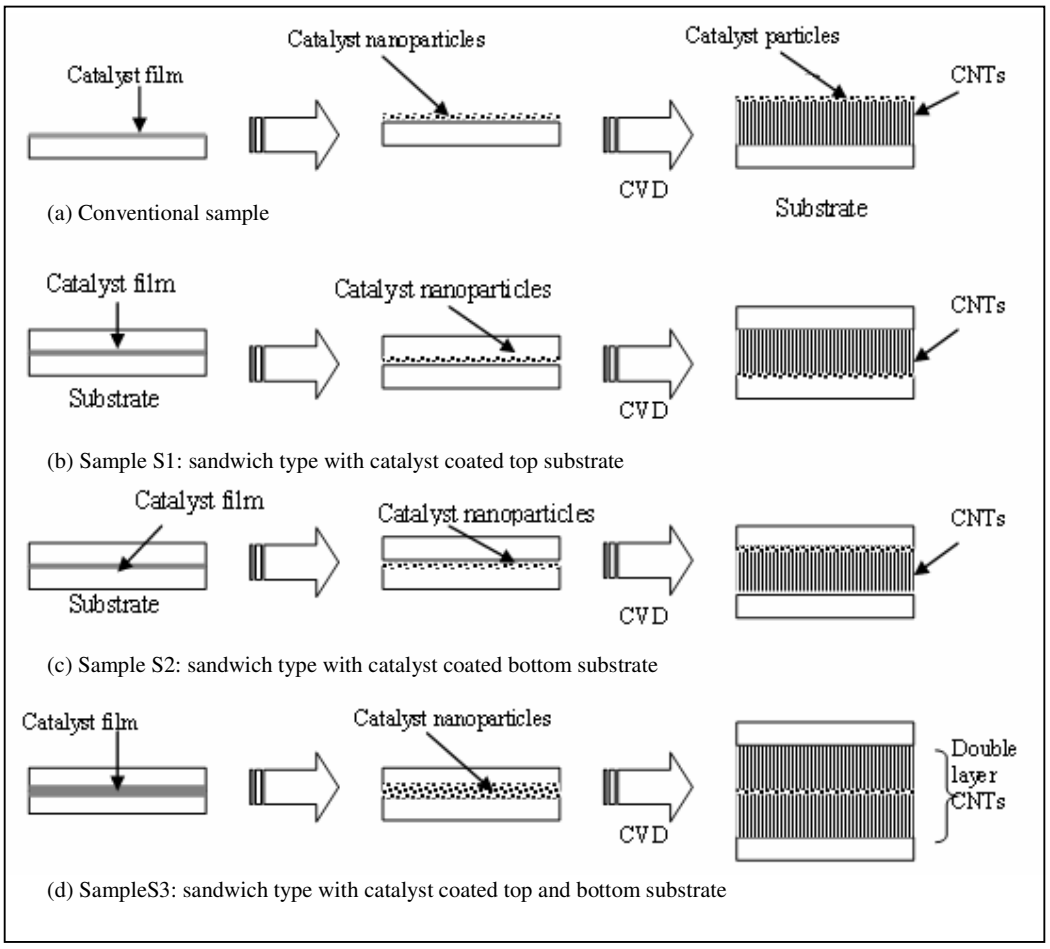

Figure 4.18 Conventional (a) versus sandwich (b, c and d) growth of vertically aligned CNTs by thermal CVD method

Prior to SEM analysis, the samples are analyzed with Raman spectroscopy to verify the presence of CNTs. Table 4.5 illustrates the Raman spectra of these samples. It can be seen that CNTs grown in the condition whereby only a single wafer containing the catalyst layer, the nanotubes obtained has lower I_D/I_G ratio or less defective. This is further confirmed by the EDX (Figure 4.20) done on the particles found on the tips of the nanotubes in Sample S3, which is identified as amorphous carbon whereas particles found on tips of the nanotubes in Sample S1, Sample S2 and conventional sample contain traces of Fe, probably an indication of tips growth. All of

them have catalyst nanoparticles located at the tips of the nanotubes. Thus, this indicates that the CNTs film undergoes tip growth mechanism.

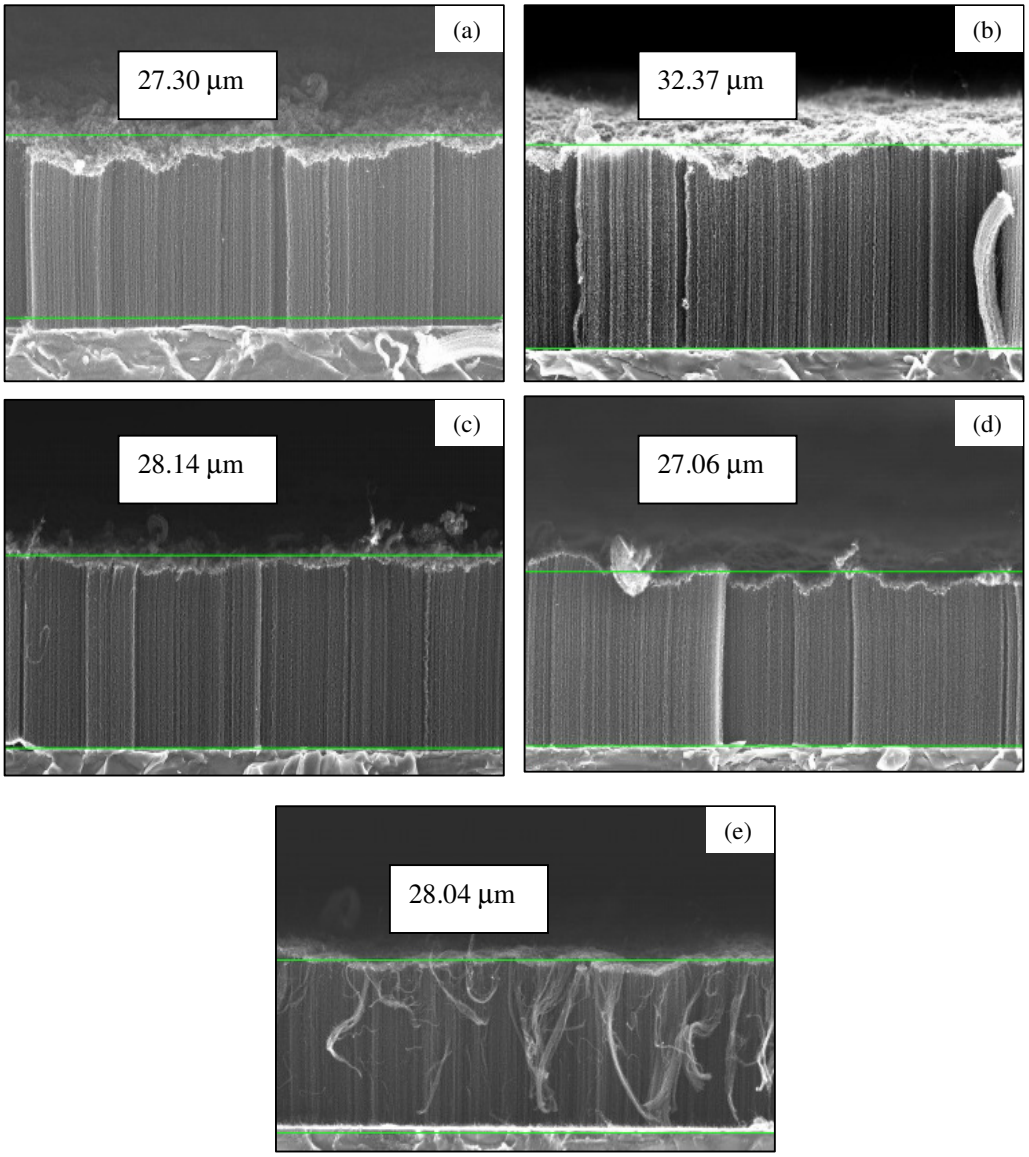

Figure 4.19 SEM images of CNT film from (a) Sample S1 (b) Sample S2 (c) Sample S3 bottom substrate (d) Sample S3 top substrate (e) Conventional

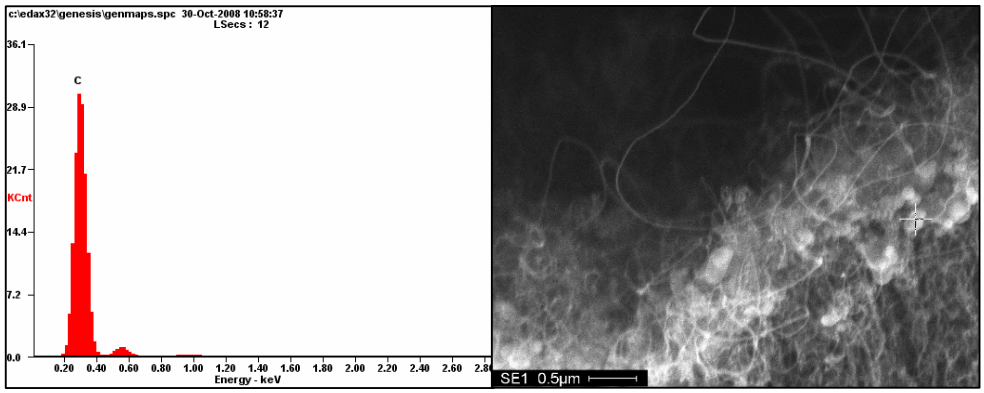

Figure 4.20 EDX on particles at the tips of CNT

Table 4.4 CNTs film thickness

	Film thickness (µm)
Sample S1	27.30
Sample S2	32.37
Sample S3 (Top substrate)	27.06
Sample S3 (Bottom substrate)	28.14
Conventional	28.04

Table 4.5 Raman spectra of samples

	I_D	I_G	I_D/I_G
Sample S1	65.6	73.2	0.90
Sample S2	67	71.5	0.94
Sample S3 (Top substrate)	77.3	68.3	1.14
Sample S3 (Bottom substrate)	59.4	57.3	1.04
Conventional	61.3	66.4	0.93

From the results obtained, none of the sandwich configurations in this study was found to exhibit these. The CNTs film thickness derived from SEM images ranged from 27 µm to 32 µm, compared to 28 µm using the conventional method. But, if the thickness of CNTs film from both substrates in Sample S3 is totaled, that is twice the length of CNTs in conventional sample. For Sample S3, the catalyst nanoparticles are found meeting midway between the cover and substrate, similar to Chen's findings. This finding may have provided some explanation to Chen's results. As the CNTs from Chen's work are of tip growth mode, the bonding between the catalyst and the

substrate is believed to be weak. Thus, during the CNT growth process using plasma CVD, the ions may have knock off some of the catalytic particles from the bottom substrate and landed onto the top surface. This resulted in both surfaces having catalytic particles and the longer CNTs observed could have been made up of two nanotubes instead of a single nanotube.

As for Sample S1 and Sample S2, the location of the catalyst whether on the top or bottom substrate seems to be insignificant towards the CNTs produced. The crystallinity and film thickness is almost the same with the conventional sample. The significance of this finding is that the catalyst film may not necessarily be exposed directly to the hydrocarbon feedstock in order for CNTs to grow. The CNTs film also does not exhibit any buckling or bending as a result of the weight of the top substrate, demonstrating the high strength of CNTs.

On the presence of amorphous carbon found in Sample S3, it could be due to the ineffectiveness of the H_2 in removing them due to the over-crowdedness in region between the two substrates as CNTs are growing from both ends. It should be highlighted that H_2 was purged continuously throughout the growth process for the purpose of removing amorphous C (refer to Table 3.1 for the growth procedure) to obtain CNTs of high purity as evidence from the SEM images of previous samples synthesized using the conventional methods.

4.5 Integration of Carbon Nanotubes

In reference to Figure 3.9, due to the presence of the buffer layer (oxidized Al), electrical conductivity does not occur via the surface but rather underneath the surface because only the top layer of the Al is oxidized.

To measure the stability of the sensing capability of CNTs, a study is made to measure the values of the resistance in the CNTs when exposed to a constant pressure over a long period of time (Figure 4.21). It is observed that at ambient pressure the resistance decreases gradually from its initial value until it becomes stable and remains almost unchanged over 2 hours period. At the same time, the temperature of

the sample and the air inside the enclosed chamber is also recorded using thermocouples. In order to determine the changes in resistance of the CNTs film with applied pressure (Figure 4.22), the resistance of the film is plotted against the pressure inside the enclosed chamber. A linear curve is obtained in which the resistance increases with pressure and this is a fundamental principal for consideration in a good operating sensor.

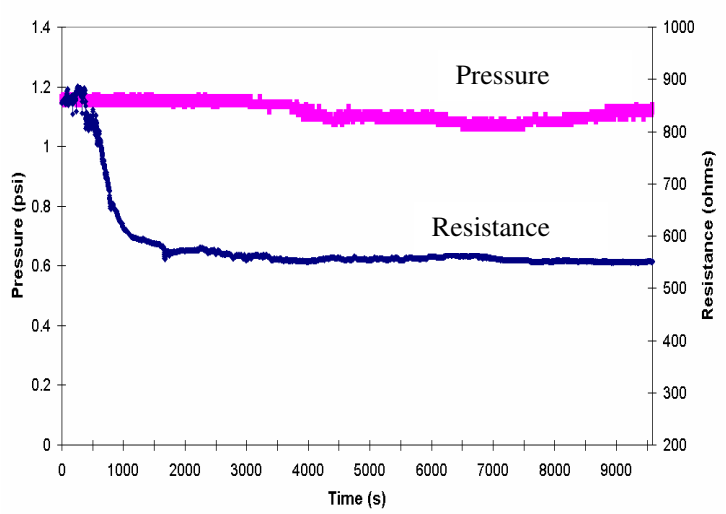

Figure 4.21 Resistance of the CNTs film over an extended period of time in ambient pressure in enclosed chamber

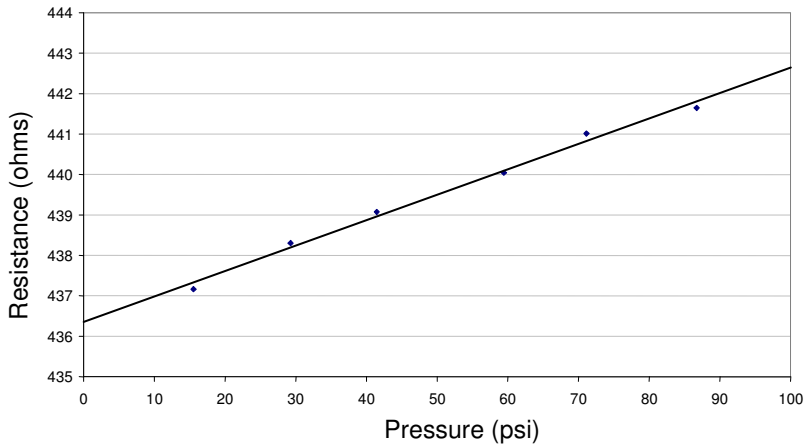

Figure 4.22 Resistance of CNTs vs applied pressure

However, the resistance does not seem to return to its initial value upon releasing the N_2 gas inside the chamber. Close interpretation reveals that the Al plate used is still pressing against the CNTs film, thus nanotubes are not able to recover their original state. It is also found that CNTs are easily scratched, as the nanotubes are delicate structures due to their nanosize. For that, it is not suitable to make contact point directly on top of the CNT film but rather on the substrate. Thus, some adaptation is made whereby top electrode (Al plate) is replaced by a thin film of Cu deposited on top of the CNTs film as well as some on the substrate using the e-beam evaporation process (Figure 3.10). Unfortunately as can be seen in Figure 4.23, it does not seem to be responsive towards the pressure inside the chamber. The Cu thin film may not be able to cause the CNTs to undergo deformation. Thus, a better model is required; one that is able to detect variation in pressure and that allows recovery of the CNTs.

In view of the above results, it was found that there could be some variables that have not been fully understood. Thus, it was then decided to use weights to generate pressure on the CNTs film using the setup in Figure 3.11, as discussed in the following section.

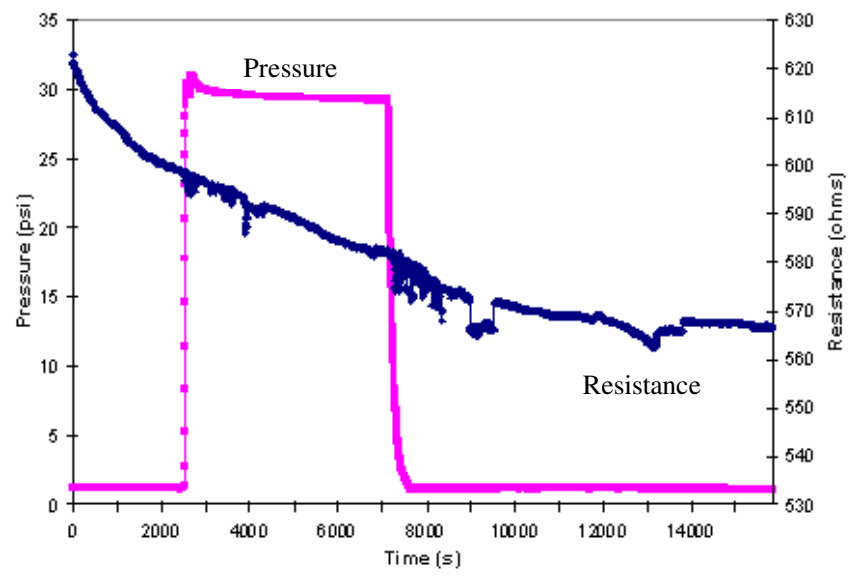

Figure 4.23 Variation of resistance with pressure over time

4.6 Electromechanical Measurement of Carbon Nanotubes Film

As described in Figure 3.11, the measurement unit is consists of double layer CNTs film. Using SEM analysis (Figure 4.24), CNTs was confirmed to grow on the catalyst-coated are while catalyst-free area are just exposed buffer layer. By doing so, electrical measurement can actually be performed on as-grown CNTs film instead of having to transfer to a conductive substrate, like Cu [136,137]. Such transfer, although is possible to carry out may have certain complication like incomplete transfer of CNTs film and unsuitability of conductive paste (normally epoxy-based) where resistant to high temperature or corrosive environment are critically required.

On the buffer layer, de los Arcos [89] reported that CNTs only grows on Al_2O_3 and not bare Al. However, Al_2O_3 is known to be non-conductive. Since the buffer layer is oxidized Al, it can be made to become electrically conductive with a resistance value of about 5 Ω (Figure 4.25), merely by reducing the amount of O_2 that was purged into the tubular furnace. This way, the buffer layer is still able to promote aligned growth of CNTs and yet remain conductive. EDX analysis confirmed that the conductive buffer layer has lower oxide level compared to the regular buffer layer (Table 4.5).

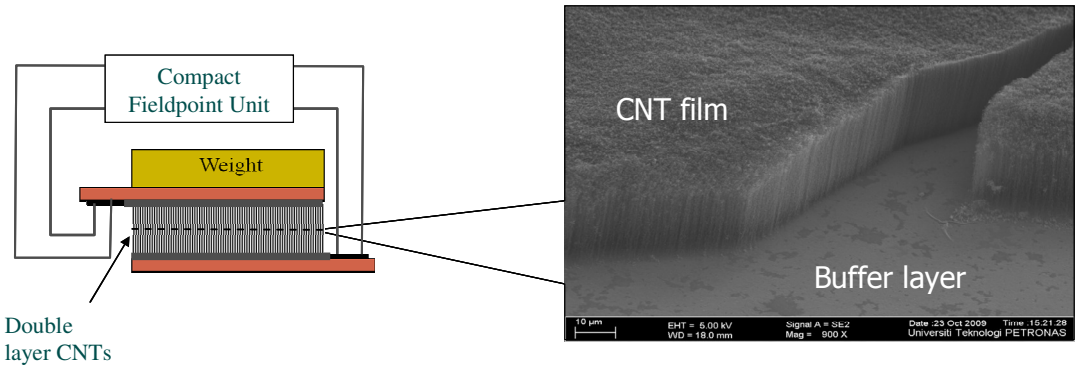

Figure 4.24 SEM image displaying clear separation between the CNTs and part of the buffer layer that is catalyst-free

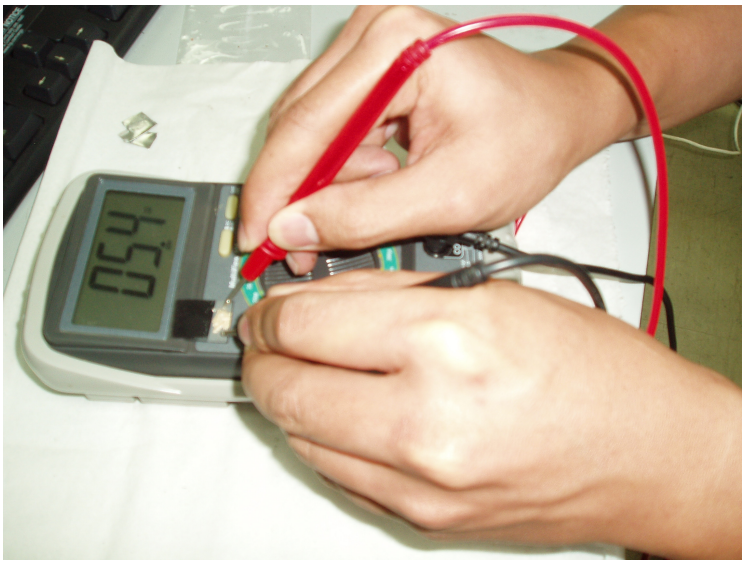

Figure 4.25 Photograph image showing the resistance of the conductive buffer layer

Table 4.5 EDX analysis of conductive and regular buffer layer

Element	Conductive buffer layer (%)	Regular buffer layer (%)
Al	12.62	2.74
O	26.81	32.77
Si	61.57	65.59

From Figure 4.26, it has been shown that a change in the resistance was observed whenever weight is added on top of the measurement unit and remains stable. At intervals of 10 s, as depicted in Figure 4.27, a steady pattern of instantaneous decrease in the resistance against weights added is portrayed. This is followed by gradual increase or recovery as these weights was removed, thus confirming reversibility of the process. However, no fixed pattern was observed when repeated with 50 s (Figure 4.28) or 100 s intervals (Figure 4.29). This could be indication that CNTs are more responsive towards rapid changes in the pressure level.

The reduction in the resistance is believed to be due to the bending of the nanotubes, resulting in an increased in the conduction channel for electrons to travel. It is noticeable that, the magnitude of the decrease is much greater initially but

became lesser as the weight increases. Figure 4.30 shows how the resistance of the CNTs changes with applied weight for loading time interval of 10 s and 100 s.

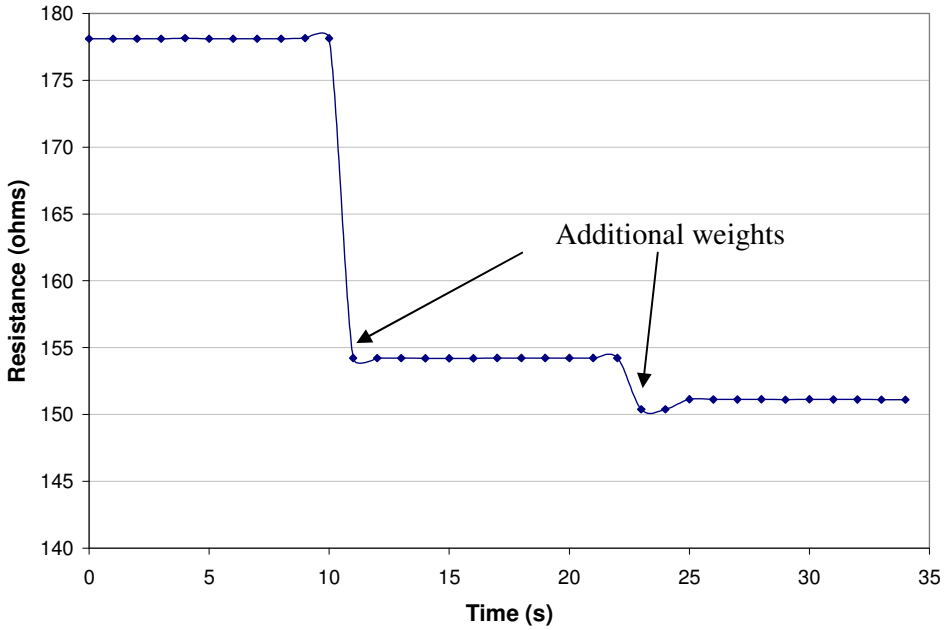

Figure 4.26 Graph showing changes in resistance of CNTs film only occurs when weights are added

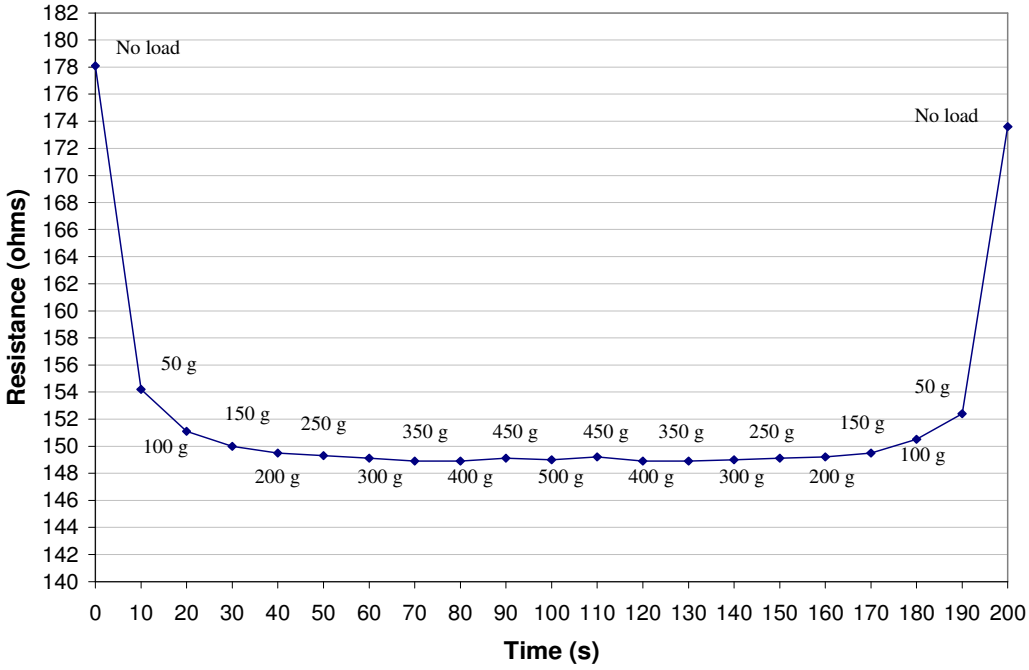

Figure 4.27 Graphs comparing resistance changes within CNTs as a result of increasing weights in the order of 50 g at 10 s intervals

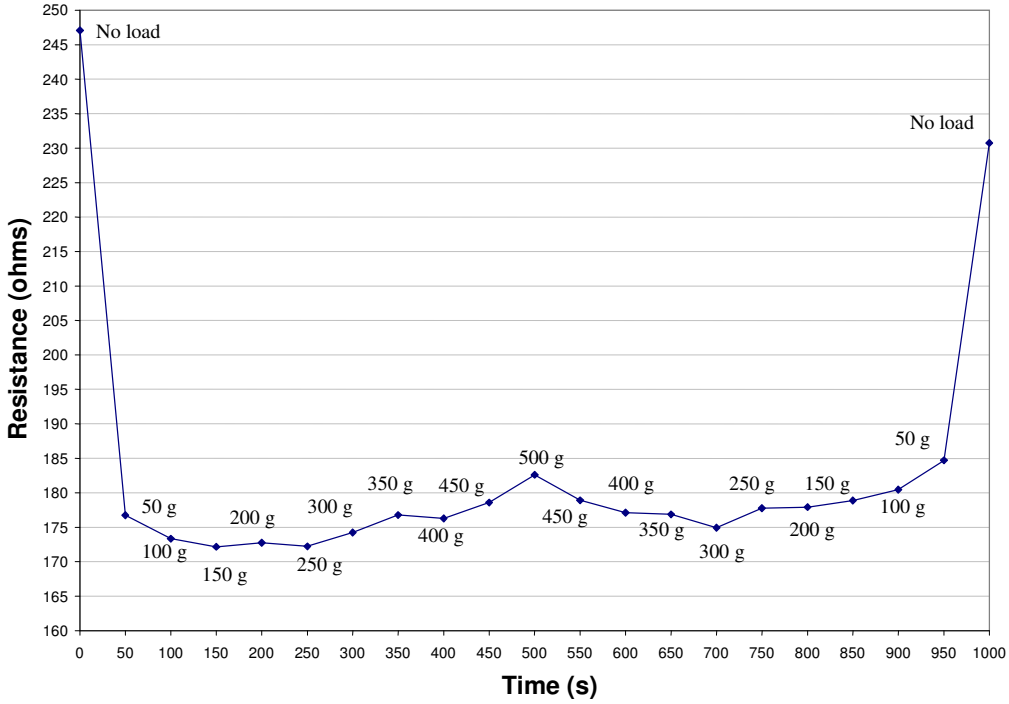

Figure 4.28 Graphs comparing resistance changes within CNTs as a result of increasing weights in the order of 50 g at 50 s intervals

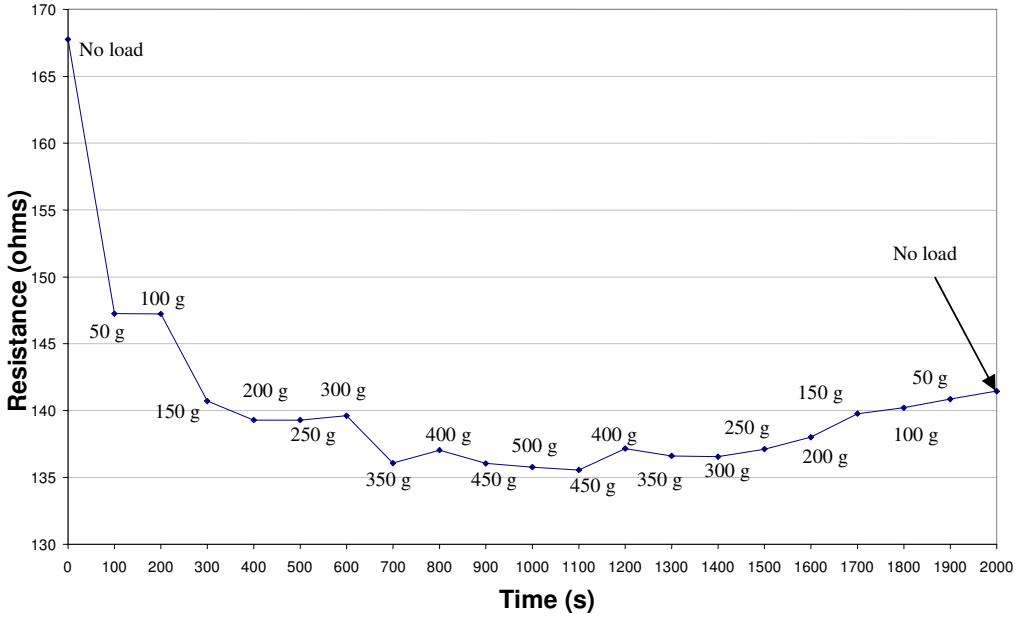

Figure 4.29 Graphs comparing resistance changes within CNTs as a result of increasing weights in the order of 50 g at 100 s intervals

For 10 s interval, it can be seen that the magnitude of the change is greater initially, until it reaches a plateau at 350 g whereas in 100 s interval, the rate of recovery during weight removal is much less compared to the corresponding increase in the resistance when the weight is added. As explained by Semet [130], in the beginning, the spacing between nanotubes is greater and thus easier for bending to take place. As the number of bends increases with stress, as proven by Yaglioglu [160], it resulted in a denser body and would require a higher stress level to achieve the same amount of strain increment at the later stage, as if there's a increased in the modulus, ε.

At the same time, the difference between the initial and final resistance of the CNTs film (when there is no load) also seem to increase when repeated using a longer time interval. One contributing factor is that, CNTs are found to undergo creep deformation when exposed to pressure over time. Creep deformation refers to the phenomenon whereby a material that is subjected to constant stress, experiences increased in strain over time. Yaglioglu [160] reported that, for carbon nanotubes, the compressive force required for sustaining a certain amount of strain (0.275), decreased from 140 MPa to around 80 MPa over a period of about 75 s, a reduction of about 43%. This could be attributed to the nanostructure of CNTs because their smaller size is more susceptible to creep, owing to their large volume to mass ratio.

To understand the effect of temperature on the resistance as the load is been applied to the nanotubes array, measurement were also carried out by varying the temperature from 30°C to 180°C. When the weights of 100 g and 500g were applied to CNTs film, linear decrease in resistance values were registered as described in Figure 4.31. This corresponds to the previous reports [139, 140], indicating the semiconducting behavior of MWCNTs. In Koratkar's report [139], it was mentioned that the presence of amorphous carbon (a-C) at the top of the CNTs film lead to an increase in the resistant, at temperature between 50°C and 200°C. Upon purification by performing plasma etching to remove the a-C, the curve became a linear curve with negative gradient (decreasing). Here, such increase of resistance was not observed, possibly because the CNTs obtained is largely free of a-C (as proven by the SEM images from previous sections), again confirming the high quality of CNTs film

obtained. Values of the gauge factor could not be calculated as the strain measurement was not carried out experimentally here.

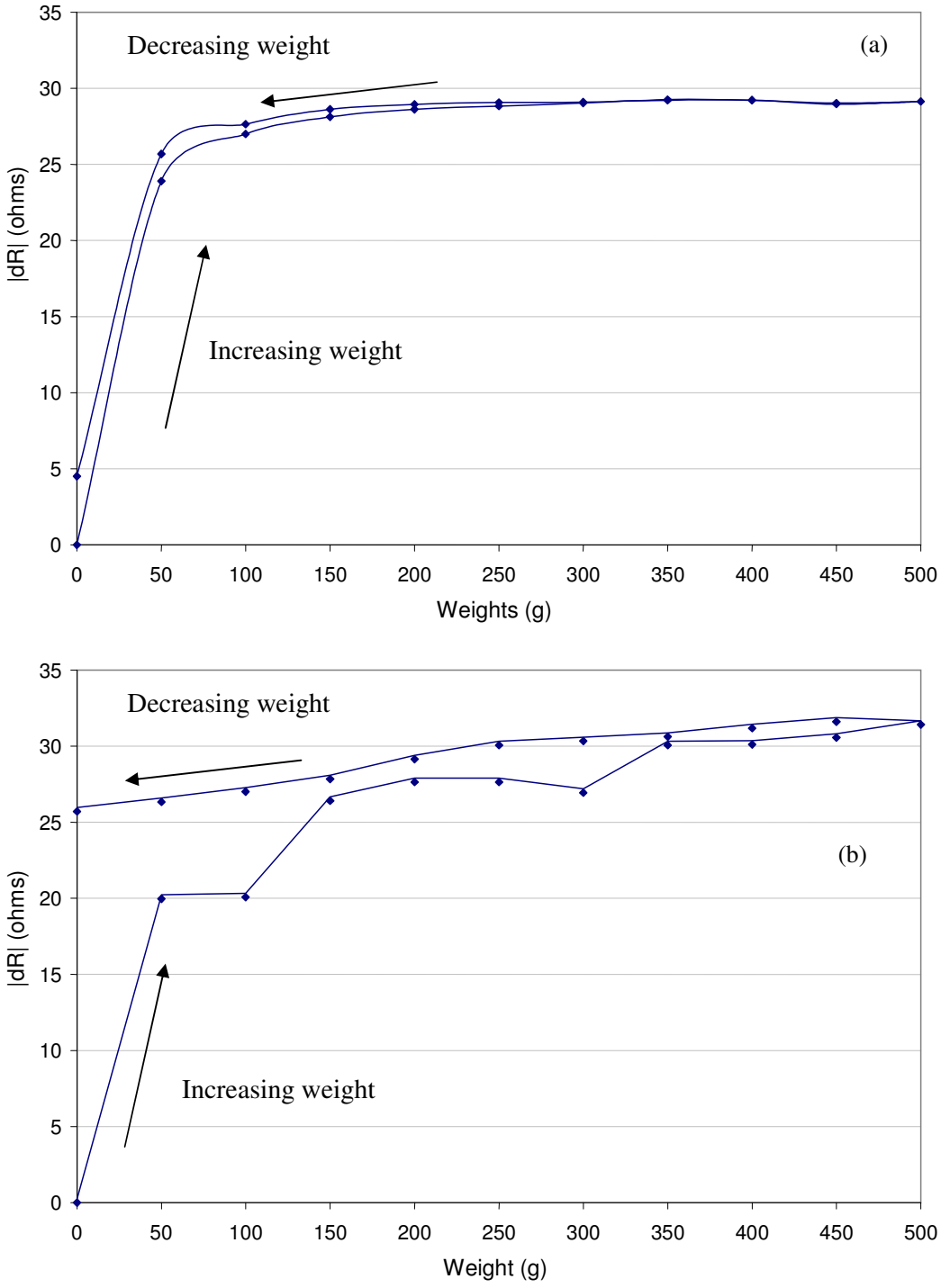

Figure 4.30 Change in the resistance, |dR| (ohms), as a function of the applied weight, W (g) for loading interval time of (a) 10 s and (b) 100 s

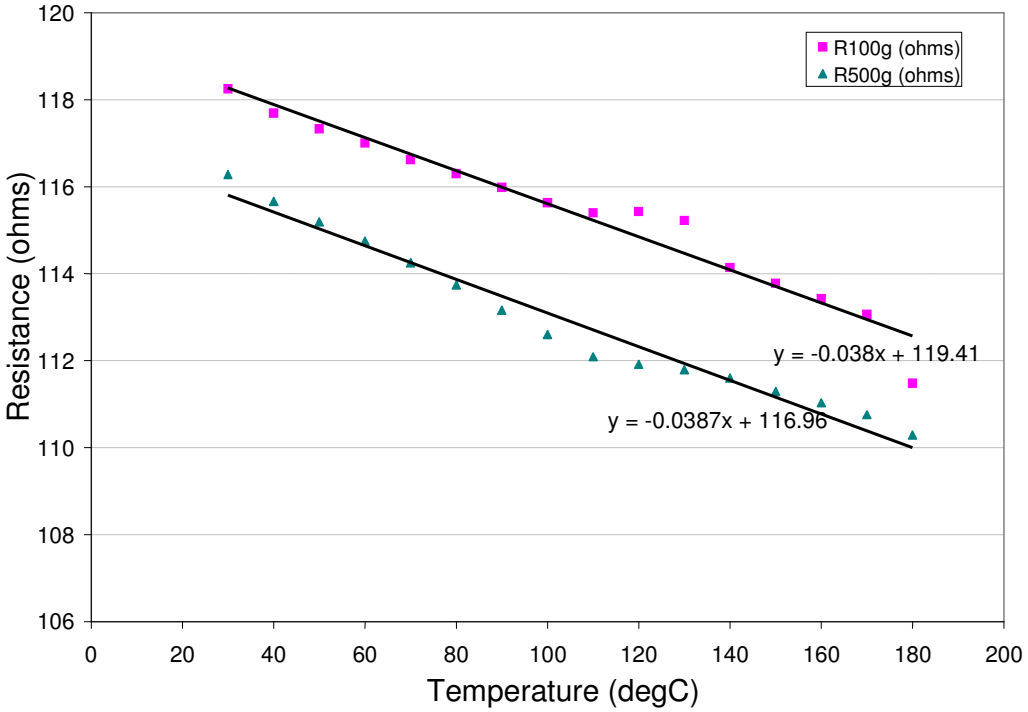

Figure 4.31 Plot of resistance (ohms) against temperature (deg C) for 100 g (■) and 500 g (▲) load

From the graph, it is noticed that at 500 g, the resistance of the CNTs film is constantly lower compared to the resistance of 100 g weight. This is consistent with the earlier finding where the resistance decreases with increasing weight. However, the slope of curve, dR/dT, which is about -0.038 Ω/°C seems to be independent of the applied weight or pressure. Furthermore, this value is similar to that value extracted from the graph of the work carried out by Koratkar (~-0.044 Ω/°C). Unlike the work carried out here, Koratkar had performed on measurement on the CNTs without any weight as the purpose was to investigate the electrical resistance of the MWCNTs across a range of temperature.

4.7 Summary

This section summarizes all the experimental findings in this chapter:

a) Growth of aligned multi-walled carbon nanotubes

MWCNTs were successfully grown using Fe powder as catalyst at temperature of 700^{o}C using ethylene. Incorporation of Al_2O_3 buffer layer helped to attain aligned growth of MWCNTs. A buffer layer refers to an intermediate thin film located between the substrate and metal catalyst. Al_2O_3 is selected because it is known to be a CNTs growth promoter. Results showed that the addition of Al_2O_3 buffer layer leads to a denser CNTs film and this contributed to highly directional growth of MWCNTs.

b) Different methods of preparing aluminum oxide buffer layer

Comparisons were made against several methods of Al_2O_3 buffer layer preparation, either direct deposition of Al_2O_3 or different methods of oxidizing the as-deposited Al. CNTs obtained using as-deposited Al_2O_3 has the highest crystallinity (I_D/I_G =0.98) while oxidizing Al in air produces CNTs of the highest film thickness (60.21 μm) and with highest growth rate.

c) Comparison of Fe powder with Fe pellet as catalyst source

Crystallinity and film thickness of the aligned MWCNTs grown using the Fe powder and Fe pellet as catalyst source were compared. The two samples were found to exhibit almost identical results between these two. The only significant difference observed was the presence of particles, believed to be Fe coated with carbon, in that sample that uses Fe powder as catalyst source.

d) Sandwich stacking orientation and its implication on the CNTs growth

Vertically aligned CNTs film, having good film density and diameter distribution, has been successfully grown using all three configurations. This could be a significant finding as it shows that the catalyst film may not necessary be exposed directly to the hydrocarbon feedstock in order for the CNTs to grow. The CNTs film also does not

exhibit any buckling as a result of the weight of the top substrate, demonstrating the high strength of the CNTs.

e) Electromechanical measurement of CNTs film

A conductive buffer layer allows resistance measurement to be performed on as-grown CNTs. Resistance of MWCNTs is found to decrease with increasing weight. As the film becomes denser, there is more contact between the nanotubes thus increasing the number of conduction channel and subsequently improving the conductivity. When the temperature was raised from 30^{o}C to 180^{o}C, the resistance of the nanotubes decreased, exhibiting a semiconducting behavior. Although higher weight loading led to further decrease in the resistance while heating at the same time, the gradient of the curve, dR/dT remained constant. Another aspect to look into is to perform the sandwich growth with both substrates instead of the approach suggested in this thesis when performing the electromechanical measurement.

CHAPTER 5

CONCLUSIONS

5.1 Conclusions

The objective of the research is to develop nanostructured carbon nanotubes as the active element for pressure sensing applications that can operate at wider temperature range. This is achieved by carrying out the following research activities:

a) Synthesis and characterization of vertically aligned carbon nanotubes using thermal chemical vapor deposition method through optimization of the growth parameters.

b) Electrical characterization of carbon nanotubes as sensing element into a test unit and evaluation of its performance when subjected to pressure and temperature.

The objectives of the project have been met. Aligned multi-walled carbon nanotubes have been successfully synthesized using thermal CVD method before being integrated into a test measurement unit for the electromechanical characterization.

In order to produce good quality, highly aligned MWCNTs, a series of experimental work was carried out. The outcome has shown that the quality and quantity of the CNTs film depends greatly on the processing parameters. The growth rate of the CNTs has been shown to vary significantly just by altering the oxidation process of the Al_2O_3 buffer layer, as seen from the different film thickness obtained. Sample with as-deposited Al_2O_3 has the highest R_{ms} value yet resulted in CNTs having the best level of crystallinity.

The buffer layer with the lowest R_{ms} value is obtained by oxidizing the Al film in air at 600^{o}C but without having to purge in Ar during the heating up stage and this resulted in the thickest CNTs film and highest growth rate.

It is also possible to grow CNTs using metal powder instead of solid i.e. pellets and disc without compromising on the quality and quantity. Raman spectra of both samples registered an almost identical I_D/I_G ratio. SEM images of CNTs obtained from Fe powder and pellets show both have similar film thickness, 47.49 μm and 49.71 μm, respectively. This may allow flexibility in selecting the composition of the metal catalyst since a combination of two or more elements have been proved to be better, especially for growing single-walled CNTs.

Sandwich stacking configuration proved that it is not necessary for the catalytic layer to be exposed to the feedstock gases in order to grow CNTs and the outcome is just as good as via conventional method. CNTs film thickness in all these samples is similar while the crystallinity of the film is almost identical except for sample S3. However, with sample S3 the thickness of the CNTs film is twice the thickness of the other samples since CNTs are growing from both catalyst-containing substrate. This is shown by the Raman spectra and SEM images of sample S1, S2 and S3 and compared to the sample produced using conventional method. This could be helpful for future application whereby the catalyst layer can be deposited at concealed location and yet CNTs can still be synthesized.

A test measurement unit, consists of as-grown CNTs on an electrically conductive Al_2O_3 buffer layer, was used for studying the electromechanical behavior of the CNTs array by means of adding weights on top of the unit. This was conceived upon unsuccessful attempts using previous setups. By default, this configuration has a low resistance (< 250 Ω) thus only requires a low voltage power source (~1 V), and is practical for actual sensing applications. Beside the electromechanical properties, their performance under varying temperature was also measured as pressure sensors are sometimes subjected to temperature changes as well. The electrical resistance MWCNTs was found to be decreasing with pressure and temperature, thus exhibiting

semiconducting behaviour. The temperature sensitivity of CNTs was found to be independent of the applied pressure.

5.2 Benefits

1. The study on the effect of growth parameters of CNTs (buffer layer preparation, catalyst precursor and substrate stacking configuration) provides further information on the CNTs growth. The outcome of MWCNTs synthesized i.e. alignment, crystallinity, film thickness, are critically dependent on these parameters.

2. It is believed that this is the first report on successful sandwich growth of MWCNTs using equal size substrates. Production of good quality, highly aligned MWCNTs in between the substrate allow for development of active element that is connected to two electrodes as in two-terminal devices.

3. The success in designing a working sensor configuration based on as-grown CNTs helps to eliminate the hassles of transferring the CNTs film onto a conductive substrate like finding suitable paste and having complete transfer of the CNTs film. This is the first time a one-step process of producing sensing element that can be applied directly into the CNT-based sensor configuration.

4. Establish a working principle of the pressure sensor based on the correlation between the changes of resistance with varying pressure in the temperature range of 30^{o}C to 180^{o}C. Development of this working principle would enable the construction of thermally stable pressure sensor using nanostructured MWCNTs as the active elements, operating in the wider temperature range (up to 180^{o}C). No previous attempts to study the effect of pressure with temperature on the electromechanical properties of CNTs film had been came upon so far.

5.3 Recommendations for Future Work

In order to apply this concept in the pressure sensor, some work need to be done to develop the prototyp that can be tested for field trial.

1. Adaptation of sandwich growth of preparing MWCNTs film as sensing element

Current method of configuring the measurement unit is by placing together two MWCNTs films grown using the conventional method. The next course of study is applying the concept from the sandwich growth would allow CNTs to be grown even at covered locations. Other benefits expected from the outcome of this adaptation includes better conductivity as a result of better connection between the two layers of CNTs film and eliminate the hassle and complication of CNTs transfer.

2. Piezoresistance study of the CNTs film in a pressure chamber

Although weights were be used to generate pressure on the array of CNTs, it is still necessary to perform the study inside a pressure chamber. Weights only act in a unilateral direction while pressurized gas inside the chamber will be pressing from the top and all four sides of the substrate.

The chamber is airtight to avoid leakage and needs to be able to withstand the high pressure inside, generated by purging gas into it similar to that of inflating a tire. It should consist of a gas inlet and gas outlet, a pressure release valve, a needle valve to control gas outlet flow, an electrical feed-through for electrical connection between the external and internal connectivity, a stage assembly (for holding the sample and carrying out electrical measurement), thermocouple for measuring temperature of the sample, pressure gauge, temperature and etc. Inside the chamber, necessary measuring probes are installed to monitor the pressure as well as recording the voltage, current and temperature.